

TECHNISCHE UNIVERSITÄT MÜNCHEN

Fakultät für Ernährung, Landnutzung und Umwelt

Lehrstuhl für Humanbiologie

Mechanosensitivity in isolated myenteric neuronal networks

Eva Maria Kugler

Vollständiger Abdruck der von der Fakultät Wissenschaftszentrum Weihenstephan für Ernährung, Landnutzung und Umwelt der Technischen Universität München zur Erlangung des akademischen Grades eines

Doktors der Naturwissenschaften

genehmigten Dissertation.

Vorsitzender: Univ.-Prof. Dr. M. Klingenspor

Prüfer der Dissertation:

1. Univ.-Prof. Dr. M. Schemann
2. apl. Prof. Dr. H. K. H. Adelsberger
3. Prof. Dr. K.-H. Schäfer
Hochschule Kaiserslautern

Die Dissertation wurde am 28.05.2014 bei der Technischen Universität München eingereicht und durch die Fakultät Wissenschaftszentrum Weihenstephan für Ernährung, Landnutzung und Umwelt am 30.09.2014 angenommen.

Publications

Original Manuscripts

Kugler E.M., Mazzuoli G., Demir I.E., Ceyhan G.O., Zeller F., Schemann M.
FRONTIERS IN NEUROSCIENCE, 6 (2012)

Activity of protease-activated receptors in primary cultured human myenteric neurons.

Schemann M., **Kugler E.M.**, Buhner S., Eastwood C., Donovan J., Jiang W., Grundy D.

PLoS ONE, 7(12):e52104 (2012)

The mast cell degranulator compound 48/80 directly activates neurons.

Buhner S.*, Braak B.*, Li Q.*, **Kugler E.M.***, Klooker T., Wouters M., Donovan J., Vignali S., Mazzuoli-Weber G., Grundy D., Boeckxstaens G., Schemann M.

(*) Authors equally contributed to the manuscript

EXPERIMENTAL PHYSIOLOGY Oct 1;99(10):1299-311 (2014)

Nerve activation by mucosal biopsy supernatants from Irritable Bowel Syndrome patients is linked to visceral sensitivity.

Published Abstracts

Kugler E.M., Zeller F., Schemann M., Mazzuoli G.
NEUROGASTROENTEROLOGY AND MOTILITY 24, 25-25

Mechanosensitive properties of isolated enteric neuronal networks

Kugler E.M., Michel K., Kirchenb uchler D., Dreissen G., Merkel R., Schemann M., Mazzuoli G.

AUTONOMIC NEUROSCIENCE 177 (1), 29-29

Physiological mechanical stimulation activates isolated myenteric neurons

Funding

German Research Foundation (Deutsche Forschungsgemeinschaft - DFG), MA-5202/1-1,
"Mechanosensitivity in the enteric nervous system"

Collaboration

Parts of the present study were performed in collaboration with the research center Jülich - institute of complex systems - biomechanics (ICS-7).

The technique for the production of the elastic surfaces was learned at the ICS-7. From there we got the silicon waver to produce the micropatterned surfaces and also the software to analyze the deformation of the stretched neurons.

Especially the following persons collaborated with us:

Prof. Dr. Rudolf Merkel

Dr. David Kirchenbüchler (now at the Weizmann Institute of Science, Rehovot, Israel)

Georg Dreissen

I want to thank them for the collaboration.

Contents

Publications	i
Funding	ii
Collaboration	iii
Zusammenfassung	1
Abstract	3
1 Introduction	5
1.1 The Enteric Nervous System	5
1.2 Mechanosensitivity in the gut	8
1.3 Classification of mechanical forces into physical terms	10
1.4 Experimental techniques used to detect mechanosensitivity in various cell systems	10
1.5 Mechanisms of mechanotransduction	11
2 Material and Methods	15
2.1 Primary culture of different neuronal cell types	15
2.1.1 Culture of guinea pig myenteric neurons from small intestine and stomach	15
2.1.2 Culture of human myenteric neurons	17
2.1.3 Culture of dorsal root ganglia neurons of guinea pig	18
2.1.4 Culture of sympathetic chain ganglia neurons of guinea pig	18
2.2 Production of elastic surface culture dishes	19
2.3 Ultrafast neuroimaging technique	20
2.3.1 Principle of the ultrafast neuroimaging technique	20
2.3.2 Staining and data acquisition	21
2.4 Testing viability of myenteric neurons	22
2.5 Mechanical stimulation	22
2.5.1 Normal stress	24
2.5.2 Shear stress	27
2.6 Measurements of cell length changes induced by stretch	28
2.7 Pharmacology	28
2.8 Immunohistochemistry	31
2.9 Transfection protocol	31

2.10 Data analysis and statistics	32
3 Results	36
3.1 Growth of primary cultured myenteric neurons of guinea pig	36
3.2 Presence of different cell types in primary cultures of myenteric neurons from guinea pig and human	36
3.3 Success rate of culturing human myenteric neurons	40
3.4 Preliminary experiments: transfection of primary cultured myenteric neurons of guinea pig	41
3.5 Identification of the properties of mechanosensitive myenteric neurons with a contact method	41
3.5.1 Mechanosensitivity is a property of enteric neurites as well as somata	41
3.5.2 Mechanosensitive properties of other cultured neurons	45
3.5.3 Characterization of mechanosensitive myenteric neurons	49
3.5.4 Pharmacological treatment of mechanosensitive neurons	53
3.5.5 Responses of multipolar neurons to multifocal mechanical stimulation	54
3.5.6 Mechanosensitivity is a property of entire neurites rather than hotspots	56
3.5.7 Reduced soma excitability affects spike invasion into neurites . . .	58
3.5.8 Mechanosensitive enteric neurons encode dynamic rather than sustained deformation	60
3.5.9 The site of mechanical stimulation is the site of origin of the electrical signal	60
3.5.10 Conduction velocity	60
3.5.11 Timing of neuronal and non-neuronal responses	64
3.5.12 Primary culture of human myenteric neurons show similar behaviour in response to mechanical stimulation	64
3.6 Identification of mechanical stimulus modalities exciting primary cultured myenteric neurons with non-contact methods	67
3.6.1 Normal stress	67
3.6.2 Shear stress	73
3.6.3 Summary normal and shear stress	77
4 Discussion	78
4.1 Comparison primary cultured myenteric neurons of guinea pig and human	78
4.2 Properties of mechanosensitive myenteric neurons identified with a contact method	79
4.3 Identification of the mechanical stimulus modalities exciting myenteric neurons	87
Bibliography	91
List of Tables	105

CONTENTS

List of Figures	106
Abbreviations	108
Acknowledgements	109
Curriculum Vitae	110

Zusammenfassung

Der Magen-Darm Trakt ist fortwährend mechanischer Spannung ausgesetzt, die aus der physiologischen Bewegung seiner Muskelschichten (zirkulärer Muskel und longitudinaler Muskel) resultiert. Der myenterische Plexus, der zwischen diesen Muskelschichten liegt, ist die lokale neuronale Kontrolle der Peristalsis. Direkte Aktivierung myenterischer Neurone durch mechanische Stimuli wurde gezeigt. Allerdings ist die genaue Stimulus Modalität, die myenterische Mechanosensoren aktiviert, bisher nicht bekannt. Die Muskelaktivität überträgt sowohl Tangential- als auch Normalspannung auf den myenterischen Plexus. Das Ziel dieser Arbeit ist es, die Eigenschaften der mechanosensitiven myenterischen Neurone zu beschreiben und diese mit anderen sensorischen Nervenzellen erster Ordnung zu vergleichen. Des Weiteren sollte die Art der mechanischen Stimulus Modalität bestimmt werden, die mechanosensitive myenterische Neurone aktiviert.

Primärkulturen myenterischer Neurone wurden benutzt, um Einflüsse von nicht neuronalen Zellen auszuschließen. Die neuronale Aktivität wurde hauptsächlich mit einer Neuroimaging Methode in Verbindung mit einem spannungssensitiven Farbstoff gemessen. Diese Technik macht es möglich von mehreren Nervenzellen gleichzeitig abzuleiten. Um die Eigenschaften der mechanosensitiven Neurone zu beschreiben wurde ein ultrafeines von Frey Haar benutzt. Normalspannung wurde mittels zwei Techniken angewandt: hydrostatischer Druck, um phasische Kontraktionen nachzuahmen und Dehnung, um tonische Kontraktionen nachzuahmen. Tangentialspannung wurde mittels eines Flüssigkeitsstroms in einem Mikrokanal appliziert.

Die vorliegende Arbeit zeigte, dass mechanosensitive myenterische Neurone keine spezialisierten Regionen für Mechanotransduktion besitzen. Stattdessen sind diese Neurone entlang des gesamten Fortsatzes und des Zellkörpers mechanosensitiv. Aktionspotentialmuster, die als Antwort auf dynamische und anhaltende Deformation einer kleinen Region der Nervenzelle auftreten, zeigten, dass diese primär auf dynamische Änderungen während der Deformation reagieren. Das elektrische Signal entsteht an der Stelle an der mechanisch gereizt wird. Signale, die in den Nervenfortsätzen entstehen, werden an das Soma und weitere Nervenfortsätze weitergeleitet. Die Multifunktionalität dieser mechanosensitiven Fortsätze wurde gezeigt. Diese übertragen sensorische Informationen und übertragen zugleich das Signal an andere Zellen. Dies zeigt ihre Funktion als motorische Fortsätze. Es wurde gezeigt, dass die Transduktion mechanischer Signale von dem Erregungszustand des Somas abhängig ist. Dies suggeriert, dass neuronale Antworten moduliert werden können, was für eine angemessene Antwort auf Umweltsignale entscheidend ist. Mechanosensitive myenterische Neurone teilen einige Eigenschaften mit anderen sensorischen Nervenzellen. Allerdings weisen sie auch spezi-

fische Eigenschaften auf, die wahrscheinlich eine Anpassung an ihre physiologische Funktion im Darm darstellen. Mechanosensitive Eigenschaften sind ähnlich in verschiedenen Spezies, was für Meerschweinchen und Human gezeigt werden konnte. Die Antworten auf Normalspannung sind reproduzierbar und weisen eine Abhängigkeit von der Kraftstärke auf, wohingegen Tangentialspannung nur eine unbedeutende Wirkung hat. Daraus wurde gefolgert, dass Normalspannung der primäre Stimulus für mechanosensitive myenterische Neurone ist. Stimuli, die phasische und tonische Kontraktionen nachahmen, haben beide eine aktivierende Wirkung, aber weisen ein unterschiedliches Antwortmuster auf. Phasische Kontraktionen scheinen schnell adaptierende mechanosensitive enterische Neurone (RAMEN) anzuregen, wohingegen tonische Kontraktionen vermutlich langsam adaptierende mechanosensitive enterische Neurone (SAMEN) anregen. Beide Mechanosensoren können auf der gleichen Zelle exprimiert sein, da ein Teil der mechanosensitiven neuronalen Population auf beide Stimuli reagiert.

Die vorliegende Arbeit hilft, die komplexen Vorgänge bei der neuronalen Mechanotransduktion zu verstehen und die neuro- motorischen Muster aufzuklären, die eine wichtige Rolle bei der Peristalsis unter physiologischen und pathophysiologischen Umständen spielen. Viele Erkrankungen des Magen-Darm Traktes wie das Reizdarmsyndrom und Obstipation stehen im Zusammenhang mit einer Motilitätsfunktionsstörung. Darum ist das Verständnis der komplexen Mechanotransduktion notwendig um neue therapeutische Ansätze für diese Erkrankungen zu finden.

Abstract

The gastrointestinal (GI) tract is constantly under mechanical stress, which results from physiologic movements of its muscle layers (circular muscle and longitudinal muscle). The myenteric plexus (MP), which is sandwiched between these muscle layers, is the local neural controller of peristalsis. Direct activation of myenteric neurons by mechanical stimuli has been shown. However, the precise stimulus modalities that excite myenteric mechanosensors are so far unknown. Muscular activity imposes shear stress and normal stress on the MP. The aim of the present study was to describe the properties of mechanosensitive myenteric neurons and to compare them with other first order sensory neurons. Furthermore, the nature of mechanical stimulus modalities that excite mechanosensitive myenteric neurons should be clarified.

Primary cultured myenteric neurons were used to exclude non-neuronal influences. Neuronal activation was mainly recorded with a neuroimaging technique with voltage-sensitive dye that made it possible to study multiple neurons simultaneously. To describe properties of mechanosensitive neurons an ultra-fine von Frey hair was used. Normal stress was applied by two techniques: hydrostatic pressure to mimic phasic contractions and stretch to mimic tonic contractions. Shear stress was applied by fluid flow through a micro channel.

The present study revealed that mechanosensitive myenteric neurons had no specialized regions for mechanotransduction. Instead, mechanosensitivity occurred along the entire neurites and the soma. Spike discharge patterns in response to dynamic and sustained deformation of small spots on neurons, revealed that they primarily encode dynamic changes during deformation. The electrical signal originated at the site of the mechanical stimulation. Neurite signals propagated towards the soma and also invaded other neurites. The multifunctionality of mechanosensitive neurites was shown. They transmit sensory information and spread the signal to other cells, which demonstrate a function as motor neurites. It could be shown that the excitability state of the soma is critical for the transduction of mechanical signals. This suggests that neuronal responses can be modulated, which would be crucial to provide appropriate responses to environmental signals. Mechanosensitive myenteric neurons share some properties with other sensory neurons but also exhibit specific features, very likely reflecting adaptation to their physiological function in the gut. Mechanosensitive properties are conserved across species as shown for guinea pig and human. Responses to normal stress were reproducible and force strength dependent, while shear stress showed only a marginal effect. Thus, it was concluded that normal stress is the primary stimulus for mechanosensitive myenteric neurons. Stimuli mimicking phasic and tonic contractions were excitatory with differing

response patterns. Phasic contractions seem to activate rapidly adapting mechanosensitive enteric neurons (RAMEN) whereas tonic contractions activate slowly adapting mechanosensitive enteric neurons (SAMEN). Both mechanosensors can be expressed on the same neuron, because a fraction of the mechanosensitive neuronal population responded to both stimuli.

The present study helps to understand the complex process of neuronal mechanotransduction and to clarify different neuro-motoric patterns involved in the regulation of peristalsis under physiological and pathophysiological situations. Many GI diseases such as irritable bowel syndrome and constipation are correlated with motility disorders. Therefore, the understanding of the complex mechanotransduction pathways is crucial to find new treatments for such diseases.

1 Introduction

1.1 The Enteric Nervous System

The enteric nervous system (ENS) is part of the autonomous nervous system, although it differs from the rest of it. The ENS can control all its vital functions independently of the central nervous system and is therefore also named the “second brain” (Gershon 1999).

The science studying the ENS, called Neurogastroenterology, became a new research field after the discovery of the enteric neurons that are organized in ganglionated plexi in the intestinal wall (Meissner 1857; Auerbach 1862). The independency of the ENS was first postulated in 1899 by investigating the local reflexes in isolated or extrinsically denervated intestine of dogs and rabbits (Bayliss and Starling 1899). The peristaltic reflex consisting of an oral contraction and an anal relaxation when pressure is applied at the inner surface of the intestine was described (Bayliss and Starling 1899). Further on, it has been shown in *in vitro* experiments that the ENS is a self-regulating nervous system that functions without the input from the brain and the spinal cord (Trendelenburg 1917). Since then a vast amount of knowledge about the ENS has been collected. The ENS consists of many hundred million of nerve cells, grouped in ganglia located in the gut wall. These ganglia are interconnected by bundles of nerve processes and form two major ganglionated plexi: the myenteric plexus (MP; also called Auerbach plexus) located between the circular and longitudinal muscle layer, and the submucous plexus (SMP; also called Meissner plexus) located between mucosa and circular muscle layer. The MP is present along the whole gut from the upper esophagus to the internal anal sphincter, whereas the SMP is only significant present in the small and large intestine (Schabadasch 1930; Schofield 1960; Stach et al. 1975; Christensen and Rick 1985; Furness et al. 1991; Schemann et al. 2001; Colpaert et al. 2002; Izumi et al. 2002). Another difference is the size of the ganglia, in the SMP the ganglia are generally smaller and the interconnecting strands finer as in the MP (Furness 2006). Moreover, the MP mainly regulates motility and the SMP mainly secretion (Furness 2006). The most extensive studied species in this field is the guinea pig.

The enteric neurons can be divided into different classes by their morphology, electrophysiological behavior, functions, projections, neurochemical and pharmacological properties.

Morphological classification of enteric neurons

A detailed description of different shapes of enteric neurons was done more than 100 years ago, but is still valuable until present (Dogiel 1895). Generally, enteric neurons are divided into three classes, Dogiel type I, Dogiel type II and Dogiel type III.

Dogiel type I neurons are flattened, slightly elongated neurons with stellate or angular outlines that have 4 – 20 lamellar dendrites and a long process, which is likely the axon (Dogiel 1895). Their cell bodies have a large diameter of 13 – 35 μm and a small diameter of 9 – 22 μm .

Dogiel type II neurons in contrast have large oval or round somata. They have a large diameter of 22 – 47 μm and a small diameter of 13 – 22 μm . Dogiel proposed that they have 3 – 10 dendrites and one axon (Dogiel 1895), but nowadays it is believed that they are multiaxonal (Stach 1981; Hendriks et al. 1990). They are numerous and make up 10 – 25% of the MP population of the small and large intestine. 80 – 90% of the Dogiel type II neurons of guinea pig myenteric ganglia are immunoreactive for the calcium- (Ca^{2+}) binding protein calbindin (Furness et al. 1988; Iyer et al. 1988; Song et al. 1991; Costa et al. 1996). Furthermore the majority of them is immunoreactive for choline acetyltransferase (ChAT) (Steele et al. 1991).

Dogiel type III neurons are filamentous neurons that have 2 – 10 dendrites. The dendrites are short, become thinner and are branching. The axon can arise from a protrusion of the cell body or from a dendrite (Dogiel 1899).

Electrophysiological classification of enteric neurons

The electrophysiological classification in AH and S neurons was introduced in 1974 (Hirst et al. 1974). AH stands historically for after-hyperpolarizing whereas S stands historically for synaptic.

AH neurons are characterized by large amplitude and greater duration of the action potential compared to S neurons. Furthermore, they have a Ca^{2+} -hump on their falling phase. There are normally two phases of hyperpolarization an early and late phase (Hirst et al. 1974; Hirst et al. 1985b). Part of their spike component is driven by Ca^{2+} influx. They rarely receive fast synaptic input but generate slow excitatory postsynaptic potentials (EPSPs). In the guinea pig ileum all AH neurons have Dogiel type II morphology. The action potentials of AH neurons show a tetrodotoxin (TTX) sensitive Na^+ current and a TTX insensitive Ca^{2+} current component (North 1973; Hirst et al. 1985a; Rugiero et al. 2003).

In contrast S neurons exhibit brief action potentials that lack the slow hyperpolarization. They receive fast EPSPs and their action potentials are TTX sensitive. Typically they show Dogiel type I morphology and have a single axon (Hirst et al. 1974). In the guinea pig small intestine they never have Dogiel type II morphology (Furness 2006).

Functional classification of enteric neurons

Functionally enteric neurons can be divided into motor neurons, interneurons, intestinofugal neurons and sensory neurons.

Functional groups are made on the basis of the combination of studies concerning morphological aspects of the enteric neurons, of their projections and of their neurochemical coding.

Motor neurons can be excitatory or inhibitory and innervate the longitudinal, the circular muscle and the muscularis mucosae throughout the GI tract. They are uniaxonal neurons with S type electrophysiology. The excitatory motor neurons have acetylcholine and tachykinins as primary transmitters. Inhibitory motor neurons have different kind of neurotransmitters such as nitric oxide, vasoactive intestinal peptide (VIP) and adenosine triphosphate (Furness 2006).

Interneurons are present in all gut regions; nevertheless their variation between different regions is huge. In guinea pig small intestine there are 3 classes of descending interneurons and one class of ascending interneurons (Costa et al. 1996; Furness 2006). The class of ascending interneurons is composed of neurons with Dogiel type I morphology with a unique chemical coding (ChAT, calretinin, substance P, neurofilament protein, enkephalin) (Brookes et al. 1997). Ascending interneurons make up 5% of all myenteric neurons (Costa et al. 1996). Descending interneurons in guinea pig small intestine can be immunoreactive for ChAT and somatostatin, ChAT and nitric oxide synthase (NOS), VIP and other substances, ChAT and 5-hydroxytryptamine (5-HT) (Furness 2006).

Intestinofugal neurons show in guinea pig small intestine Dogiel type I morphology (Tassicker et al. 1999). Their somata lay in the gut wall and their processes project to prevertebral ganglia forming synapses with postganglionic sympathetic neurons (Kuntz 1938; Szurszewski and Miller 1994). The intestinofugal neurons in the small intestine are immunoreactive for VIP and ChAT, and calcitonin gene-related peptide, but not for NOS in contrast to the large intestine (Anderson et al. 1995; Mann et al. 1995). The innervated sympathetic neurons have inhibitory function for motility and secretion (Furness 2006).

Sensory neurons make up $\sim 20\%$ of all neurons in the ENS (Furness et al. 1998; Furness 2006). These are the first neurons involved in reacting to chemical and mechanical stimuli within the gut. It was suggested that intrinsic primary afferent neurons (IPANs) are the only sensory neurons in the gut (Bornstein 1994; Furness et al. 1998) They have all Dogiel type II morphology and AH electrophysiology (Bornstein et al. 1989; Evans et al. 1994). IPANs show calbindin, substance P and ChAT immunoreactivity (Furness et al. 1984; Kirchgessner et al. 1992). They project within submucous ganglia, to the mucosa and the MP (Bornstein et al. 1989; Kirchgessner et al. 1992; Song et al. 1992; Evans et al. 1994).

1.2 Mechanosensitivity in the gut

Mechanical forces are constantly present in the GI tract triggered by muscle movement. There are different types of muscle activity in the gut occurring induced by two antagonists acting in the intestine, the circular muscle and the longitudinal muscle. With contraction of the circular muscle the diameter of the contracted segment is decreased. Contraction of the longitudinal muscle induces a shortening of the length of the segment. Movement of the two muscle layers against each other induces mechanical stress on the MP situated between these two layers. In addition contractions of the GI smooth muscle can be divided in phasic and tonic contractions. Phasic contractions can be defined as short periodic contractions followed by relaxation. In contrast tonic contractions are maintained contractions without regularly following relaxations. It has been shown that myenteric ganglia undergo deformation during gut muscle activity (Mazzuoli and Schemann 2009). Neuronal cell bodies as well as interganglionic fibers are deformed (Mazzuoli and Schemann 2009). Anyway the mechanism how the ENS is activated by mechanical stimuli is still under debate. Are the enteric neurons directly activated by mechanical stimuli or indirectly by the release of other transmitter substances? An example for an indirect activation is the release of 5-HT by enterochromaffin cells subsequent to mechanical stimulation of the mucosa (Bertrand and Bertrand 2010). Furthermore, in the gut there are other cells as smooth muscle cells and interstitial cells of Cajal (ICC) that can directly respond to mechanical stimuli (Kraichely and Farrugia 2007). The ICC have pacemaker function, whereas smooth muscle cells are the effector cells for contraction and relaxation (Barajas-Lopez et al. 1989; Ward et al. 2000; Lyford and Farrugia 2003; Kraichely and Farrugia 2007).

It is also challenging to detect the initiator of the peristaltic reflex. Partially contradictory results have been reported in the years. Early on a crucial role of the mucosa was postulated after the discovery that the peristaltic reflex was absent in preparations without mucosa (Bulbring et al. 1958). On the contrary, other scientists observed the peristaltic reflex without the presence of mucosa (Ginzel 1959; Diamant et al. 1961). It was also found that the absence of the MP inhibited the peristalsis (Evans and Schild 1953). These experiments and experiments, in which normal peristalsis was detected in preparations without mucosa and SMP, proposed the MP as the neural site of the initiation of the peristaltic reflex (Tsuji et al. 1992; Spencer and Keating 2011). This suggests that neurotransmitters secreted by mucosal non-neuronal cells may have only modulatory action on the mechanotransduction pathway.

Electrophysiological studies on the MP clearly showed direct neuronal excitation by various mechanical stimuli (Mayer and Wood 1975; Kunze et al. 2000; Mao et al. 2006; Smith et al. 2007; Mazzuoli and Schemann 2009; Mazzuoli and Schemann 2012).

Myenteric neurons receive from the muscle layers, they are embedded in, the crucial information and at the same time they control the muscle cell activity, forming a self-reinforcing network.

A specialized group of neurons early on has been suggested to have sensory function, the IPANs (Bornstein 1994; Furness et al. 1998; Bertrand and Thomas 2004; Furness et al. 2004; Gershon 2005). The IPANs in guinea pig ileum were characterized as Dogiel

type II neurons with AH electrophysiology (Iyer et al. 1988; Hendriks et al. 1990; Kunze and Furness 1999). IPANs communicate with slow EPSPs and most of them show immunoreactivity for calbindin (Furness et al. 1988; Iyer et al. 1988; Quinson et al. 2001). The mechanosensitivity of IPANs has been shown by an ongoing spike discharge in response to circumferential stretch and muscle contraction (Kunze et al. 1998; Kunze and Furness 1999). In addition excitatory action of mechanical stimuli have been only shown for interganglionic nerve processes, whereas compression of the neuronal soma in IPANs has an inhibitory effect (Kunze et al. 2000).

The concept that there is only one specialized group of enteric neurons with sensory function is now in evolution. There are more and more evidences indeed that not only this specialized group of neurons is mechanosensitive, but also other myenteric neurons are activated by mechanical stimuli. For instance there are regions as the guinea pig gastric corpus where AH-neurons are completely absent (Hirst et al. 1974; Wood and Mayer 1978; Hodgkiss and Lees 1983; Schemann and Wood 1989b). For the first time it was shown in 2004 that also S interneurons are activated by circumferential stretch (Spencer and Smith 2004). Further studies showed that different enteric neurons like interneurons and motor neurons fulfill multiple functions and give rise to a concept of multifunctional sensory neurons (Smith et al. 2007; Mazzuoli and Schemann 2009; Schemann and Mazzuoli 2010; Mazzuoli and Schemann 2012).

The concept of multifunctional myenteric neurons proposes moreover a neuronal regional specialization based on the different kind of motor activity. It is a fact that enteric neurons from different gut regions have to fulfill different functions. In mouse it was shown that mechanosensitive myenteric neurons from ileum all encoded dynamic deformation, whereas from colon they partly encoded sustained deformation (Mazzuoli and Schemann 2012). The terms rapidly adapting mechanosensitive enteric neurons (RAMEN) and slowly adapting mechanosensitive enteric neurons (SAMEN) were introduced previously (Mazzuoli and Schemann 2009; Mazzuoli and Schemann 2012). Another example are the neurons situated in the stomach, which have to fulfill different functions than the ones in the small intestine. Therefore, a difference in the electrophysiological and synaptic behavior of their neurons is not surprising (Wood 1987a; Wood 1987b; Wood 1989; Schemann and Wood 1989b; Schemann and Wood 1989a). In addition, myenteric neurons in the stomach receive only fast synaptic input unlike small intestinal myenteric neurons (North 1986; Hodgkiss and Lees 1986; Schemann and Wood 1989a). Fast synaptic input strongly suggests a modulatory activation. The concept of gating of enteric neuronal responses was proposed early on (Wood and Mayer 1979), but was never experimentally proven up to know. Recently it was found that all mechanosensitive myenteric neurons from guinea pig small intestine receive fast synaptic input (Mazzuoli and Schemann 2009). Differences in the mechanotransduction pathway in myenteric neurons derived from regions with different motor activity as stomach and small intestine would be plausible and need to be investigated.

1.3 Classification of mechanical forces into physical terms

Mechanical forces can be classified in two major physical terms. First, normal stress is a force perpendicular to a given surface divided by the respective surface. It results in a volume/length change of the object (Hoeffling 1985).

Second, shear stress is a force parallel to a given surface divided by the respective area. It induces no volume change, but a shape change (Hoeffling 1985).

In the present study mechanical force classification was based on their primary loading modality.

1.4 Experimental techniques used to detect mechanosensitivity in various cell systems

Mechanosensitivity plays a key role in a great variety of biological systems. Reacting to external environmental changes and modulating physiological processes are situations that require an adequate response to various mechanical stimuli. This study area is of extreme importance in different research fields. Mechanosensors can become novel therapeutic targets in the clinical use. Indeed, it has been shown that in many pathological conditions mechanical stress increases the cell sensitivity (Kamkin and Kiseleva 2005). The somatosensory system is a well-studied research field in mechanosensitivity. There is a diverse array of specialized mechanosensitive neurons responding to specific mechanical forces in an appropriate way. The mechanosensitive functions are fulfilled by specialized primary afferent neurons with their cell bodies located in trigeminal ganglia and dorsal root ganglia (DRG) projecting long axons to the skin and deeper body structures. Specific neurons detect external mechanical stimuli, whereas others transduce self-generated stimuli (Belmonte and Viana 2008; Basbaum et al. 2009). There are subtypes of mechanosensitive neurons that do not only sense different mechanical stimulus modalities, but also encode specific sensitivity thresholds (Lumpkin and Caterina 2007; Belmonte and Viana 2008). All these neurons have in common mechanotransducing channels on sensory nerve endings. These channels are able to transform mechanical forces into electrical signals. This depolarizes receptor fields, which locally give rise to receptor potentials. These may generate action potentials that are then further propagated to the central nervous system.

Several experimental strategies have been developed to study mechanotransduction in different cell systems.

Normal stress can be applied by different techniques. Von Frey hairs are pressed down onto the target and compress the compartment beneath it. This technique was already successfully used to stimulate enteric neurons (Mayer and Wood 1975; Kunze et al. 2000; Mazzuoli and Schemann 2009). Hydrostatic pressure can be locally applied by fluid flow through the micropipette. This technique has been used to stimulate cardiomyocytes

(Kong et al. 2005; Sanchez et al. 2008); and erythrocytes, epithelial cells and DRG neurons (Sanchez et al. 2008). Stretch as normal stress can be applied by various techniques. Special designed stretch apparatus' have been already used to stretch gut whole-mount preparations (Kunze et al. 1998; Zagorodnyuk and Spencer 2011). For local stretch application an elastic surface, on which the cells adhere, can be pulled. This technique was already applied to myofibroblasts (Kirchenbuchler et al. 2010) and DRG neurons (Cheng et al. 2010; Lin et al. 2009). Shear stress can be applied with fluid flow through a micro channel. Micro channels have been already used to stimulate fibroblasts (Hung et al. 1997); Schwann cells (Chafik et al. 2003); cancer cells (Couzon et al. 2009) and endothelial cells (Meer et al. 2010).

Studies, which cover all kind of mechanical stimulus modalities, are the first step to unravel the mechanical properties of cells. Such studies are unfortunately missing in the ENS.

It has to be considered that *in vivo* cells are exposed to not exclusively one stimulus modality but to multiple modes of mechanical stimulation. It was shown that different stimulus modalities can cause different cell responses. In endothelial cells, for example, shear stress and circumferential stretch but not pressure is able to modulate Cx43 expression, which plays a role in gap junctional communication under pathological conditions (Kwak et al. 2005). In rat skeletal muscle it was shown that different factors play a role in stretch- and shear-stress induced angiogenesis, which influences the expression of these factors (Milkiewicz et al. 2007). In intestinal epithelial cells it was shown that stretch enhances the cellular proliferation, whereas shear stress influences the adhesion (Gayer and Basson 2009).

Thus an important question to answer is if myenteric neurons respond to different stimulus modalities and how do they respond.

Another central question is if mechanoreceptors primarily sense stress, which is defined by force per cross sectional area, or strain, which is a non-dimensional measure of deformation.

1.5 Mechanisms of mechanotransduction

Molecular basis of mechanotransduction

The basis of a membrane protein to be mechanosensitive is that it changes its property in result of mechanical deformation. A two-state channel can have a closed and open conformation, which may be caused by changes in bilayer tension, thickness, or local curvature or by direct pulling on the membrane protein by cytoskeletal or extracellular tethers. It is important to identify the parameter conferring mechanosensitivity on the membrane protein (Hamill and Martinac 2001). The cytoskeleton gives the cells the needed stability as well as deformability and is referred to have also a critical role in the modification of the cells mechanical response (Elson 1988).

Mechanosensitive channels

Until present a wide array of various stretch-sensitive and mechanosensitive channels have been detected. In the following paragraphs a small selection of mechanosensitive channels are described.

Transient receptor potential (TRP) channel superfamily

The TRP superfamily can be divided into six cation-selective subfamilies in mammals, which are promising candidates to be mechanosensitive channels (Damann et al. 2008). Most of them are linked to mechanosensation (Christensen and Corey 2007). The ankyrin subfamily TRPA has one member, the canonical TRPC family has 7 members, the vanilloid TRPV family has 6 members, the melastin TRPM has 8 members, the polycystin TRPP has 3 members and the distantly related mucolipin TRPML has 3 members (Sharif-Naeini et al. 2008). TRPs are present in various species and regions and fulfill a number of functions such as sensation of physical stimuli like light, osmolarity, temperature and pH and chemical stimuli like odours, pheromones and nerve growth factor (Minke and Cook 2002). At least 10 mammalian TRPs exhibit mechanosensitivity: TRPC1,5,6; TRPV1,2,4; TRPM3,7; TRPA1 and TRPP2 (Christensen and Corey 2007; Sharif-Naeini et al. 2008; Inoue et al. 2009). In cultured DRG neurons a role in mechanosensation of TRPA1 was found in a subtype of neurons, which show slowly adapting mechanically-activated currents (Vilceanu and Stucky 2010). A role in sensing membrane stretch was shown for TRPV2 and hypotonic cell swelling and shear stress for TRPV4 (O'Neil and Heller 2005).

Piezo proteins

As other promising candidates for mechanosensation the Piezo proteins have been recently identified (Coste et al. 2010; Coste et al. 2012). In vertebrates there are two Piezo members, Piezo1 and Piezo2, which were previously known as FAM38A and FAM38B, respectively. Piezo2 is substantially expressed in DRG, whereas Piezo1 is rarely found (Delmas et al. 2011). Mechanosensitive currents were observed in heterologous expression of Piezo1 and Piezo2, but with different kinetics (Coste et al. 2010). It is not known if Piezo proteins themselves conduct currents or if they confer mechanosensitivity to pore-forming subunits by heterodimerization (Delmas et al. 2011). Nevertheless Piezo-dependent mechanosensitive currents can be blocked by classical mechanical blockers such as gadolinium and ruthenium red (Delmas et al. 2011). Later on, it was claimed that Piezo proteins are indeed ion channels (Coste et al. 2012). Piezo1 can be furthermore specifically blocked by GsMTx4 (Bae et al. 2011).

Aim of the study and study design

The aim of the present study is to describe the properties of mechanosensitive myenteric neurons and to compare them with other first order sensory neurons. Furthermore, the nature of mechanical stimulus modalities exciting mechanosensitive myenteric neurons is clarified.

Primary cultured myenteric neurons are used for this study. With this approach possible influences of other cell types, in particular muscle cells, are at least controllable if not excluded. Furthermore mechanical stress can be locally applied to a defined small region and the requirements for the experimental design can be adjusted. The neuroimaging technique with voltage-sensitive dye was used as a rather non-invasive recording method to detect neuronal responses. This technique in combination with independent component analysis (ICA) make it possible, firstly, to detect signals from the neuronal cell body as well as from single neurites; and secondly, to follow the signals conducted from the site of mechanical stimulation to the soma and other neurites. Different types of mechanical stimuli were chosen to mimic the physiological neuronal deformation, which appears during muscle contraction and relaxation of the gut wall.

The first part of the thesis studied in details the response patterns of primary cultured myenteric neurons after probing neurites or somata with an ultra-fine carbon fiber of 8 μm diameter. This was done with the purpose to understand where the mechanotransduction site is located. It has been proposed that IPANs respond differentially to mechanical stimulation of neurites and somata in guinea pig small intestine tissue preparations (Kunze et al. 2000). The experiments of the present study were not focused only on a specific neuronal population, but following the concept of multifunctionality to study the responses on a large population of myenteric neurons. In order to compare features of mechanosensitive myenteric neurons with well-established mechanosensors in the central nervous system, experiments on primary culture of DRG neurons were performed. Cultured sympathetic chain ganglia (SCG) neurons were also tested as negative control as they are supposed to be not mechanosensitive (McCarter et al. 1999). With pharmacological experiments the involvement of some known mechanosensitive channels in myenteric mechanotransduction was tested.

The second part of this thesis identifies the nature of the mechanical stimulus modality exciting myenteric neurons. Until now, there is no study existing testing the full array of mechanical stimulus modalities on enteric neurons. Normal stress may affect the enteric neurons during muscle contraction and relaxation. Shear stress may occur when the two perpendicular muscle layers move against each other. In the gut up to now the effect of different stimulus modalities was shown only on intestinal endothelial cells (Gayer and Basson 2009).

In this part of the study only non-contact methods for the application of mechanical (normal or shear) stress were used. These techniques allowed to stimulate simultaneously whole neuronal clusters. In addition two techniques to apply normal stress were used in order to mimic the deformation that may occur during phasic and tonic contractions. Phasic contractions were mimicked by hydrostatic pressure through a micropipette. With this technique a short lasting deformation was obtained. Tonic contractions were mimicked with stretch by pulling an elastic surface, on which the neurons adhered. This stimulation technique induced a dynamic phase of the deformation and a long-lasting sustained phase. Shear stress was applied by fluid flow through a micro channel. These results represent a step forward to understand, which stimulus modalities contribute to the process of neuronal mechanotransduction in the enteric network.

This could help to clarify the different neuro-motoric pattern involved in the regulation of peristalsis and to understand pathophysiological situations. Many GI diseases are in fact correlated with dysmotility, such as irritable bowel syndrome and constipation (Di Nardo et al. 2008). Therefore the understanding of the complex mechanotransduction pathway would be the next step to find new therapeutic targets to treat motility disorders.

2 Material and Methods

2.1 Primary culture of different neuronal cell types

2.1.1 Culture of guinea pig myenteric neurons from small intestine and stomach

All studies with guinea pigs were conducted according to the German guidelines for animal care and welfare. Cultures were prepared with 100 male guinea pigs (*Dunkin Hartley, Harlan Winkelmann, Borcheln, Germany*) after the protocol from Vanden Berghe et al. (Vanden Berghe et al. 2000). The guinea pigs were kept under standardized conditions at the Human Biology institute in appropriate airflow-cabinets (*Uni-Protect, Ehret, Emmendingen*). They were fed with standard food (*Altromin Spezialfutter GmbH & Co. KG, Lage, Germany*) and drinking water ad libitum. In the airflow-cabinets was an optimal temperature of 20-24 °C and a humidity of 60%. The day and night cycle was automatically regulated with 14:10 h. The guinea pigs were kept at least for one week at the institute before using them, and then they had a weight of 371 ± 63 g (mean \pm standard deviation) (range 238 – 558 g). The animals were killed by cervical dislocation and exsanguination (approved by the local animal ethical committee and in accordance with the German guidelines for animal care and welfare). The abdomen was opened with surgical scissors (14001-13; *Fine Science Tools (FST), Heidelberg, Germany*) and tissue forceps (11023-10; *FST*). The abdomen was held with forceps with flat corrugated tips (11000-14; *FST*). To obtain primary culture of small intestinal myenteric neurons a 10-15 cm piece of the small intestine orally to the ileocecal sphincter was quickly removed with scissors (14010-15; *FST*) and two times rinsed with sterile, ice-cold, carbogenated (95% CO₂, 5% O₂; *Andeldinger, Freising, Germany*) Krebs solution (containing in mM: 1.2 MgCl₂, 2.5 CaCl₂, 1.2 NaH₂PO₄, 120.9 NaCl, 14.4 NaHCO₃, 11.5 Glucose, 5.9 KCl; pH=7.4) that is also used for the other preparation steps, filled in a sterile 24 mL syringe (*Henry Schein, Melville, NY, USA*). All further steps were performed under a sterile bench (Maxi Safe 2010; *Heto-Holten A/S, Allerød, Denmark*) with sterile preparation instruments (sterilized at 180 °C for 2 h). The tissue was cut in a sterile glass petri dish (*Schott, Mainz, Germany*) containing sterile Krebs solution into 10-20 mm segments with preparation scissors (14028-10; *FST*). The gut segments were pulled on a glass pipette with a diameter of ~ 5 mm and then the longitudinal muscle - myenteric plexus layer (LMMP) was cut with a sterile scalpel, thereby the circular muscle was not cut. Then the LMMP was stripped with forceps (*Dumostar #5; Dumont, Switzerland*). To obtain primary culture of myenteric neurons of the stomach the corpus of the stomach was prepared. The preparation steps were performed in a sterile glass petri dish

(Schott) with a sylgard surface (Sylgard [®] 184; Dow Corning, Wiesbaden, Germany) under a stereomicroscope (Olympus, Hamburg, Germany). For all the preparation steps that were not performed under the hood all instruments and surfaces were sterilized before. Surfaces were cleaned with 80% ethanol and Descosept AF (Dr. Schumacher GmbH, Melsungen, Germany). The tissue was roughly pinned with insect pins (26002-10; FST). The stomach was opened along the big curvature. The two stomach parts were pinned in separate petri dishes. The corpus part of the stomach was separated from the other parts. The tissue was softly stretched and pinned facing the mucosal side up. The tissue was dissected in order to obtain LMMPs. The same procedures were performed with both parts of the stomach. Then the tissue was transferred to a sterile bench (Heto-Holten A/S). The obtained LMMP tissue samples from both regions were 3 times washed with sterile, ice-cold, carbogenated Krebs solution by placing them in further sterile glass petri dishes (Schott). Then the tissue samples were transferred in a small, sterile glass bottle filled with 4.5 mL sterile, ice-cold, carbogenated Krebs solution. Then the LMMPs were cut with scissors (14028-10; FST) as small as possible ($\sim 1 \text{ mm}^2$ pieces) to increase the surface for the enzymes. An enzymatic solution containing 0.9 mg/mL protease type I from bovine pancreas (Sigma, Steinheim, Germany), 1.2 mg/mL collagenase type II from Clostridium histolyticum (Gibco, Karlsruhe, Germany) and 3.7 mg/mL bovine serum albumin fraction V (Serva, Heidelberg, Germany) was added in the small glass bottle. Then the tissue was digested for 20-35 min at 37 °C in a shaking water bath (Gesellschaft für Labortechnik, Burgwedel, Germany). After the enzymatic digestion the solution was transferred to a 15 mL Falcon (Greiner Bio-One, Frickenhausen, Germany) and filled with sterile, ice-cold, carbogenated Krebs solution up to 14 mL. The Falcon was centrifuged (Z513K; Hermle Labortechnik GmbH, Wehingen, Germany) at 4 °C with 1000 rpm for 5 min. After centrifugation the supernatant was removed with a sterile glass pipette (Brand, Wertheim, Germany) and a vacuum pump (NKF Neuberger, Freiburg, Germany). The pellet was then re-suspended in Krebs solution and the same procedure was performed another two times. After the third centrifugation step sterile M199 Medium (GlutaMAX; Gibco) was added up to 10 mL. Then the cell suspension was transferred in a sterile glass petri dish to identify the myenteric ganglia under the light microscope (DMIL, 4x objective, phase contrast; Leica, Wetzlar, Germany). The identified ganglia were picked with a 20-200 μL pipette (Finnpipette; Thermo Scientific, Dreieich, Germany). The characteristic property of the ganglia was a shiny surface and the typical ganglia shape in which different somata and fiber tracts can be seen (Figure 2.1). To study the effect of different mechanical stimulation techniques different culture dishes were used. For the application of targeted stress with von Frey hair and for normal stress via hydrostatic pressure were used normal cell culture dishes (μ -dish 35mm, ibiTreat coated; Ibidi, Martinsried, Germany). For the application of stretch were special culture dishes used with an elastically supported surface (ESS) (μ -dish 35mm, ESS, uncoated, 28kPa; Ibidi) or self-made culture dishes with an elastic surface. These were previously coated before inoculation (description follows). For the application of shear stress micro channels (ibidi μ -Slide I Luer, ibiTreat-coating; Ibidi) were inoculated. Each culture dish was inoculated with 100-300 μL ganglia suspension. The dishes were then transferred into a CO₂-incubator (CB, 5% CO₂, 37 °C;

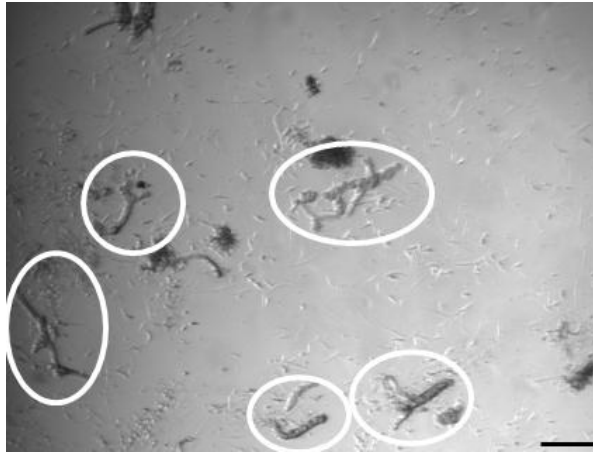


Figure 2.1: Cell suspension during the procedure of fishing myenteric ganglia. Ganglia are encircled in white. Scale bar: 100 μm

Binder, Tuttlingen, Germany). 3-4 h were waited and then culture medium M199 was added with the following additives: 1% Penicillin/Streptomycin (Gibco), 30 mM glucose, 50 ng/mL mouse nerve growth factor 7S (*Alomone Labs, Jerusalem, Israel*) and 10% fetal bovine serum (*Gibco*). The medium was changed every 2-3 days and supplied with 2 μM cytosine- β -D-arabinofuraside (*Sigma*) to suppress the proliferation of other cell types. It was waited for at least 6 days before performing an experiment.

2.1.2 Culture of human myenteric neurons

The culture procedures from guinea pig were adapted for human myenteric neuronal cultures (Kugler et al. 2012). All procedures were approved by the ethical committee of the Technische Universität München (1746/07; informed consent was obtained from all patients). The tissue samples for culturing were obtained from 90 patients (46x male, 41x female, for the remaining 3 there are no specifications available) undergoing surgery at the medical clinics of Freising and *Rechts der Isar* in Munich. The mean age of the patients was 66 ± 13 years (mean \pm standard deviation) (range 19-88 years). Diagnoses that led to surgery were 66 carcinoma, 6 polyp, 8 diverticulitis, 3 ileostoma and 7 various diagnoses. After surgery, tissue samples were placed in sterile, ice-cold, carbogenated Krebs solution (as described before and used also for all the other culture steps) and immediately transferred to our institute. After arriving the tissue samples were washed 3 times with sterile, ice-cold, carbogenated Krebs solution and then transferred in a sterile glass petri dish (*Schott*) with a sylgard surface (*Dow Corning*). For all the preparation steps that were not performed under the hood all instruments and surfaces were sterilized before. Surfaces were cleaned with 80% ethanol and Descosept AF (*Dr. Schumacher GmbH*). The tissue was roughly pinned with insect pins (26002-10; *FST*). The following dissection was done under a stereomicroscope (*Olympus*). If the resectate was still a closed piece of the intestine it was opened with scissors (14028-10; *FST*) and forceps (Dumostar #5; *Dumont*), otherwise it was directly pinned with the mucosa down. First

the tissue sample was separated in LMMP - circular muscle and submucosa – mucosa with fine scissors (15013-12; *FST*) and forceps (Dumostar #5; *Dumont*) that were also used for the following steps. Then the LMMP - circular muscle was stretched pinned with the circular muscle down. To obtain enough material for culturing used pieces were at least 2 cm². In a first step the serosa was removed. Then the tissue was turned around and the circular muscle was carefully removed. During the preparation the sterile, ice-cold, carbogenated Krebs solution in the petri dish was changed every 10 min. After the LMMP lay open the tissue was transferred to the sterile bench (*Heto-Holten A/S*). There the tissue was pinned in a new sterile petri dish and then washed 3 times with sterile, ice-cold, carbogenated Krebs solution. The tissue was cut in ~ 0.5 cm² pieces and transferred in a sterile small glass bottle. From there on the procedures were the same as in the guinea pig except that the digestion time was extended; in mean it was 62 ± 18 min (mean ± standard deviation) (range 20-117 min).

2.1.3 Culture of dorsal root ganglia neurons of guinea pig

Cell culture procedures from above were adjusted for primary culture of DRG neurons. After removal of the intestinal tissue for other experiments, all the internal organs were removed. Then the fur of the guinea pig was removed and the spinal column was isolated. The spinal column was washed with sterile Krebs solution and stored in a sterile bottle filled with Krebs solution. The spinal column was then cut into two pieces and pinned in big sterile petri glass dishes (150 x 25 mm; *Schott*) with sylgard (*Dow Corning*). The spinal column was pinned with needles facing the dorsal part up. The dissection was performed under a stereomicroscope (*Olympus*) with different forceps (Dumostar # 5; *Dumont* and 1103-13; *FST*) and scissors (14574-11; *FST*). Then the muscle layers covering the spinal column were removed. The spinal column was opened to reveal the spinal cord. Two cuts through the top of the spinal column on either part about 1 mm wide were made. Then part of the bone was removed. We removed as much bone as needed until DRG were visible along either side of spinal column near the bottom. The DRG were taken with forceps (Dumostar # 5; *Dumont*) and the nerve roots were cut on either side with microscissors (14058-11; *FST*). All DRG were collected in a small glass bottle. The DRG were then transferred to the sterile bench (*Heto-Holten A/S*). Further proceedings were as for the other cultures. The incubation time was 35-50 min. After the last centrifugation step the pellet was re-suspended in 2.4 – 3.6 mL medium. Each culture dish (μ-dish 35mm, ibiTreat coated; *Ibidi*) was inoculated with 400 μL of the cell suspension. Cultures grew for at least 7 days until the experiment.

2.1.4 Culture of sympathetic chain ganglia neurons of guinea pig

To isolate SCG neurons we handled the guinea pig as for the DRG culture, but the spinal column was pinned with the ventral side up. The cell bodies of the SCG lay close to and on either side of the spine in long chains. The preparation was done under the stereomicroscope (*Olympus*) with forceps (Dumostar # 5; *Dumont*) and rough and fine scissors (14574-11 and 14058-11; *FST*). To identify the SCG the sympathetic fibers

were followed from the rips close to the spinal cord and it was looked for a long chain crossing these fibers lateral of the spine. The whole chain was taken in once on both sides and transferred to a sterile glass bottle filled with sterile Krebs solution. All further proceedings were done as for the DRG culture. Cultures were grown for at least 6 days until the experiment.

2.2 Production of elastic surface culture dishes

The preparation of bead micropatterned elastic substrates was performed as described previously (Kirchenbuchler et al. 2010; Merkel et al. 2007). To produce the elastic substrate a two-component silicone rubber (polydimethylsiloxane, PDMS) formulation (Sylgard [®] 184; *Dow Corning*) was used composed of a base material and cross-linker. In the experiments a mixing ratio of base and cross-linker of 40:1 (w/w) was used. The two components were mixed carefully with a plastic spatula in a 50 mL Falcon tube (*Greiner Bio-One*). The developed bubbles were eliminated by placing the Falcon with the substrate in the sonicator. The remaining bubbles disappeared after leaving it overnight at -20 °C. A silicon waver with a special micropatterned surface (produced by the research center Jülich, ICS-7) were dried at 135 °C for 10 min. This silicon waver with a silanized surface had a microstructure consisting of 2 µm dots arranged in a square lattice of 3.5 µm lattice constant. 10 µL of the 40:1 elastic substrate per culture dish were mixed with 0.25 – 0.5 µL FluoSpheres (green, Ø 0.2 µm, Crimson; *Invitrogen*). The labeled substrate was then applied with a plastic spatula at the silicon waver, the excessive substrate was whipped away with lens tissue, the substrate was left only in the micropatterned surface of the silicon waver (below 1 µm thickness). Afterwards one drop of the unlabeled substrate was applied in the middle of the silicon waver. As spacers 80 µm coverslips cut in pieces with ~ 5 mm width were placed at two opposite sides of the silicone waver. Then an 80 µm coverslip was placed on top of the drop. To press the silicon waver and the coverslip together a microscope slide was placed over the coverslip and then silicon waver and slide were fixed together with book clips at the place of the spacers (Figure 2.2).

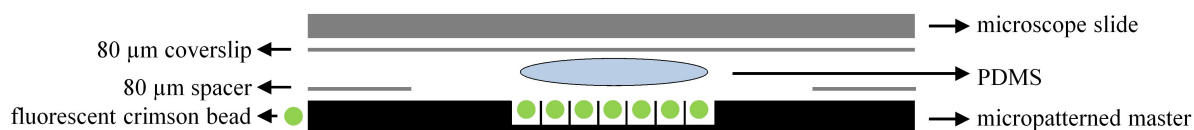


Figure 2.2: Schematic illustration of the components used for the production of the self-made elastic surface culture dishes.

With this technique a monolayer of fluorescent beads on top of the elastic surface was obtained. The so prepared surfaces were dried 18 - 20 h at 50 °C. After the drying time the clips and the microscope slide were removed. Then the master chip was carefully removed in an isopropanol filled petri dish with the use of a scalpel. The 80 µm thick elastic surface with a fluorescent bead monolayer in the upper layer was then on top of

the 80 μm thick coverslip. The coverslip with the elastic surface was glued with PDMS with a mixing ratio of 10:1 to a plastic petri dish (\varnothing 3.5 cm) with predrilled 1.5 cm holes and then dried for 2 h at 50 $^{\circ}\text{C}$. As described elsewhere this specific elastic surface had a Poisson's ratio of 0.5 and a Young's modulus of 80 ± 14 kPa (Cesa et al. 2007).

For coating this hydrophobic surface different coating procedures were tested:

- 0.01% Collagen I (*Sigma-Aldrich*) for 2 h at room temperature (RT)
- 0.01% Poly-L-Lysine (*Sigma-Aldrich*) for 1 h at RT
- 0.05 mg/mL Laminin (*Boehringer, Mannheim, Germany*) for 1 h at 37 $^{\circ}\text{C}$, 5% CO_2
- 0.05 mg/mL Fibronectin (*BD Biosciences*) for 1 h at RT
- 15 $\mu\text{g}/\text{mL}$ Collagen IV (*BD Biosciences*) 1 h at RT
- 5 $\mu\text{g}/\text{cm}^2$ Poly-D-Lysine (*BD Biosciences*) and 5 $\mu\text{g}/\text{cm}^2$ human extracellular matrix (*BD Biosciences*) for 1 h at 37 $^{\circ}\text{C}$, 5% CO_2

2.3 Ultrafast neuroimaging technique

2.3.1 Principle of the ultrafast neuroimaging technique

To record neuronal responses the ultrafast neuroimaging technique was utilized in combination with a voltage- or Ca^{2+} - sensitive dye (Figure 2.3).

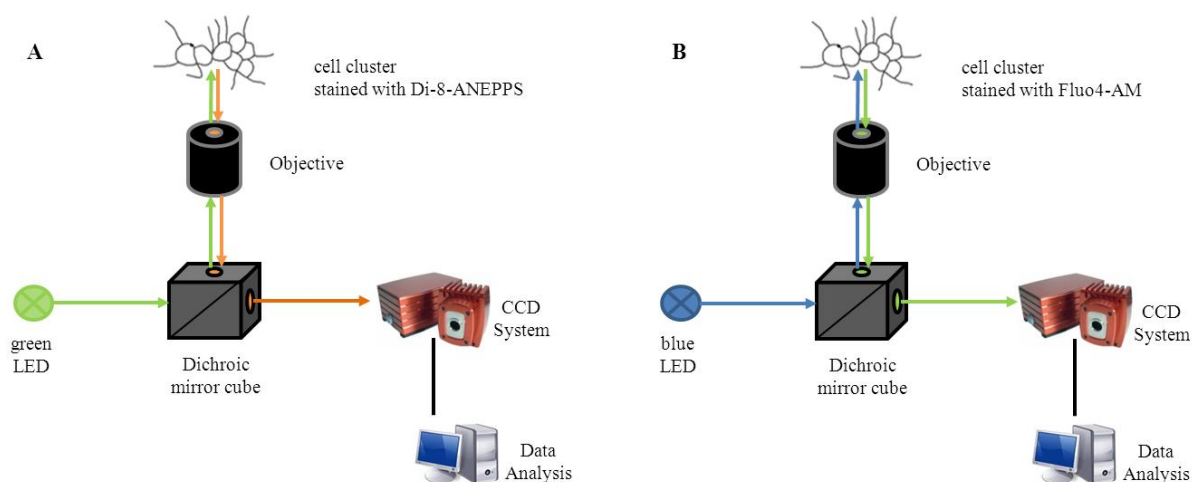


Figure 2.3: Schematic illustration of the neuroimaging set-up used to record from primary cultured neuron clusters stained with Di-8-ANEPPS (A) or Fluo4-AM (B).

This technique has been described previously in detail (Neunlist et al. 1999; Scheumann et al. 2002; Michel et al. 2011). As a voltage-sensitive dye Di-8-ANEPPS (1-(3-sulfonato-propyl-4-[β -[2-(di-n-octylamino)-6-naphthyl]vinyl]pyridinium betaine; *Molecular Probes, Eugene, OR, USA*) was used. Di-8-ANEPPS is incorporated into the cell membrane and changes its absorption and emission spectra with the membrane potential (Fromherz and Lambacher 1991). The fluorescence change is reflecting the real time membrane potential change and thereby action potentials can be detected. This fast voltage changes expressed in fluorescence changes can be recorded with a cooled charged-coupled device (CCD) chip technology. As a Ca^{2+} -sensitive dye Fluo4-AM (*Invitrogen*) was used that enters the cell. The Ca^{2+} -sensitive dye binds free cytosolic Ca^{2+} , and increases its fluorescence intensity if binding to Ca^{2+} . Not only neurons show an increase of the intracellular Ca^{2+} ($[\text{Ca}^{2+}]_i$) level if activated but also non-neuronal cell types as enteric glia and fibroblasts. The $[\text{Ca}^{2+}]_i$ level can rise, because of Ca^{2+} release from $[\text{Ca}^{2+}]_i$ stores or via extracellular influx through Ca^{2+} -channels. The experiments provide us with electrical data that are in this neuroimaging technique transferred into optical data. Every neuron in the field of view is projected on numerous photodiodes. This photodiodes can be separately marked and thereby the activity of multiple neurons can be simultaneously recorded and analyzed. The main advantage of the ultrafast neuroimaging technique is that the activity of a whole network can be simultaneously recorded with high spatial ($\sim 4 \mu\text{m}^2$ per pixel with the 100x objective) and temporal (up to 10 kHz) resolution. Furthermore, it is a non-invasive method providing information from all neurons in the field of view with no change of the physiological properties of the neurons. The voltage-sensitive dye imaging technique gives information about the activity state of neurons and shows thereby clear bursting patterns. It is a reliable tool to record fast neuronal responses. On the other hand, the Ca^{2+} -sensitive dye imaging technique can record activity states of different cell types. Furthermore, this technique is able to detect slow changes and is useful to record long lasting responses of neurons.

2.3.2 Staining and data acquisition

For staining with the voltage-sensitive dye a stock solution of Di-8-ANEPPS of 15 mM in a 50% / 50% mixture of DMSO “extra dry” (*Acros Organics, Geel, Belgium*) and Pluronic F-127 (20% in DMSO; *Invitrogen*) was used. For the 1 mM stock solution of the Ca^{2+} -sensitive dye 1 mg of Fluo4-AM was dissolved in 910 μL DMSO “extra dry” (*Acros Organics*). The dishes were placed in an appropriate special custom-made Plexiglas holder. The thickness of the bottom of the culture dishes was 180 μm and directly usable for high resolution microscopy with an inverted microscope. The culture medium was removed with a plastic Pasteur pipette and a 10 μM Di-8-ANEPPS / 10 μM Fluo4-AM solution diluted with HEPES modified Krebs solution (in mM: 1 MgCl_2 , 2 CaCl_2 , 150 NaCl , 10 HEPES, 10 Glucose, 5 KCl + 1.25 Probenecid for Ca^{2+} -imaging) was added and incubated for 15-20 min at RT in the dark. After incubation the staining solution was for 10 min washed out with a 37 $^\circ\text{C}$ warmed HEPES buffer (+ 1.25 mM Probenecid for Ca^{2+} -imaging) via a peristaltic pump (Minipuls® 3; *Gilson, Middleton, WI, USA*) connected with plastic tubes (Tygon R3607) to the culture dish. During the

experiment the culture dish was continuously perfused with this solution from a 500 mL reservoir at a rate of 12 mL/min. The experiments were performed with an inverted microscope (Zeiss Axio Observer.D1 microscope; *Zeiss, München, Germany*) and the NeuroCCD imaging system from RedShirt Imaging (*Decatur, USA*). The NeuroCCD imaging system was build up with a fast CCD camera and the Neuroplex software for acquisition and analysis. The set-up was equipped with a modified Cy3 filterset (545±15 nm excitation interference filter, 565 nm dichroic mirror and 580 nm emission; *AHF Analysentechnik, Tübingen, Germany*) to detect the Di-8-ANEPPS signals. The voltage-sensitive dye was excited with a green LED (LE T S2W and LE T A2A; *Osram, München, Germany*). Appropriate for detection of Fluo4-AM was a FITC filterset (HD475/35 excitation, BS499 dichroic mirror, HC530/43 emission, Brightline FITC HC Basic BP-Filterset; *AHF Analysentechnik*). The Ca²⁺- sensitive dye was excited by a blue LED (3W blue and 3W royal blue, Philips Lumiled; *Conrad, München, Germany*). To find clusters a 10x objective (NA=0.25; *Zeiss*) was used and for recording the neuronal responses a 100x oil immersion objective (NA=1.35; *Olympus*) was utilized. The relative fluorescence changes ($\Delta F/F$) of the dyes are linearly related to changes in the membrane potential (Neunlist et al. 1999) or the [Ca²⁺]_i and are detected with a CCD camera made up of 80 x 80 pixels. The frame rate was between 125 Hz and 10 kHz. The optical signals were further processed with the Neuroplex software (*RedShirt Imaging*). To detect the signals of individual neurons the image of the cluster and the signals were overlaid (Michel et al. 2005).

2.4 Testing viability of myenteric neurons

The integrity of the neurons was proven by application of nicotine (100 µM; *Sigma*) through pressure ejection from a glass pipette with a fine opening (~ 8 µm). The pipette was positioned ~ 500 µm from the cell cluster and the ejection induced no visible mechanical deformation of the cells. Excitation of the neurons by nicotine proved their integrity. Instead of nicotine sometimes also 50 mM KCl was used as a standard stimulus. Furthermore electrical stimulation proved the integrity of neurons if EPSPs can be observed. Either carbon fiber electrodes with 50 mA were used or platinum wire electrodes with 5-50 mA.

Acquisitions without any stimulus were performed to check for spontaneously active neurons.

2.5 Mechanical stimulation

As a von Frey hair a single carbon fiber strand (Ø 8 µm; *Conrad*) was used that was inserted by hand in a glass capillary (0.58 x 1.00 x 100 mm; *Science products, Hofheim, Germany*) and then pulled (Puller P87; *Sutter instruments, Novato, CA, USA*)(Figure 2.4).

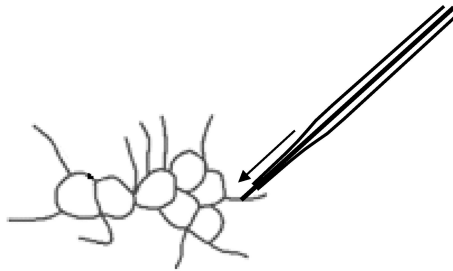


Figure 2.4: Schematic drawing of a stimulation of a neuronal cluster with a von Frey hair made of carbon fiber.

The carbon fiber was cut that it extended the pipette 400 - 900 μm .

To use the carbon fiber as an electrode additional to the previous steps Wood's metal and then a copper wire were inserted in the pulled pipette. By melting the Wood's metal the carbon fiber and the copper wire got connected. The tip of the carbon fiber outside the glass pipette was dipped into nail polish for isolation. To stimulate a nerve fiber 50 mA were used.

To stimulate the neurons the ultra-fine tool was controlled with a motorized step micromanipulator (PM-10 with DC-3K; Märzhäuser, Wetzlar, Germany), which allows for fine movements (step 1 - 10 μm). With this tool it was possible to obtain a targeted stimulation of only part of the cluster or even single neurons. The maximal exerting force was $436 \pm 49 \mu\text{N}$. The force was measured by pressing the carbon fiber with a 10 μm piezo step perpendicular on a force transducer (MLT1030/a; AD instruments Ltd, Oxford, UK). 3 different carbon fibers were tested each pressed 3 times with a 10 μm step on the force transducer (AD instruments Ltd). To calibrate the obtained values water drops with 5 μL , 10 μL , 25 μL , 50 μL and 100 μL were applied each 3 times on the force transducer (AD instruments Ltd). The force could be then calculated (Equation 2.1). With this values a straight calibration line was obtained with the equation $y = 2,807.4 x$. From the calibration line the force of the carbon fiber was determined.

$$F = m * g \quad (2.1)$$

F: force

m: mass

g: $9.81 \frac{\text{m}}{\text{s}^2}$

The angle of the carbon fiber to the culture dish bottom during the experiment was $74 \pm 4^\circ$. With this stimulation tool it was possible to stimulate only a small membrane region ($\sim 50 \mu\text{m}^2$) of either the neuronal soma or the neurite. At the beginning of the recording after 50-400 ms the carbon fiber was pressed down onto the target. The recording time was either 2 s, 5 s or 10 s. The target for mechanical stimulation was differently chosen depending on the experimental design.

2.5.1 Normal stress

Two different techniques were used to apply normal stress on the cultured neurons to mimic the deformation occurring during phasic and tonic contractions.

Hydrostatic pressure

Hydrostatic pressure was used to mimic phasic contractions. A short lasting (200 ms) pulse of the same HEPES modified Krebs solution as superfused during the experiment was ejected with a micropipette (Figure 2.5).

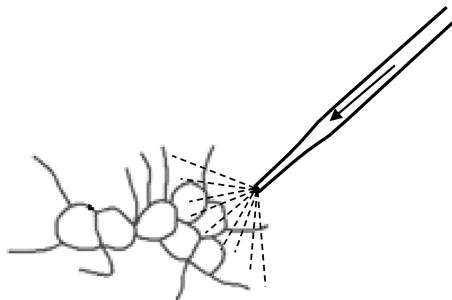


Figure 2.5: Schematic drawing of a stimulation of a neuronal cluster with hydrostatic pressure via micropipette.

During the pulse the maximal exerting force was immediately reached and held for the pulse duration. The micropipettes had a tip opening of $\sim 10 \mu\text{m}$. The pipette was placed $\sim 80 \mu\text{m}$ away from the neuronal cluster in the parallel plane. The distance was so adjusted that the whole cluster was visible deformed. The micropipette was connected to a microejection system (PDES-2L; *npi electronic, Tamm, Germany*; A310 Accupulser; *world precision instruments, Sarasota, USA*). With this microejection system the pressure was adjusted to 0.7 bar and 1.0 bar. The applied force varied with the exact position of the pipette and the tip opening. With a pressure of 0.7 bar a force of $45 \pm 35 \text{ nN}$ was exerted, whereas with 1.0 bar $88 \pm 63 \text{ nN}$. The force was measured with an atomic force microscopy (AFM) cantilever (spring constant: 0.12 N/m and surface area: $12,222 \mu\text{m}^2$, Standard Silicon Nitride Probes; *Veeco Instruments Inc., Plainview, NY, USA*). The exerting force was deflecting the AFM cantilever. The force values were obtained from 3 different pipettes with at least 12 individual deflections per pressure. The analysis of the deflection was done with Igor Pro 6.22A (*Wavemetrics Inc., Lake Oswego, OR, USA*) in a subpixel range based on intensity (Thevenaz et al. 1998). The angle of the micropipette to the culture dish bottom was 60° . Application of hydrostatic pressure resulted in normal and shear stress. The calculation of the proportion of normal force to shear force with the tangent showed that the normal force exceeds the shear force by 73% (Figure 2.6 and Equation 2.2). Therefore the predominant stress modality is normal stress.

$$\tan 60 = 1.73 = \frac{\text{normal force}}{\text{shear force}} \quad (2.2)$$

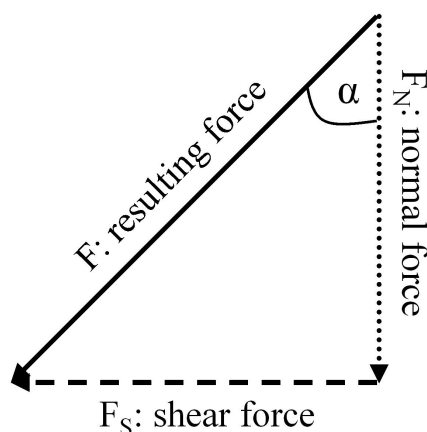


Figure 2.6: Illustration of the resulting force by its decomposition in normal force and shear force. The angle correlates to the angle of the micropipette to the culture dish bottom.

To examine neuronal properties in a paired manner and to exclude differences, because of different application parameters, the micropipette was positioned once per cluster and two consecutive applications were done. In this way the reproducibility and force strength dependency of the response to hydrostatic pressure was examined. For most experiments the stimulation parameter for pulse duration was 200 ms and recording time 2 s. To test if variation of the pulse duration had an influence on the response longer applications of 1 s and 2 s were made with a recording time of 3 s.

In another set of experiments was the fluid applied in different angles onto the cluster. Therefore a custom-made arch was used on which a micromanipulator with a pipette holder was fixed (*Narishige, Tokyo, Japan*; Figure 2.7). Angles of 45 ° and 90 ° were tried with a distance of $\sim 150 \mu\text{m}$ to the cluster. With the application angle of 90 ° only normal stress is applied and of 45 ° normal stress and shear stress have the same strength (Equation 2.3).

$$\tan 45 = 1 \quad (2.3)$$

$$\text{normal force} = \text{shear force}$$

Stretch

As another kind of normal stress stretch was applied to mimic tonic contractions. Two different methods were used to induce stretch.

For the first method the ESS-dishes (*Ibidi*) were used. To induce a deformation in the nearby cluster a blunt glass pipette (tip diameter 1-2 μm) was poked 10 μm into the surface 5-20 μm away from the cluster. The glass pipette was connected to a piezo-driven manipulator (PM-10 with DC-3K; *Märzhäuser*) and had an angle of $\sim 70^\circ$ to



Figure 2.7: Custom-made arch for application of hydrostatic pressure with different angles used on the experimental set-up.

the bottom surface.

For the second stimulation technique special self-made culture dishes with elastic surfaces were used. In order to induce decaying deformation fields at the neuronal clusters an elastic substrate was used that was deformed with the tip of a gauge needle ($\text{\O} 0.9 \text{ mm}$; *Heiland, Hamburg, Germany*; Figure 2.8).

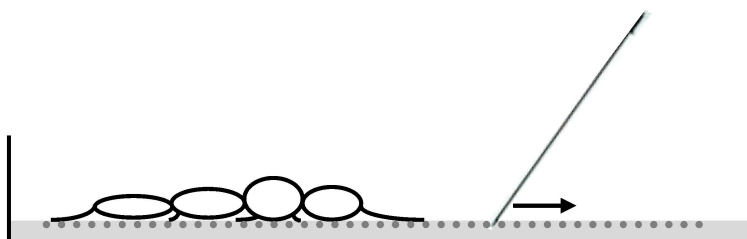


Figure 2.8: Schematic drawing of the application of stretch on cultured neurons adherent to a micropatterned elastic surface by side movement of a gauge needle dipped into the elastic surface.

The gauge needle was fixed at the piezo-driven manipulator (*Märzhäuser*). To avoid touching neurites surrounding neurons the distance to the cluster varied between 20–80 μm . The angle of the needle to the surface was $\sim 70^\circ$. To stretch the cell cluster the needle was poked 10 μm into the elastic surface and then moved 10 μm sideways away from the cluster. Additional high resolution pictures (AxioCam Icm 1; *Zeiss*) of the fluorescent beads in the elastic surface and of the cell cluster in the same position were taken for the later analysis of the decaying deformation fields. Pulling the needle induced a decaying deformation field in the whole cluster. The needle was moved at the

beginning of a 5 s recording and stayed then for the rest at the same position. Thus with this stimulation technique a short dynamic and a long sustained phase was induced. The reproducibility of stretch was examined by two consecutive applications of the same stimulus by retracting the needle and performing the sideways step again.

2.5.2 Shear stress

Shear stress was applied by fluid flow through a micro channel. Micro channels with different dimensions (ibidi μ -slide I 0.2, 0.4, 0.6, 0.8 Luer, ibiTreat-coating; *Ibidi*) were tested to achieve an appropriate shear stress range. Later on only one type of micro channels (ibidi μ -slide I 0.4 Luer, ibiTreat-coating; *Ibidi*) was used (Figure 2.9).

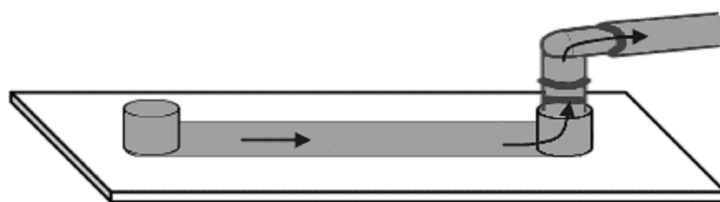


Figure 2.9: Schematic drawing of the stimulation of cultured neurons with shear stress by fluid flow through a micro channel.

This micro channel had the following parameters: height: 400 μm , width: 5 mm, length: 50 mm and volume: 100 μL . To extend the reservoir of the channel on one side a syringe without plunger was connected. The other reservoir was connected to the aspirating tube of the peristaltic pump (*Gilson*). The flow rate was defined by aspirating a defined volume with a certain speed of the peristaltic pump. With the flow rate the shear stress can be calculated (Equation 2.4).

$$\tau = \frac{6\mu Q}{h^2 w} \quad (2.4)$$

fluid viscosity: $\mu=8.5 \cdot 10^{-4} \text{ Pa s}$

flow rate: $Q \left[\frac{\text{m}^3}{\text{s}} \right]$

height of the channel: $h= 400 \mu\text{m}$

width of the channel: $w= 5 \text{ mm}$

The flow rates were adjusted to obtain a shear stress range from 0.2 to 0.8 Pa. The force obtained with this shear stress range was 0.4 - 1.6 μN . This stimulation technique stressed all neurons in the micro channel at the same time. For the preliminary experiments the pump was started by hand during the recording. Later on the stimulus pulse was controlled with the Accupulser system (A310 Accupulser; *world precision instruments*) and lasted for 2 s. The recording time was 3 s.

2.6 Measurements of cell length changes induced by stretch

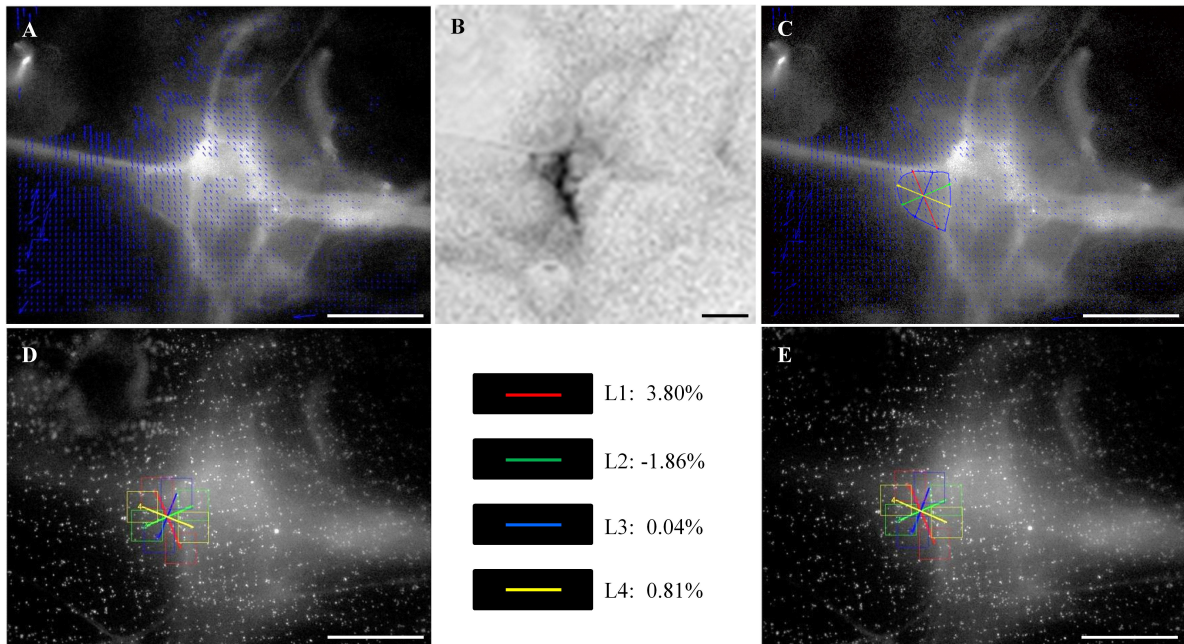
A bead tracking software was used to analyze the decaying deformation field induced by stretch. The micropatterned elastic surfaces were the basis for the analysis. Pictures of the bead surface in the position of the cluster of interest were taken before pulling the surface and after in the stretched state. The images obtained with the high resolution camera were processed with Image J (1.45m; *National Institutes of Health, USA*) to obtain a stack of the cluster of interest and the bead positions before and after. A software on the basis of MATLAB (8.2 R2013b; *MathWorks, Natick, MA, USA*) to analyze the deformation was written in the research center Jülich. First the bead pictures were smoothed with a binomial filter (3 x 3 pixels). Then mask areas of 49 x 49 pixels were created in the bead picture of the relaxed state. These mask areas were generated in regular distances every 20 pixels. In the bead pictures of the stretched state these mask areas were searched using a cross-correlation. The bead position in the relaxed state and the stretched state were compared and on this basis a deformation field was generated. The deformation of the beads was displayed with arrows pointing to the stretching direction (Figure 2.10 A).

A cluster picture of the same field of view was used to mark the neuron of interest. Mechanosensitive neurons previously identified by an independent component analysis (ICA, see section Data analysis and statistics) were the basis for marking the neurons (Figure 2.10 B). The somata were encircled with a polygon and the midpoint of the soma was marked with a cross. The first line was set in direction of the deformation field as calculated before. Additional 3 lines were automatically plotted in 45 ° distance to the first line (Figure 2.10 C). The length change of the line defined by the points of intersection with the polygon was then calculated. Therefore from the endpoints of the lines in the relaxed state (bead picture) masks of 99 x 99 pixels were generated (Figure 2.10 D). These masks were cross-correlated with the stretched state (bead picture) (Figure 2.10 E). As an output the line length before and after was obtained. The relative and absolute length change was calculated.

The maximum stretch of a neuron was represented by the biggest change with a positive value. Whereas, the maximum compression of a neuron was expressed by the biggest change with a negative value. For every mechanosensitive neuron a summed (\sum) stretch was calculated by summing all positive values and a \sum compression by summing all negative values.

2.7 Pharmacology

To block synaptic activity in the culture 0.02 μ M ω -conotoxin GVIA (*Alomone Labs*; specific blocker of voltage dependent N-type Ca^{2+} channels; irreversible action) (Cruz and Olivera 1986; Cunningham et al. 1998) diluted in 50 mL HEPES modified Krebs solution was superfused.



2. MATERIAL AND METHODS

10 μM AP-18 (*Sigma*) diluted in 50 mL HEPES modified Krebs solution was superfused for 20 min to block TRPA1 channels (Petrus et al. 2007).

75 μM Tranilast (*Selleck Chemicals, Houston, TX, USA*) diluted in 50 mL HEPES modified Krebs solution was superfused for 30 min to block TRPV2 channels (Mihara et al. 2010).

To destabilize microtubules 1 μM cytochalasin D (*Sigma*) was added to the culture medium M199 and incubated for 28-45.5 h (according to Vanden Berghe et al. 2004).

For local blockade of nerve activity TTX (*Biozol Diagnostica, Eching, Germany*) was applied, which blocks voltage gated fast sodium channels (Colquhoun and Ritchie 1972; Narahashi et al. 1964). The concentration in the spritz pipette was 10 μM . To achieve only a local blockade of the neurites TTX was applied with a micropipette. This pipette had a fine tip opening of $\sim 3 \mu\text{m}$ and was positioned $\sim 5 \mu\text{m}$ away from the fiber tract. With this technique a local TTX block was achieved on a small area on the fiber tract (Figure 2.11).



Figure 2.11: Picture of the experimental set for the local blockade of neuronal activity with tetrodotoxin (TTX). The neuronal cluster is encircled in white, the micropipette filled with 10 μM TTX is marked with a black arrow and the carbon fiber is marked with a white arrow. Scale bar: 20 μm .

The distribution of the substance was proven by application of fast green (*Sigma*; data not shown). TTX was applied 3 times for 60 s. As control for neuronal blockade the fiber tract was electrically stimulated just behind the TTX pipette with a carbon fiber electrode. Electrical stimulation always resulted in a compound action potential, a single peak. The nerve fiber was stimulated with 50 mA. The neurite was mechanically stimulated with the carbon fiber just above the microelectrode and also electrically stimulated before, during and after TTX application (10 min washout, adequate only for local application).

To reveal if mechanosensitive responses can be modulated adenosine (*Sigma*) was used, which causes hyperpolarization of myenteric neurons (Zafirov et al. 1985). A final concentration of 0.5 mM adenosine dissolved in HEPES modified Krebs solution was locally applied as described for TTX for 10 s.

2.8 Immunohistochemistry

After the experiments the cultured neurons were fixed overnight at 4 °C. For human culture a fix solution was used containing 4% phosphate buffered formaldehyde. For guinea pig the fix solution contained additionally 0.2% picric acid. After fixation the dishes were washed (3 x 10 min) with phosphate buffer. For long time storage phosphate buffered saline (PBS) with NaN_3 was added to inhibit the growth of microorganisms. If the cultures contained PBS/ NaN_3 the dishes were washed (3 x 10 min) with PBS. A blocking serum containing PBS with 0.5% Triton X-100, 0.1% NaN_3 and 4% horse serum was incubated for 1 h at RT. This was followed by 12 h incubation with 200 μL solution containing the primary antibody (Table 2.1). A washing step with PBS followed (3 x 10 min). Then the secondary antibody (Table 2.1) was incubated for 1.5 h. This step was followed by 3 x 10 min washing steps with PBS. To reduce the auto fluorescence cultured neurons were treated with 1 mM CuSO_4 in 50 mM ammonium acetate buffer for 1.5 h. Before and after application of CuSO_4 the culture dish was shortly washed with distilled water. An additional PBS (3 x 10 min) washing step followed. To mount the cells they were cover slipped with a solution containing PBS (pH 7.0) and 0.1% NaN_3 with 80% glycerol (cover slip \varnothing 20 mm; *Menzel, Braunschweig, Germany*). For examination the culture dishes were turned around and the cells analyzed through the bottom. An epifluorescence microscope (BX61W1; *Olympus*) equipped with appropriate filter blocks was used. The acquisition system consisted of a video camera connected to a computer and was controlled by a Scion image software (Cell P; *Scion Corp., Frederick, MD, USA*).

2.9 Transfection protocol

To transfect myenteric neurons of the small intestine from guinea pig 6-well plates (*Greiner BIO-One GmbH*) were inoculated and grown for at least 7 days. 3 culture dishes (*Ibidi*) were pre-equilibrated with culture medium M199 at 37 °C, 5% CO_2 . Just before transfection the neurons were detached from the 6-well plate with 0.25% trypsin (*CC-Pro, Oberdorla, Germany*). First the medium was removed, and then the 6-well plate was washed twice with PBS (RT). Afterwards trypsin was incubated for 5 min at 37 °C. The process was stopped by adding 1 mL pre-warmed culture medium M199. The detached cells were carefully transferred to a 15 mL Falcon tube, if needed more medium was added to transfer all cells. The cell suspension was centrifuged for 5 min at 80 g, RT. Afterwards the supernatant was removed. The cell pellet was re-suspended in 300 μL

Table 2.1: List of antibodies used for staining primary cultured neurons.

primary antibody	dilution	company
sheep anti-PGP 9.5	1:20,000	The Binding Site
rabbit anti-calbindin	1:1,000	Chemicon
mouse anti-SOX	1:10	Prof. Wegner
rabbit anti-SK3	1:7,500	Alomone labs
rabbit anti-c-kit	1:100	Oncogene
mouse anti-smoothelin	1:100	van der Loop
mouse anti-Vinculin	1:2,000	Sigma
mouse anti-Vimentin clone 9	1:500	Dako
rabbit anti-Piezo1	1:10,000	Novus Biologicals
rabbit anti-Piezo2	1:2,000	Novus Biologicals
secondary antibody	dilution	company
donkey anti-sheep Cy5	1:500	Dianova
donkey anti-sheep Cy2	1:200	Dianova
donkey anti-mouse Cy2	1:200	Dianova
donkey anti-rabbit Cy2	1:200	Dianova
donkey anti-rabbit Cy5	1:500	Dianova
donkey anti-rabbit AMCA	1:50	Dianova

nucleofector solution (from AMAXA™ Basic nucleofector kit primary neurons; *Lonza, Basel, Switzerland*). As a first step only transfection controls were used. 12 μ L pmax green fluorescent protein (GFP) (from AMAXA™ Basic nucleofector kit primary neurons; *Lonza*) was added for transfection. 100 μ L of the cell suspension was added to each transfection cuvette (from AMAXA™ Basic nucleofector kit primary neurons; *Lonza*). Different programs of the Amaxa Nucleofector (Nucleofector™ 2b device; *Lonza*) were used: C-13 (2x); O-03; O-05; G-13; A-33

The cuvette with the cell / DNA suspension was inserted in the cuvette holder and the cells were electroporated with the chosen program. Immediately after transfection 500 μ L pre-warmed culture medium was added. Afterwards the cell suspension was gently transferred to the prepared culture dishes with the supplied pipettes (from AMAXA™ Basic nucleofector kit primary neurons; *Lonza*). After 2 - 3 days the adhered cells could be analyzed under the fluorescent microscope with the Cy2 filterset.

2.10 Data analysis and statistics

For analysis of the neuronal mechanical responses in addition to Neuroplex (*RedShirt Imaging*) an “Independent Component Analysis (ICA)” in Igor Pro 6.22A (*Wavemetrics Inc.*) and R (*R Core Team 2013*) were employed. With the ICA method it was possible to separate multivariate signals into additive subcomponents. It has been already applied

to neuroimaging data (Brown et al. 2001). This method was needed because of the following reasons: 1) due to the limited spatial resolution of the high speed camera (CCD camera; *RedShirt Imaging*) the chance of detecting signals of two or more neurons simultaneously on a single pixel is relatively high. Separating these signals manually is subjective and prone to error. 2) Following the signals from the soma to all neurites is generally not possible because the signal to noise ratio in the neurites is declining rapidly. Furthermore, if neurites of different neurons run together it is impossible to identify the origin of the different signals manually. Another advantage of the ICA is that artifacts from mechanical movements during the stimulation are removed from the traces. The trace derived from the ICA was calculated by “mixing” the original signals from all detectors to get “sources” that are statistically maximally independent. The contribution of every source to each pixel was in addition calculated. This second calculation yielded to an image, in which all pixels in the field of view with the same discharge pattern were shown (Figure 2.12).

The image obtained with the ICA revealed the soma with its corresponding neurites that conduct the electrical signal. The signals could be then followed from the site of mechanical stimulation to the soma and its projecting neurites. Thereby it could be clearly detected if the site of mechanical stimulation is itself the point where mechanotransduction occurred.

All data obtained with voltage- sensitive dye imaging were further analyzed with the ICA.

To count the action potentials in the ICA given traces the Macro Neuromatic (*Think Random, London, UK*) in Igor Pro 6.22A was employed. The traces were loaded with this software and then for every trace a threshold for counting peaks was individually set. The peaks that were counted as action potentials were controlled visually with an enlargement tool in order to recognize a clear action potential shape. Neuroplex traces were obtained by averaging the relative change in fluorescence from the pixels on the neuronal cell body. These traces could contain also signals from other “sources”, because of neurites running under the neuronal cell body (Figure 2.12). All traces shown in the figures were ICA traces if not else indicated.

For the overall spike frequency the number of action potentials was divided by the time from the start of mechanical stimulation to the end of the recording. For calculation of the burst spike frequency the number of action potentials was divided by the time from the first to the last action potential fired. For stimulation techniques that resulted in a dynamic and sustained phase this two phases were further analyzed separately. The time points of the two phases were determined by the trace below the scan movie of the Neuroplex software obtained from the point of mechanical stimulation. This trace represents the mean change of fluorescence of the given spot. The point of mechanical stimulation was manually chosen from the visible movement induced by the carbon fiber placing. The mechanical stimulation itself caused a change of fluorescence. All data were presented as median with 25% and 75% quartiles, because most data were not normally distributed. If data are displayed in another way this is indicated. For the targeted stimulation with the carbon fiber (in the myenteric, DRG and SCG neurons) the % of mechanosensitive spots was calculated on the overall number of stimulated spots. For

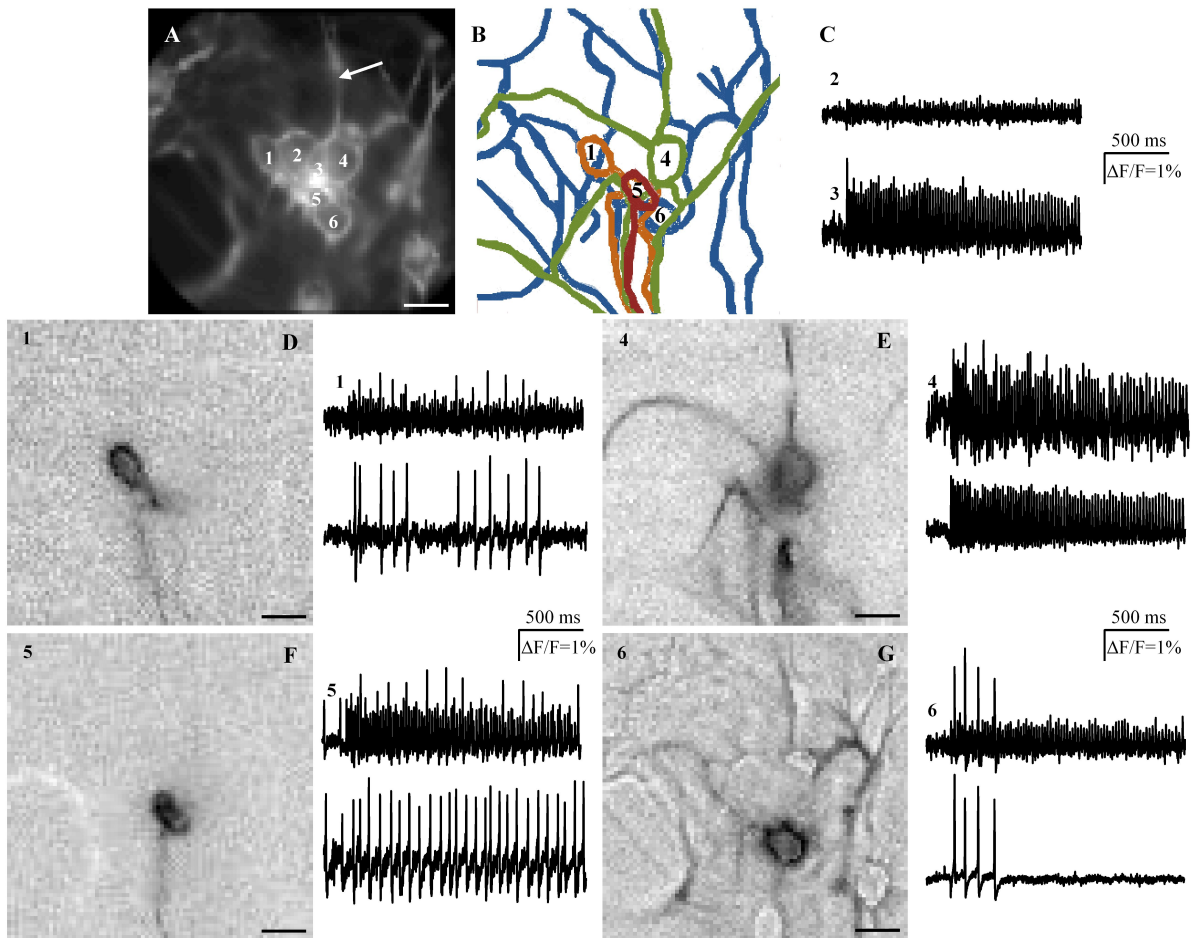


Figure 2.12: Advantages of the signal detection of single neurons with the independent component analysis (ICA). (A) shows a picture of a cluster with 6 neurons, which is stimulated on a fiber tract (white arrow) with the carbon fiber. In (B) the cluster is redrawn following the ICA images of the responding neurons. Neuron 1 is displayed in orange, neuron 4 in green, neuron 5 in red and neuron 6 in blue. An overlay of somata and neurites is visible. (C) shows the traces of the neurons 2 and 3 obtained with the software Neuroplex by averaging the signal of the pixels on the cell body. In the trace of neuron 3 many spikes are visible; this is an artifact due to the overlay with neuron 4. Indeed, neuron 2 and 3 do not appear as responders with the ICA. (D)-(G) display the ICA images of neuron 1, neuron 4, neuron 5 and neuron 6 with the corresponding Neuroplex trace of the cell body (upper trace) and ICA trace (lower trace), respectively. Every peak in the traces represents a spike. In the Neuroplex traces are often detectable overlays of different signals, which are instead separated by the ICA. Scale bar: 25 μm

the other stimulation techniques (normal and shear stress), which resulted in stimulation of the whole cluster the % of mechanosensitive neurons were given per cluster. For comparison of the % of mechanosensitive spots the z-test was used. Two paired data sets were compared if normally distributed with a Student's paired t test and if not normally distributed with a Wilcoxon Signed Rank test. Comparison of two data sets in a non-paired fashion were performed if normally distributed with a Student's t test and if not normally distributed with a Mann-Whitney Rank Sum test. More than two paired data sets were compared with the Friedman Repeated Measures Analysis of Variance (ANOVA) on Ranks; for not paired data sets with the Kruskal-Wallis One Way ANOVA on Ranks. Differences were considered as significant when $p < 0.05$.

To identify neurites belonging to the same neuron the ICA picture was used of the response to nicotine. Some neurons did not respond to nicotine. These neurons were included in the analysis only if they responded to carbon fiber stimulation. We assumed that stimulation of a large fiber tract stimulates all neurites running together in this tract. The number of mechanosensitive neurites was analyzed from all probed neurites of a mechanosensitive neuron. The spike frequency was compared of 3 mechanosensitive neurites of the same neuron.

The conduction velocity was calculated in recordings with 10 kHz. With this frame rate the field of view of the CCD camera was reduced from 80 x 80 to 80 x 12 pixels. Two pixels along one direction away from the point of stimulation where a clear signal can be detected were chosen. The distance of these two pixels was measured with Image J (Image J 1.45m; *National Institutes of Health, USA*). The traces of these two pixels were compared and the time delay between both traces was analyzed. The conduction velocity was calculated by dividing the distance by the time delay.

Ca²⁺- imaging data were analyzed differently. There the time point of mechanical stimulation could not be exactly determined. Here it was only analyzed, in which cell types the increase of [Ca²⁺]_i started first. This offered valuable clues about the involvement of different cell types in mechanotransduction, for instance it was analyzed if the neuronal response to mechanical stimulation was direct or triggered by other cell types.

3 Results

3.1 Growth of primary cultured myenteric neurons of guinea pig

Pieces of ganglia or whole ganglia (Figure 3.1 A) were fished from the cell suspension to inoculate culture dishes. The neurons did not attach to the culture dish bottom during day 0 (Figure 3.1 B). At day 1 the cells formed cell clumps and adhered to the bottom of the culture dish (Figure 3.1 C). At day 2 cell clumps started to form a monolayer and also non-neuronal cells were visible (Figure 3.1 D). At day 4 more and more single neurons were visible and growth of neurites started (Figure 3.1 E). At day 5-9 neuronal clusters were clearly visible and the neurites became longer, some neurons were also lost during medium change (Figure 3.1 F-K). After day 7 the culture dishes were ready for experiments; single neurons were clearly visible and they showed long neurites.

3.2 Presence of different cell types in primary cultures of myenteric neurons from guinea pig and human

With immunohistochemical methods different cell types were identified in the primary culture. Cultures were compared from guinea pig and human. Protein gene product 9.5 (PGP 9.5) is a marker for neuronal cells (Doran et al. 1983). PGP 9.5 was used for counting neurons and comparing clusters from guinea pig and human MP. Neurons were counted in 31 clusters from 4 guinea pigs and 19 clusters from 10 human tissues. Guinea pig clusters contained a significant higher number of neurons than human clusters (guinea pig: 15 ± 9 vs. human: 5 ± 6 (mean \pm standard deviation); $p \leq 0.001$).

Glial cells were detected with a SOX antibody (Kuhlbrodt et al. 1998). Glial cells were present in guinea pig as well as human primary cultures. In guinea pig culture besides neurons (PGP 9.5 positive cells) there were only a few glial cells within a cluster and around it (Figure 3.2 A-C). In human, on the other hand, there were only a few neurons, but a lot of glial cells within it (Figure 3.2 D-F).

Vinculin was first identified in cultured chicken fibroblast and is a cytoskeletal protein concentrated at their focal adhesions (Geiger et al. 1980). In this study vinculin was used as a marker for fibroblast-like cells. Vinculin positive cells were present in both

3. RESULTS

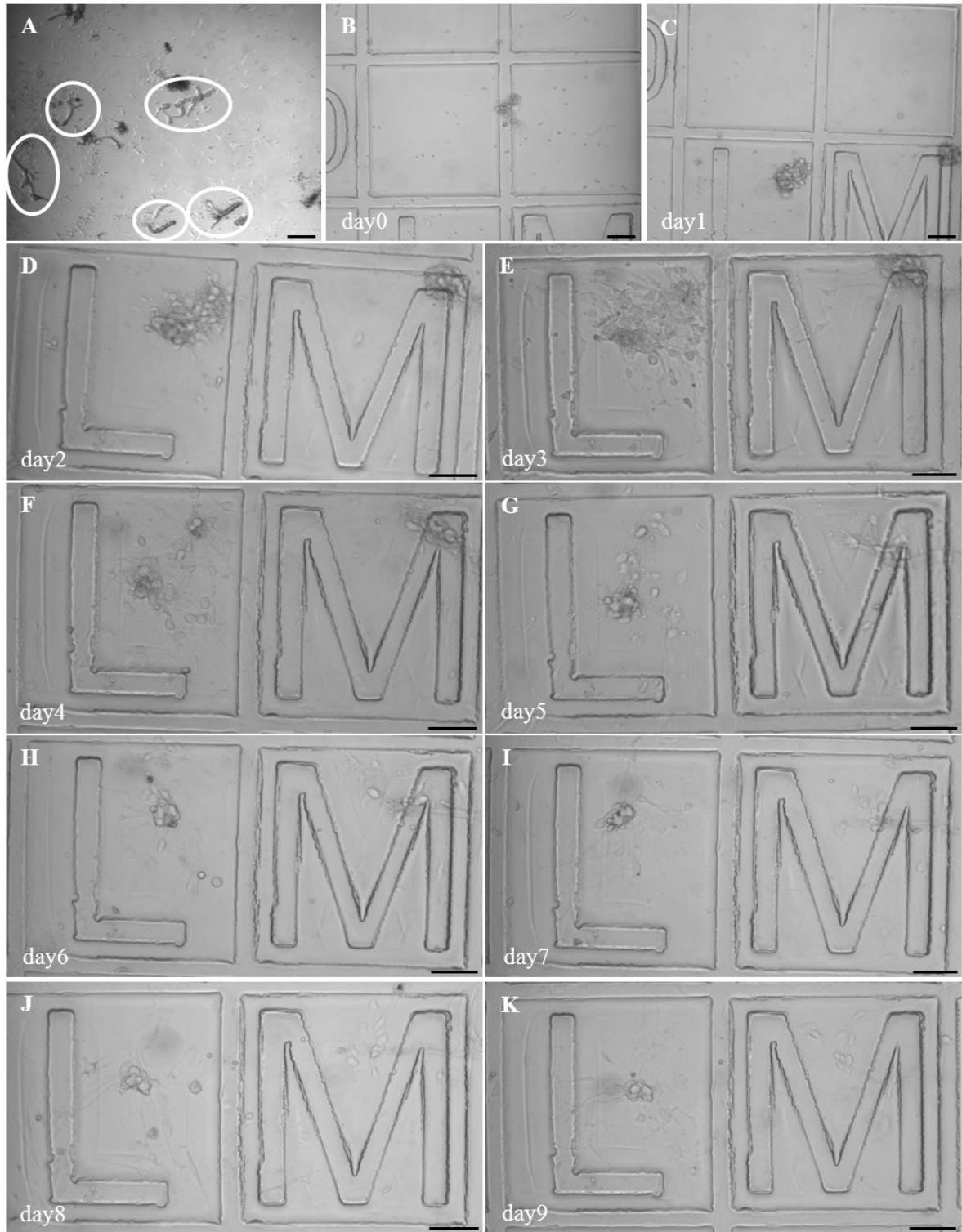


Figure 3.1: Cell growth during day 0 - 9 of the culture of guinea pig myenteric neurons. (A) shows ganglia that are fished to inoculate the culture dishes. Ganglia are encircled in white. (B)-(K) display the same cell cluster from day 0 to day 9. Scale bar: 100 μm .

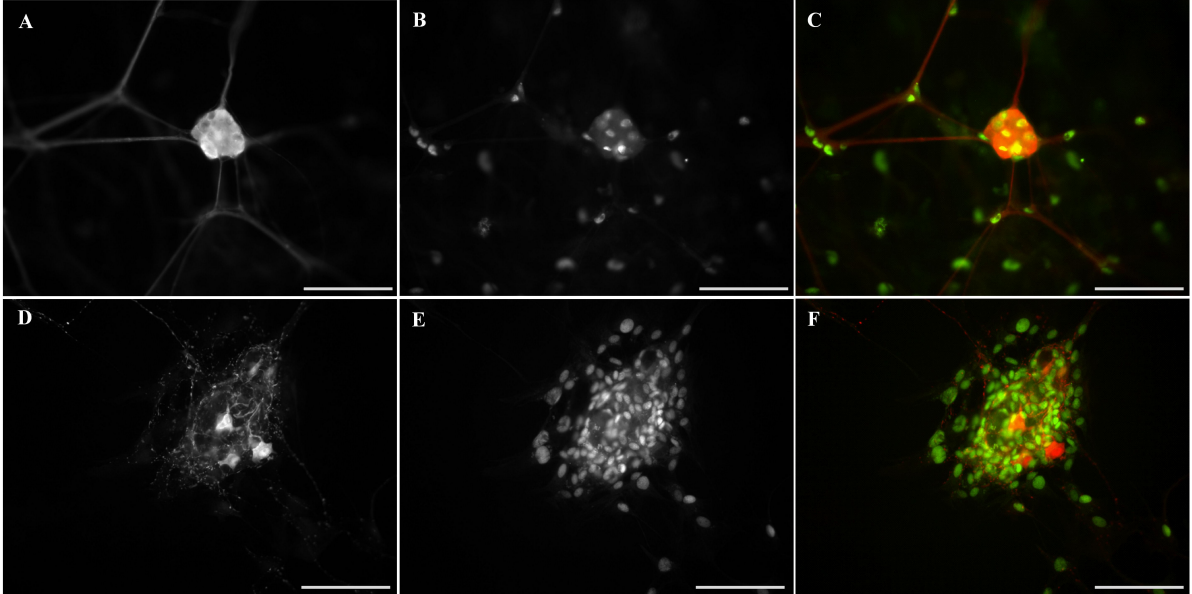


Figure 3.2: Overlay of protein gene product 9.5 (PGP 9.5) positive and SOX positive cells. Pictures in (A)-(C) are taken from guinea pig cultured myenteric neurons. Pictures in (D)-(F) are taken from human cultured myenteric neurons. (A) and (D) show PGP 9.5 positive cells (Cy5, red). SOX positive cells are shown in (B) and (E) (Cy2, green). In (C) and (F) are the pictures merged. Scale bar: 100 μm .

3. RESULTS

guinea pig and human primary culture (Figure 3.3). In guinea pig these cells formed a whole layer also under the neuronal clusters (Figure 3.3 A-C) while in human these cells were within a cluster (Figure 3.3 D-F) and formed no separate layer.

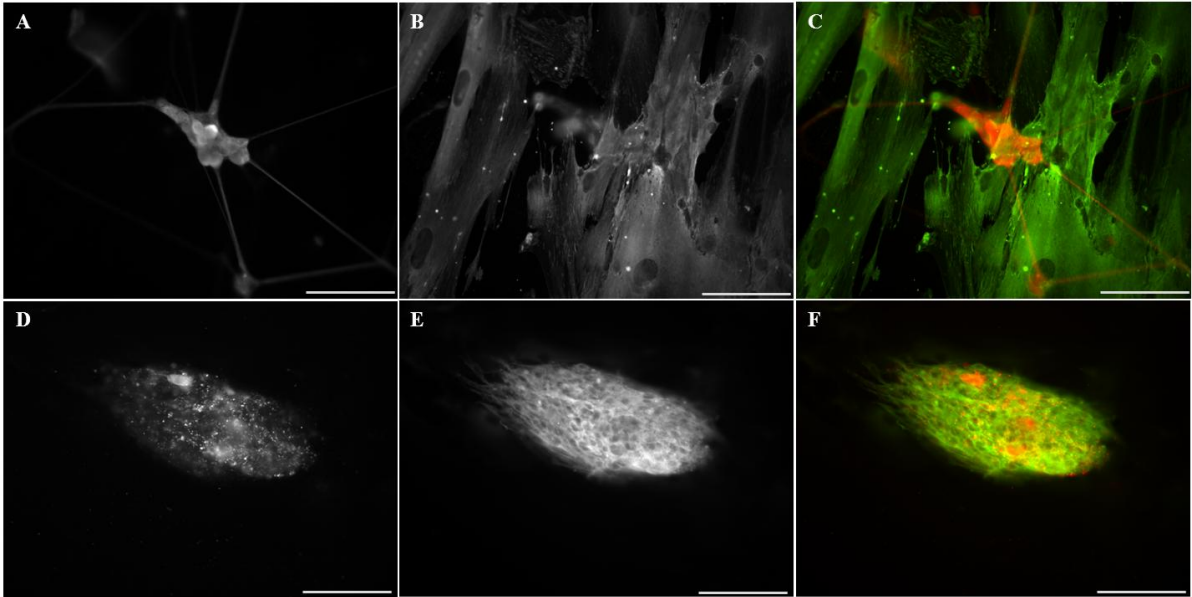


Figure 3.3: Overlay of PGP 9.5 positive and Vinculin positive cells. (A)-(C) are guinea pig; (D)-(F) are human cultured myenteric neurons. (A) and (D) show PGP 9.5 positive cells stained (Cy5, red). Vinculin positive cells are shown in (B) and (E) (Cy2, green). In (C) and (F) the pictures are merged. Scale bar: 100 μm .

Vimentin is a marker for intermediate-size filaments present in cells with mesenchymal origin (Franke et al. 1978). It is expressed in fibroblast-like cells, blood cells and endothelial cells (Schmid et al. 1979). It can be also found in ICCs (Komuro and Zhou 1996). In the culture there were no blood cells present and the presence of endothelial cells was unlikely, because the mucosa was removed. The presence of ICCs could be ruled out, because of their specific morphology. Therefore vimentin was a marker for fibroblast-like cells as vinculin in the cultures. In guinea pig vimentin positive cells were mostly found around the clusters and rarely within the clusters (Figure 3.4 A-C). In contrast in human most vimentin-positive cells were within the clusters and only some around it (Figure 3.4 D-F).

It was also stained for small conductance calcium-activated potassium channel type 3 protein (SK3). SK3 is mainly present in smooth muscle and vascular endothelium (Chen et al. 2004). Staining results with anti-SK3 antibody in the culture were unspecific (pictures not shown).

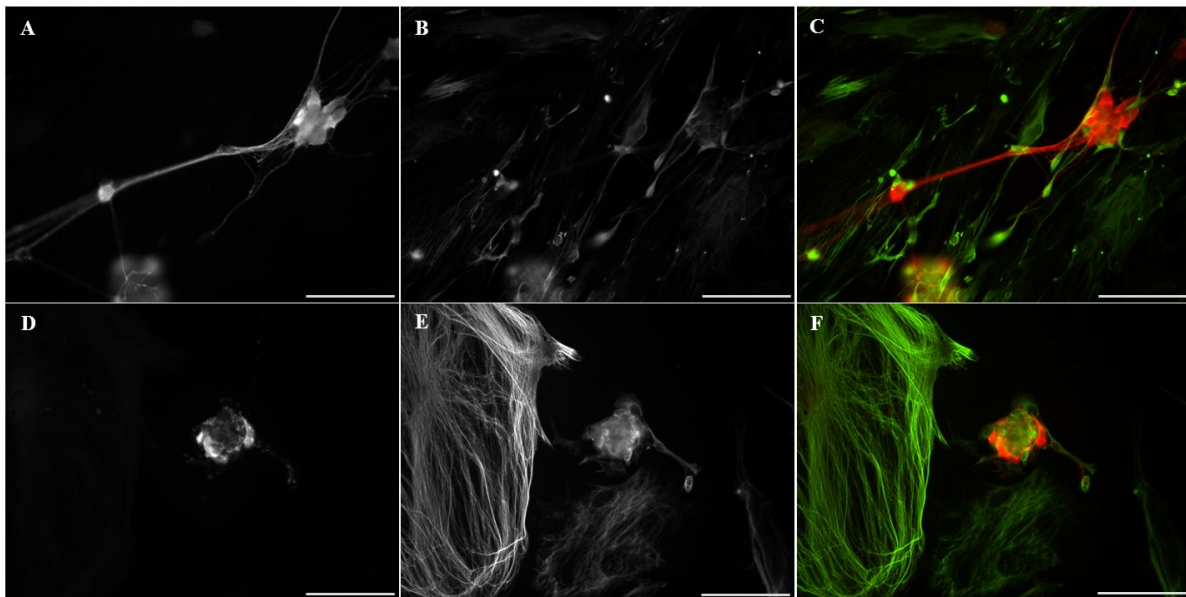


Figure 3.4: Overlay of PGP 9.5 positive and vimentin positive cells. (A)-(C) are guinea pig; (D)-(F) are human cultured myenteric neurons. (A) and (D) show PGP 9.5 positive cells stained (Cy5, red). Vimentin positive cells are shown in (B) and (E) (Cy2, green). In (C) and (F) the merged pictures are shown. Scale bar: 100 μ m.

The mast/stem cell growth factor receptor is also known as proto-oncogene c-Kit (c-Kit). C-kit positive stainings are found in mast cells and in ICCs (Nocka et al. 1989; Komuro and Zhou 1996). Staining results with anti-c-kit antibody in the culture were unspecific (pictures not shown).

As a marker for smooth muscle cells smoothelin can be used (Loop et al. 1996). Staining results with anti-smoothelin antibody in the culture were unspecific (pictures not shown).

3.3 Success rate of culturing human myenteric neurons

Culturing human myenteric neurons was challenging. 90 tissue samples were cultured. In 68% of the cultures neurons were identified during the experiments, which responded to nicotine. In 32% of the cultures the neurons either did not respond to nicotine or no cells grew in the culture dish. All in all 209 culture dishes were inoculated from these 90 tissues. In 51% of the culture dishes grew neurons that responded to nicotine. In 28% cell growth could be observed, but none of the cells responded to nicotine. In 21% there was no cell growth.

The immunohistochemical analysis of 6 culture dishes, in which no cells responded to nicotine, showed that there were neurons in 5 of them.

Comparisons were performed to identify any differences in the success rate for culturing the tissue coming from the clinic in Freising (75%) and *Rechts der Isar* (60%); between male (65%) and female (71%) patients and tissues from small intestine (64%) and large intestine (70%). There were in all cases no significant differences.

3.4 Preliminary experiments: transfection of primary cultured myenteric neurons of guinea pig

For further studies to identify the mechanism of mechanotransduction transfection was tested of primary cultured myenteric neurons from guinea pig via electroporation with a GFP vector as a control.

All programs tested killed most of the cultured neurons. After electroporation and inoculating new culture dishes with the cell suspension rarely clusters were growing in the culture dish.

3.5 Identification of the properties of mechanosensitive myenteric neurons with a contact method

All experiments were performed in primary cultured myenteric neurons from guinea pig small intestine if there are no further specifications.

3.5.1 Mechanosensitivity is a property of enteric neurites as well as somata

The carbon fiber was used for targeted stimulation on neurites or somata. In the present study 256 spots were stimulated on the neurites of 203 neuronal clusters from 30 guinea pigs. Stimulation induced in 114 of these 256 spots (45%) spike discharge at least in one neuron. The signal could be detected in the mechanical stimulated neurite, in the corresponding soma and in further neurites. Enteric cultured neurons are mostly organized in clusters and therefore it could be observed that stimulation of one spot often led to the activation of many neurons having nearby running neurites (Figure 3.5). In details, stimulation of a spot on the neurite led in 67% of the cases to the activation of only one neuron, in 20% to excitation of two neurons, in 8% to activation of 3 neurons, in 4% to excitation of 4 neurons and in 1% to activation of 5 neurons. The responding neurons fired with an overall spike frequency of 4.4 (2.2/9.8) Hz and a burst spike frequency of 13.4 (5.9/20.1) Hz.

Placing the carbon fiber on the target resulted in a membrane deformation consisting of a short dynamic phase and a sustained phase. During the sustained phase the carbon fiber was maintained pressed onto the target. The dynamic phase lasted 280 (140/401) ms. The spike frequency during dynamic phase was significantly higher than during

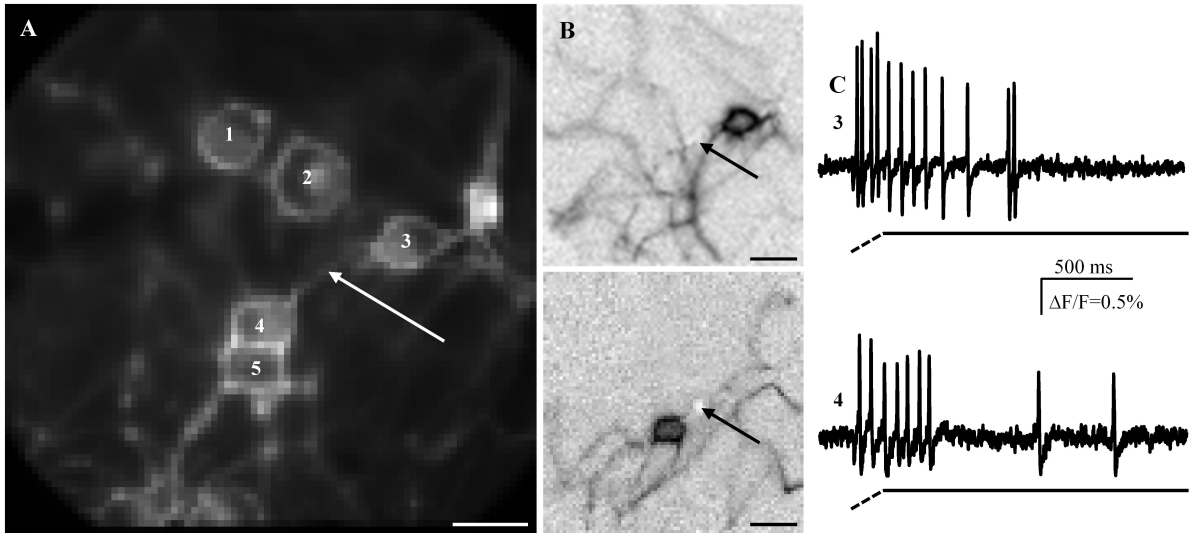


Figure 3.5: Myenteric neurons are activated by carbon fiber stimulation on their neurites. (A) shows a picture of a cluster with 5 neurons stimulated on a fiber tract (white arrow). In (B) the ICA images of the responding neurons are displayed. The upper image shows neuron 3 and the lower neuron 4. The spot of carbon fiber stimulation is marked with the black arrow in both images. In (C) are shown the traces of the responding mechanosensitive neurons. The dashed line under the trace indicates the dynamic phase of the stimulation and the continuous line the sustained phase. Scale bar: 25 μm .

3. RESULTS

sustained phase (9.4 (2.1/18.3) Hz vs. 2.6 (0.7/8.1) Hz; $p \leq 0.001$). The spike burst occurred 55 (13/153) ms after pressing the carbon fiber onto the target and lasted 1,080 (418/1,576) ms.

Experiments with stimulation on the somata of myenteric neurons were in addition performed. In this set of experiments the somata of 96 neurons in 67 clusters from 18 guinea pigs were stimulated. Soma stimulation induced spike discharge in 13 of 96 neurons (14%). The signal was detectable on the stimulated soma and on further projecting neurites (Figure 3.6).

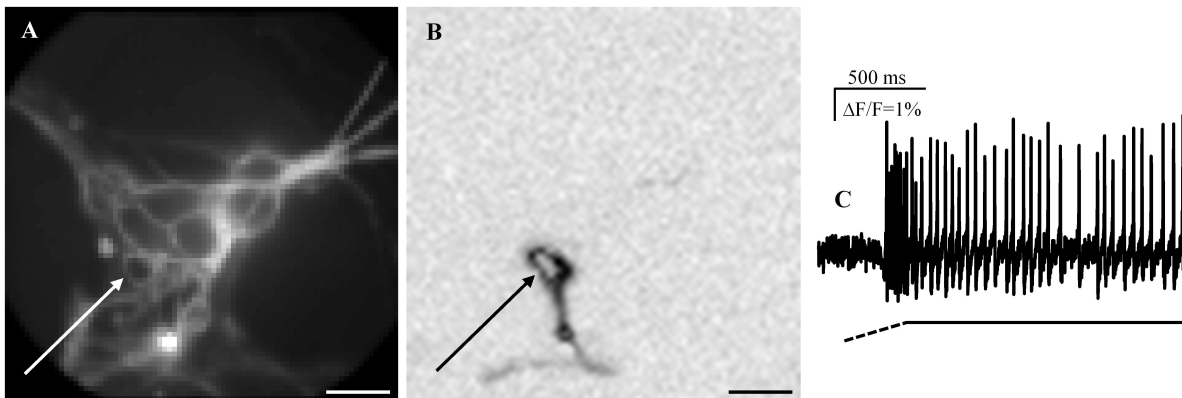


Figure 3.6: Myenteric neurons are excited by carbon fiber stimulation on their soma. (A) shows a picture of a cluster stimulated at the spot indicated by the white arrow. In (B) is displayed the ICA image of the stimulated and responding neuron. (C) shows the trace of the response of this neuron. Scale bar: 25 μm .

The mechanosensitive neurons fired with an overall spike frequency of 7.2 (3.0/16.7) Hz and a burst spike frequency of 17.0 (7.4/23.7) Hz. The dynamic phase of the stimulation lasted 420 (320/718) ms. The spike discharge was not significantly different between dynamic and sustained phase (12.8 (2.2/16.7) Hz vs. 4.6 (1.0/13.5) Hz). The neurons started firing after 163 (33/236) ms. The spike burst lasted 1,338 (875/1,680) ms.

It was demonstrated that mechanosensitivity is a property of neurites and somata. In the next step it was tested if all neurons that showed mechanosensitive properties if stimulated on the neurite were also mechanosensitive if stimulated on the soma. In this run 18 neurons from 7 guinea pigs were stimulated both on one of the neurites and on the soma. The neurons that responded to neurite stimulation were in 45% of the cases also excited by soma stimulation. The comparison of the response characteristics considering only the neurons responding to both stimuli showed a significantly higher burst spike frequency for soma stimulation ($p=0.007$), but no difference in the other response characteristics (Table 3.1). A noteworthy phenomenon was that responses to soma deformation after stimulation of the neurite were more pronounced than those obtained during soma deformation without prior neurite stimulation. Both, the burst spike frequency ($p=0.035$) as well as the spike frequency during the dynamic deformation

3. RESULTS

($p=0.058$) were higher. In addition, the spike burst occurred much faster after the deformation of the soma ($p=0.049$) strongly suggesting that mechanical stimulation of neurites sensitized the soma (Table 3.1).

Table 3.1: Comparison of the response characteristics of paired neurite and soma stimulations as well as soma stimulation with and without prior neurite stimulation. The different spike frequencies and the timing of the responses are compared of soma stimulation after neurite stimulation with neurite stimulation and soma stimulation without prior neurite stimulation. Significant differences are marked with *. Spike frequencies during dynamic and sustained phase are tested against each other within one group and marked with † if significant.

	soma	soma after neurite	neurite
burst spike frequency [Hz]	17.0 (7.4/23.7)*	31.7 (27.2/42.7)	17.9 (9.4/26.4)*
spike frequency during dynamic phase [Hz]	12.8 (2.2/16.7)*	25.0 (10.1/51.5)	13.8 (8.8/24.2)
spike frequency during sustained phase [Hz]	4.6 (1.0/13.5)	0.5 (0.0/3.0)†	1.1 (0.0/17.9)†
start spike burst [ms]	147 (29/206)*	10 (3/148)	25 (10/107)
duration spike burst [ms]	1,338 (875/1,680)*	65 (61/787)	1,005 (357/1,579)
n=(GP or tissue / cluster / neuron)	(8/14/14)	(4/8/9)	(4/8/9)

Reproducibility was tested in 39 mechanosensitive neurons in 6 clusters from one guinea pig. It was tried to stimulate exactly the same spot with the carbon fiber twice on a neurite, which was prone to errors as previously reported (Mazzuoli and Schemann 2009). Pressing onto a fiber tract excited 39 neurons; the second stimulation activated only 24 neurons (62%). The burst spike frequency comparing all 39 neurons was significantly decreased (15.2 (10.1/18.0) Hz vs. 6.1 (0.0/12.1) Hz; $p \leq 0.001$). Comparison of only the neurons responding twice was also significant different (16.9 (13.2/20.2) Hz vs. 8.7 (7.0/17.5) Hz; $p \leq 0.001$).

To detect long firing neurons the recording time was extended from 2 s to 5 s or 10 s. 17 spots of 17 clusters from 6 guinea pigs were probed that were already identified as mechanosensitive. Probing 17 spots on the neurite activated 27 neurons. Of these 27 neurons only 7 neurons (26%) did not fire longer than 2 s. The overall spike was 1.9 (0.9/3.4) Hz and the burst spike frequency 4.3 (2.3/9.7) Hz. The spike discharge started 55 (14/190) ms after touching the neurite and lasted for 5,791 (663/8,716) ms. The burst spike frequency of the dynamic phase was significantly higher than the burst spike frequency of the sustained phase (23.3 (10.1/29.9) Hz vs. 1.6 (0.5/3.1) Hz; $p \leq 0.001$).

Cultures of myenteric neurons from the gastric corpus were probed to test if myenteric

neurons from other gut regions show the same response characteristics. 52 neurons in 25 clusters from 3 guinea pigs were stimulated. Mechanical stimulation induced in 23 of 52 neurons (44%) spike discharge. The overall spike frequency of 5.7 (1.8/16.4) Hz was not significantly different to small intestinal myenteric culture. The burst spike frequency of 21.2 (11.1/27.8) Hz was significantly higher ($p=0.024$). The spike frequency during dynamic phase (8.3 (4.4/19.3) Hz) and the spike frequency during sustained phase (2.9 (0.0/15.6) Hz) was not significantly different. In addition, both were not different to cultured myenteric neurons from small intestine. The spike discharge started 85 (42/126) ms after mechanical stimulation and lasted 646 (139/979) ms. The firing onset was not significantly different, but the burst duration was significantly shorter in cultured myenteric neurons from gastric corpus ($p=0.019$).

3.5.2 Mechanosensitive properties of other cultured neurons

To validate the mechanical stimulation method, the ultra-fine tool was tested on already well-characterized mechanosensitive neurons: the DRG neurons (Howe et al. 1977; McCarter et al. 1999; Hu and Lewin 2006). Furthermore cultured SCG neurons were probed, which were characterized as non-mechanosensitive neurons (McCarter et al. 1999).

First neurite stimulation of DRG neuron was performed. 54 spots were stimulated on neurites in 26 field of view from 2 guinea pigs. Stimulation on the neurite led to excitation of at least one neuron. The ICA showed several neurites running together (Figure 3.7). In 43% of the cases stimulation of one spot activated only one neuron, in 40% two neurons, in 11% 3 neurons and in 6% 4 neurons. The firing of DRG neurons to neurite stimulation resulted in an overall spike frequency of 5.2 (2.2/12.3) Hz and a burst spike frequency of 8.9 (6.7/16.7) Hz. Pressing down the carbon fiber induced a dynamic phase of 305 (230/425) ms. The spike frequency during dynamic phase was significantly higher than during sustained phase (11.8 (6.5/18.9) Hz vs. 3.9 (0.7/9.7) Hz; $p\leq 0.001$). The spike burst occurred 9 (4/37) ms after the start of mechanical stimulation and lasted 1,503 (760/1,739) ms.

The mechanosensitive DRG neurons were divided into classes according to their size in large diameter neurons ($> 30 \mu\text{m}$), medium diameter neurons (20-30 μm) and small diameter neurons ($< 20 \mu\text{m}$) (Sommer et al. 1985). In the experiments classification by morphological evaluation was only possible for 12 neurons, since for the other neurons there were only neurites in the field of view. 24% of the mechanosensitive neurons were small diameter neurons, 68% were medium sized neurons and 8% could be classified as large diameter neurons.

Furthermore the ability of DRG somata was examined to respond to mechanical stimulation. Therefore 21 somata from two guinea pigs were stimulated. None of the stimulated neurons responded. This was the most striking difference to myenteric neurons.

Furthermore cultured SCG neurons were probed with the ultra-fine tool. 47 spots were stimulated on the neurites of 26 clusters from two guinea pigs. In 36 of 47 spots (77%) mechanical stimulation induced spike discharge in at least one neuron. Neurites running

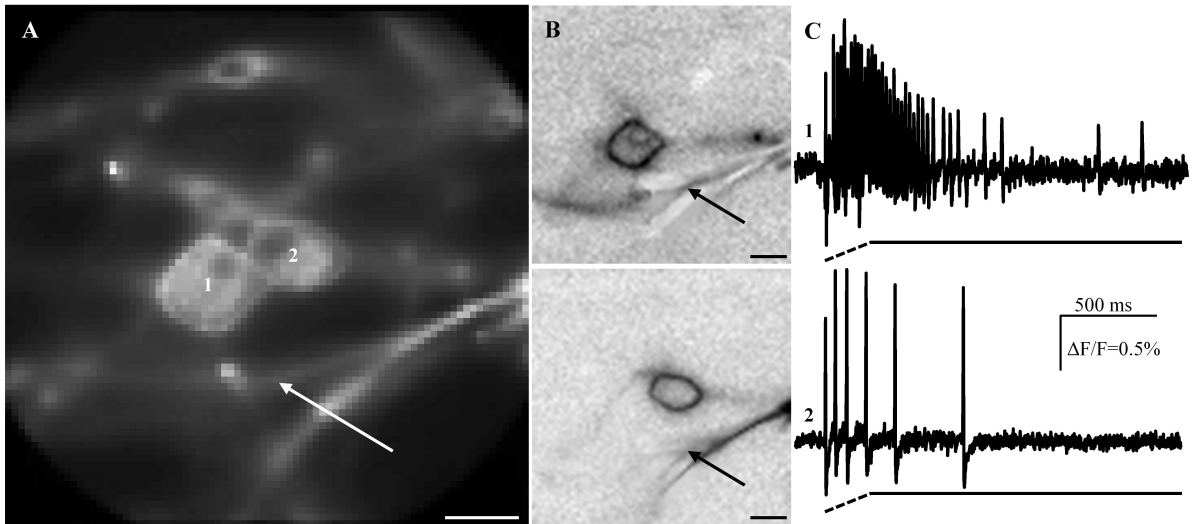


Figure 3.7: Carbon fiber stimulation on the neurites of cultured dorsal root ganglia (DRG) neurons is excitatory. (A) shows a picture of two DRG neurons in the field of view stimulated at the spot indicated by the white arrow. (B) represents the ICA images of them. In (C) are displayed the traces of the two neurons. Scale bar: 25 μm .

together were also observed for SCG neurons. Stimulation of one spot on a neurite led in 40% to excitation of only one neuron, in 21% to two neurons, in 16% to 3 neurons, in 8% to 4 neurons and in 15% to more than 4 neurons (Figure 3.8). The mechanosensitive SCG neurons fired in response to carbon fiber stimulation with an overall spike frequency of 5.0 (2.2/10.7) Hz and a burst spike frequency of 9.9 (5.8/18.4) Hz. The spike frequency during dynamic phase was significantly higher than during sustained phase (9.5 (3.9/17.6) Hz vs. 3.6 (1.5/8.9) Hz; $p \leq 0.001$). The spike burst started 88 (19/233) ms after mechanical stimulation and lasted 1,434 (878/1,653) ms.

In addition probing of 18 somata of SCG in 18 clusters from two guinea pigs showed that 6 of 18 (33%) were mechanosensitive on this site.

Comparing the response characteristics of all three types of neurons showed no significant differences except for the timing of the responses. DRG neurons started firing spikes significantly earlier ($p \leq 0.001$) compared to the other two and the burst lasted longer ($p \leq 0.001$) in DRG and SCG neurons compared to myenteric neurons (Figure 3.9). Furthermore the percentages of mechanosensitive neurites and somata were different. For neurite stimulation there was a significant difference between myenteric neurons and DRG neurons ($p = 0.012$), myenteric neurons and SCG neurons ($p \leq 0.001$) but not DRG and SCG neurons (Table 3.2). For soma stimulation there was a significant difference between DRG and SCG neurons ($p = 0.013$) but neither between myenteric neurons and DRG nor for myenteric neurons and SCG (Table 3.2).

3. RESULTS

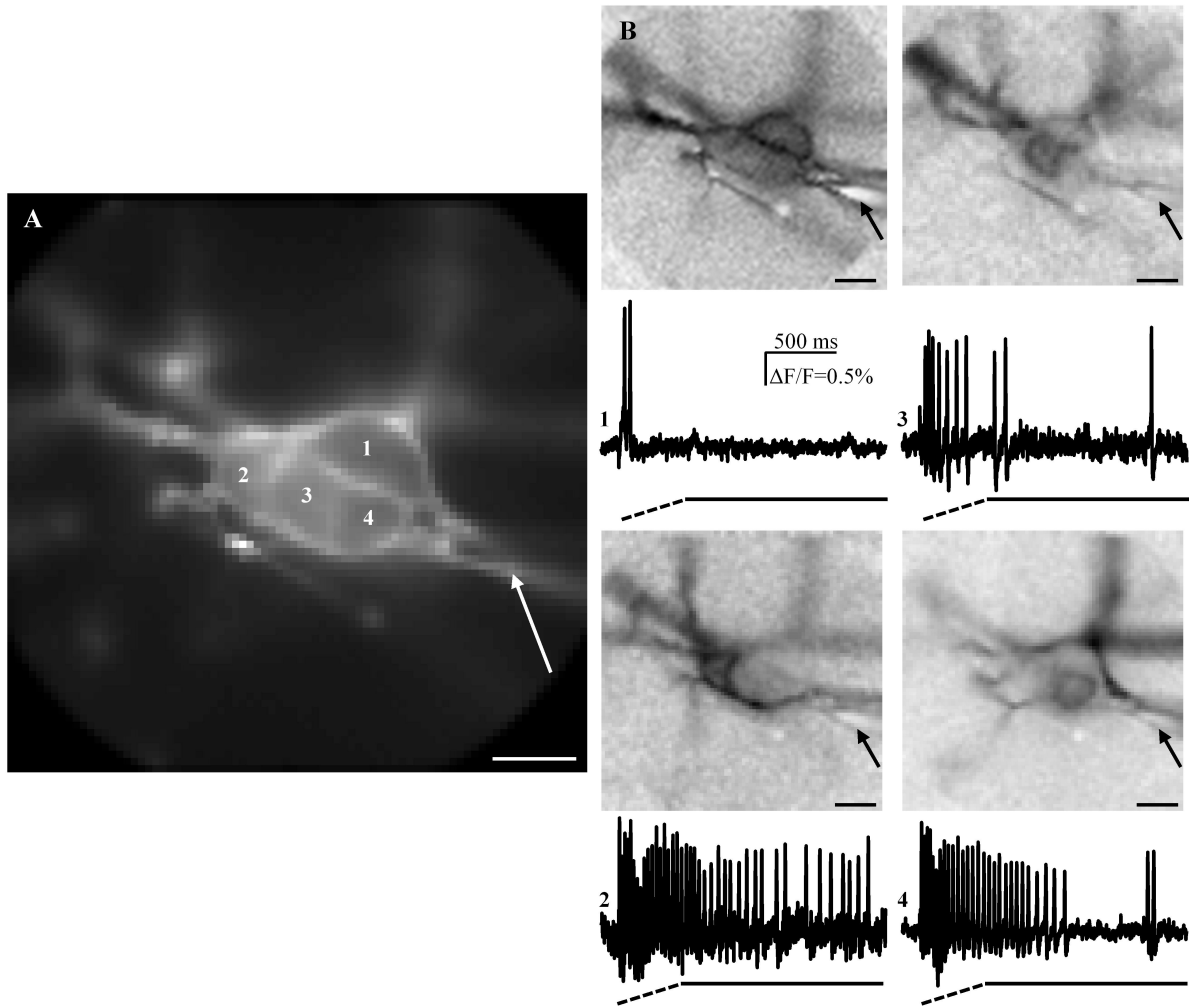


Figure 3.8: Cultured sympathetic chain ganglia (SCG) neurons are excited by carbon fiber stimulation on their neurites. (A) shows a picture of 4 SCG neurons stimulated at the white arrow. (B) displays their ICA images. All 4 neurons respond to carbon fiber stimulation. Under each ICA image is shown the corresponding trace. Scale bar: 25 μm .

Table 3.2: Comparison of percentages of mechanosensitive neurites and somata of MP, DRG and SCG neurons. Significant differences to MP neurons are marked with *. Significant differences to DRG neurons are marked with †.

	% mechanosensitive neurites	% mechanosensitive somata
MP	45†	14
DRG	65*	0
SCG	77*	33†

3. RESULTS

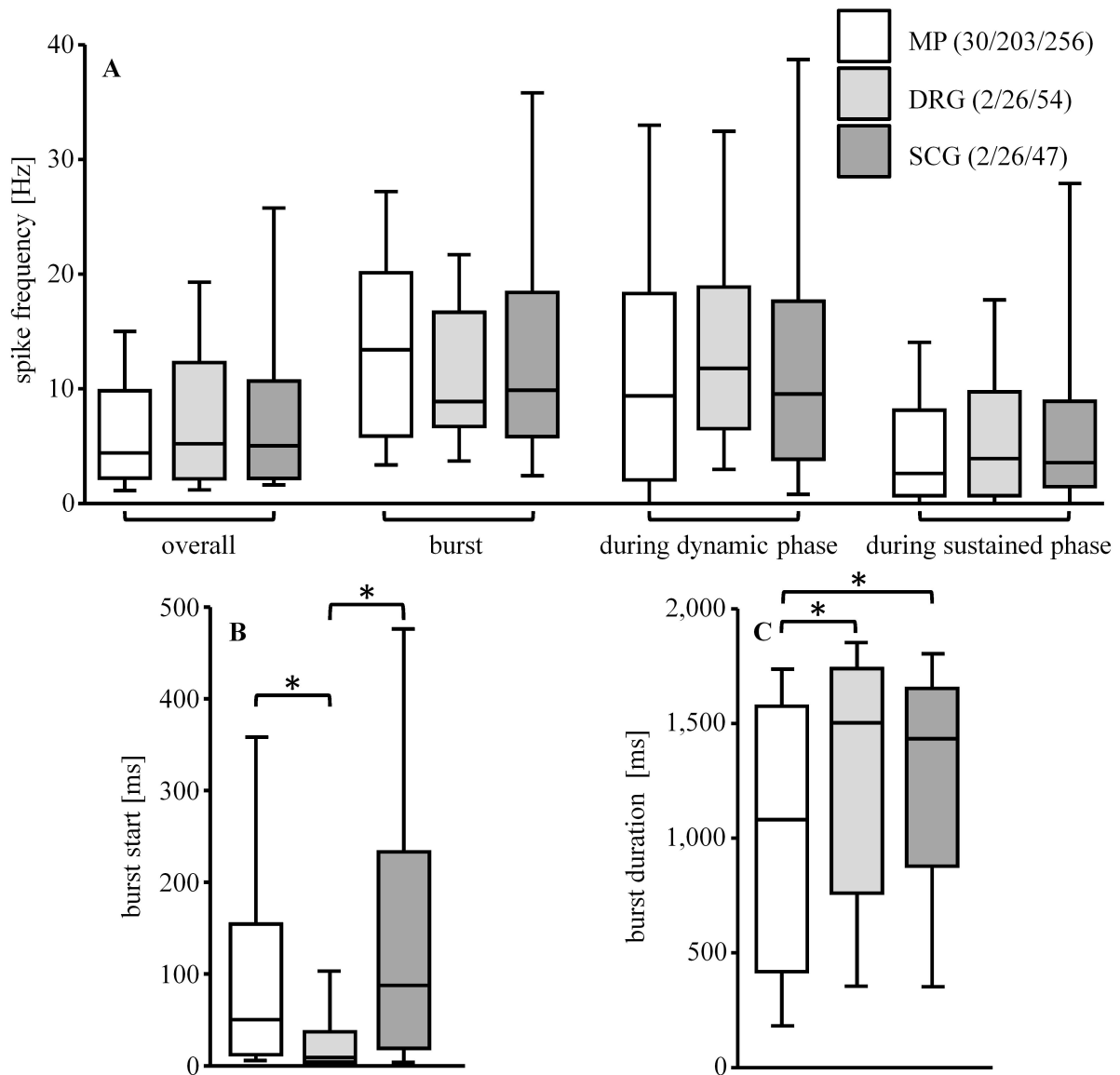


Figure 3.9: Comparison of the response characteristics of mechanosensitive myenteric plexus (MP), DRG and SCG neurons (analysis of variance (ANOVA) on Ranks test). (A) shows no differences in the overall and burst spike frequency as well as in the spike frequency during dynamic and sustained phase. (B) reveals a significant difference of the start of the spike burst between myenteric and DRG as well as between DRG and SCG neurons. (C) shows a significant difference of the duration of the spike burst between myenteric and DRG as well as between myenteric and SCG neurons. N numbers in parenthesis show the number of guinea pigs/ clusters or field of views / neurons, respectively.

3.5.3 Characterization of mechanosensitive myenteric neurons

The ICA images were used to morphometrically characterize 151 mechanosensitive neurons by measuring the large and small diameter and the number of neurites. The large diameter was 20 (16/22) μm (range 9 - 46 μm) and the small diameter was 14 (12/16) μm (range 5 - 24 μm). The number of neurites was 3 (2/4) (range 1 - 7). This may be an underestimation as action potentials may not invade all neurites. However, ICA images of 33 neurons activated by deformation were identical with images derived from activation by nicotine which is supposed to primarily evoke soma spikes (Figure 3.10). The overlap of the two ICA images at least suggested that neurites activated by mechanical deformation also conduct action potentials generated in the soma.

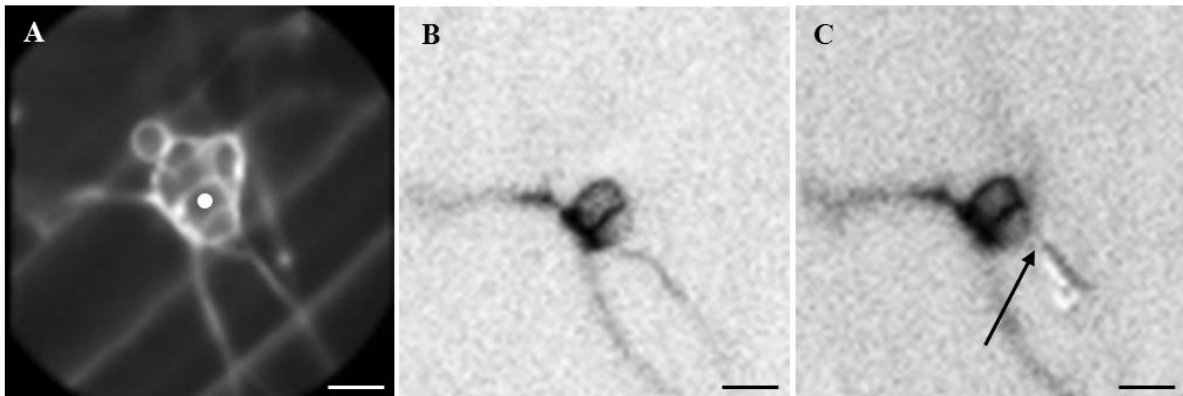


Figure 3.10: Overlap of the ICA images of a neuron in response to nicotine and carbon fiber stimulation. In (A) is shown a picture of the cluster. The neuron of interest is marked with a white dot. In (B) the ICA image of the nicotine response is shown. (C) shows the ICA image of the mechanical response of the same neuron. The neuron is stimulated at the spot marked with the black arrow. The two images are perfectly overlapping. Scale bar: 25 μm .

To address the question if all mechanosensitive neurons correspond to the previously identified IPANs double immunofluorescent labeling was used with the pan neuronal marker PGP 9.5 (Doran et al. 1983) and calbindin (Li and Furness 2000; Quinson et al. 2001). 72 mechanosensitive neurons were analyzed in 13 clusters from 2 guinea pigs. Of all mechanosensitive neurons 16 were calbindin positive (22%) and showed a Ca^{2+} hump on the falling phase of their action potentials (Figure 3.11).

To clarify the question if Piezo1 and Piezo2, which were previously identified as mechanosensors in DRG neurons (Coste et al. 2010), are also present in myenteric neurons immunohistochemistry was used. These stainings were as well performed in DRG and SCG neurons.

Piezo1 is present in somata and neurites of myenteric neurons (Figure 3.12 A-C). 22 mechanosensitive neurons in 4 clusters from one guinea pig were analyzed. 55% of

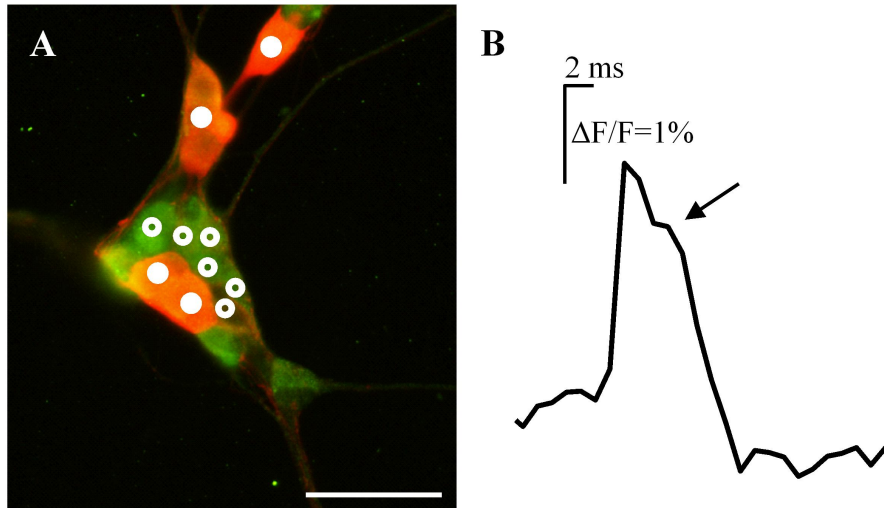


Figure 3.11: The mechanosensitive neuronal population is partly showing characteristics of intrinsic primary afferent neurons (IPANs). (A) shows a cluster with 10 mechanosensitive neurons. Mechanosensitive neurons only protein gene product (PGP 9.5) positive (green) are marked with a white circle. Part of the mechanosensitive neurons is also immunoreactive for calbindin (red), which is a IPAN marker in guinea pig; these neurons are marked with a white dot. All mechanosensitive neurons immunoreactive for calbindin showed a Ca^{2+} hump on the falling phase of their spikes. A representative spike is displayed in (B); the hump is indicated with the arrow. Scale bar: 50 μm .

3. RESULTS

mechanosensitive neurons were Piezo1 and PGP 9.5 positive, whereas 45% were only PGP 9.5 positive. Immunohistochemical staining of Piezo2 showed presence of Piezo2 in some neurites; in the somata the background fluorescence was instead too bright to detect any eventual staining (Figure 3.12 D-F). For Piezo2 staining it was not possible to analyze its presence in mechanosensitive neurons: with the 80 x 80 pixels resolution it was not possible to identify the exact spot that was mechanically stimulated in the experiment. There were Piezo2 positive and negative neurites running close by. Therefore classification of mechanosensitive neurites in Piezo2 positive and negative was not possible.

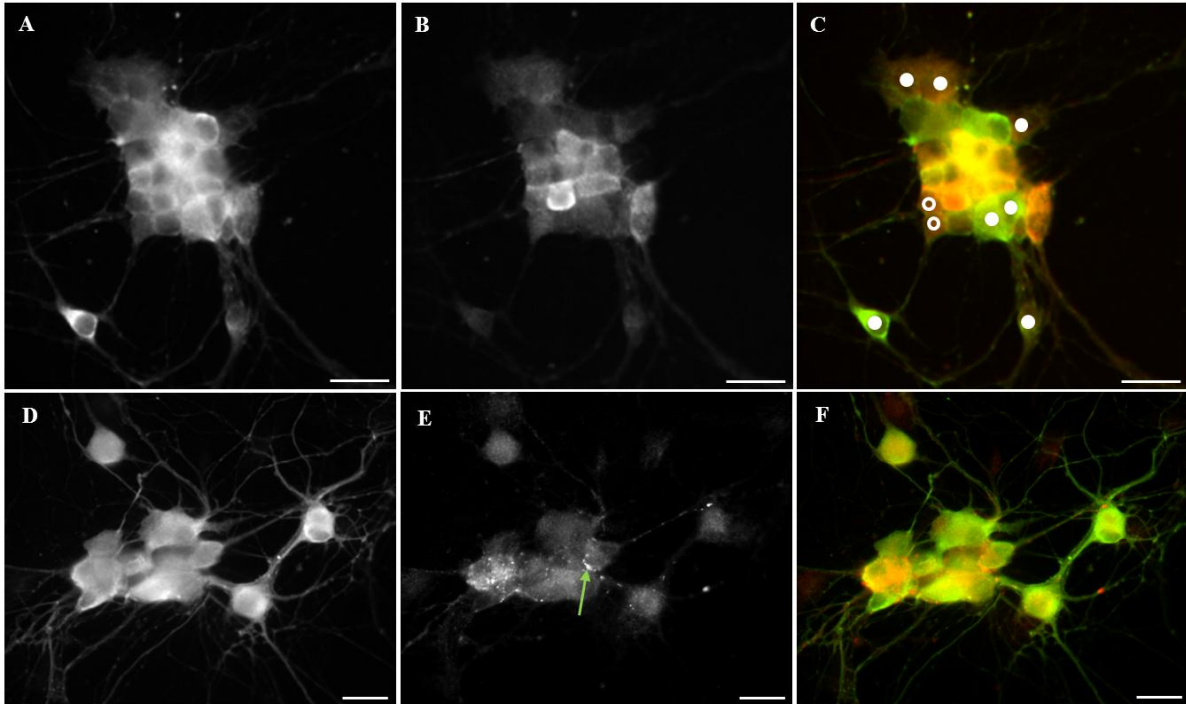


Figure 3.12: Piezo1 and Piezo2 are present in myenteric neurons. (A) and (D) show PGP 9.5 stainings. Piezo1 is present in somata as well as neurites (B). The overlay of PGP 9.5 (Cy2, green) and Piezo1 (Cy5, red) shows that the myenteric neurons are partly Piezo1 positive. The mechanosensitive neurons are marked with white dots (only PGP 9.5 positive neurons) or white circles (PGP 9.5 and Piezo1 positive neurons). Presence of Piezo2 in neurites (green arrow) as well as background staining in somata is shown in (E). Merge images are shown in (C) and (F) (PGP 9.5: green, Piezo: red). Scale bar: 25 μm .

In DRG neurons neither Piezo1 nor Piezo2 revealed any specific staining (Figure 3.13).

SCG neurons had Piezo1 positive somata and neurites (Figure 3.14 A-C). Piezo2 was present in neurites only (Figure 3.14 D-G). In SCG neurons costaining was performed

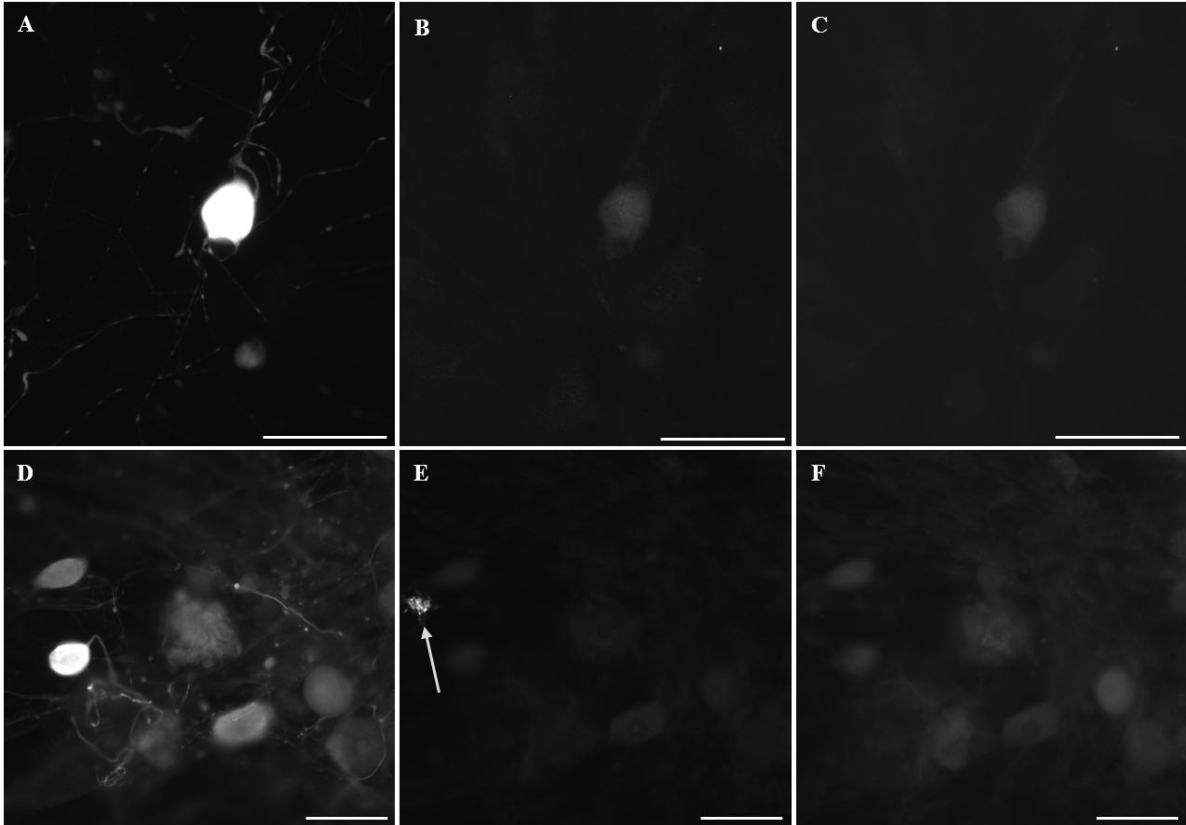


Figure 3.13: Piezo1 and Piezo2 stainings are not specific in DRG neurons. (A) and (D) show PGP 9.5 staining. Neither Piezo1 (B) nor Piezo2 (E) is present in DRG neurons. Only a structure outside the neurons is stained with Piezo2 (arrow). (C) and (F) show the autofluorescence in the AMCA filter, which is not different to the Piezo staining. Scale bar: 50 μm .

3. RESULTS

with tyrosine hydroxylase (TH), which is a marker for SCG neurons (Lund et al. 1978).

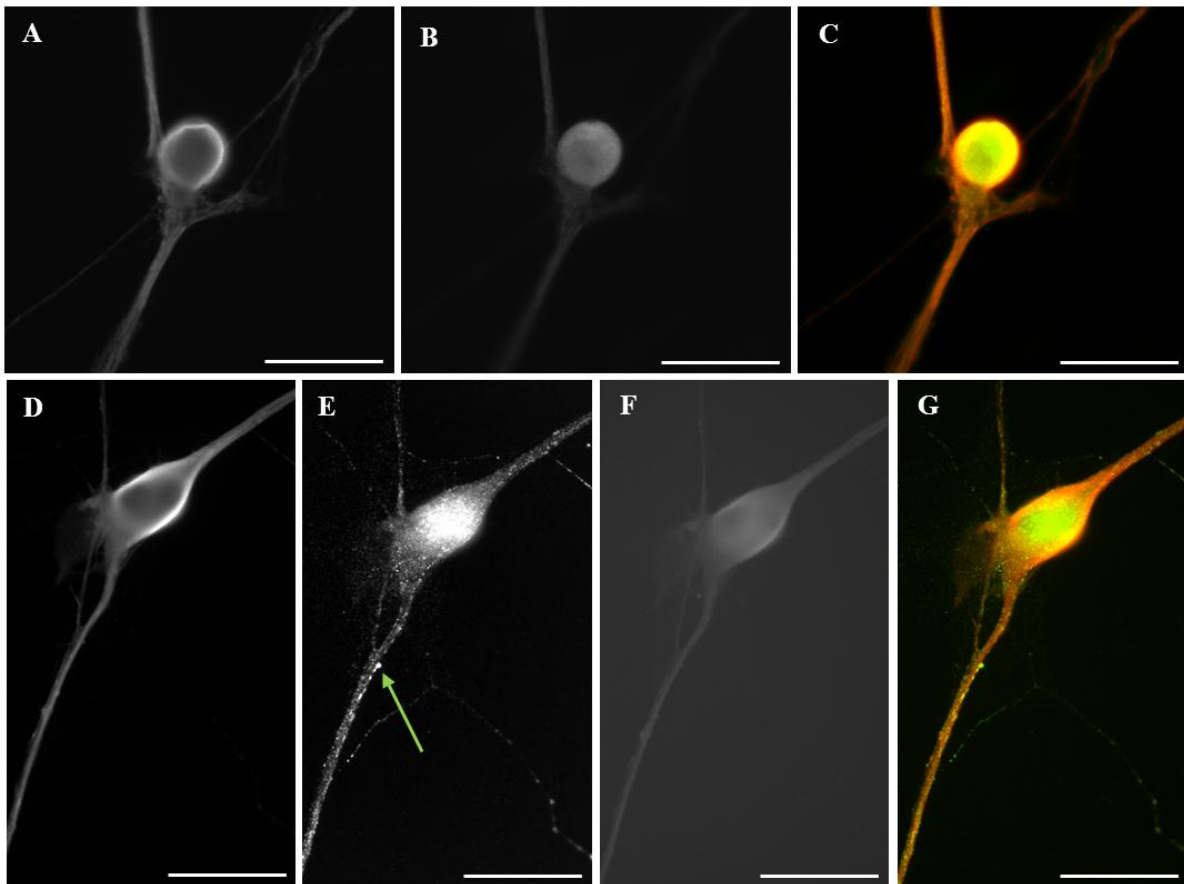


Figure 3.14: Piezo1 and Piezo2 is present in SCG neurons. (A) and (D) show tyrosine hydroxylase (TH) staining. Piezo1 is present in somata as well as in neurites (B). The overlay of TH (Cy3, red) and Piezo1 (Cy2, green) shows that SCG neurons are Piezo1 positive. The presence of Piezo2 in neurites (green arrow) as well as in somata is shown in (E). The autofluorescence in the AMCA filter is shown in (F). Merge images are shown in (C) and (G) (TH: red, Piezo: green). Scale bar: 50 μm .

3.5.4 Pharmacological treatment of mechanosensitive neurons

Effect of ω -conotoxin GVIA

Synaptic blockade with ω -conotoxin GVIA was performed in 7 clusters from 6 guinea pigs. 17 neurons responded before ω -conotoxin GVIA to von Frey hair stimulation on their neurite. Perfusion of ω -conotoxin GVIA significantly reduced the number of neurons activated by mechanical stimulation from 17 to 9 (100% vs. 53%; $p=0.005$). In addition, comparing the overall spike frequency in a paired manner showed a significant

decrease in ω -conotoxin GVIA (4.4 (1.4/6.9) Hz vs. 0.0 (0.0/1.9) Hz; $p=0.05$). The burst spike frequency was different as well (15.7 (7.1/20.3) Hz vs. 0.0 (0.0/1.9) Hz; $p=0.007$). The paired comparison of the burst and overall spike frequency of the neurons responding before and after perfusion of ω -conotoxin GVIA showed no significant difference.

Effect of AP-18

AP-18 (blocker of TRPA1) was superfused in two clusters from one guinea pig. Neurite stimulation induced in two neurons spike discharge. These two neurons fired before and after AP-18 perfusion with a similar overall spike frequency (12.9 (2.2/23.6) Hz vs. 12.9 (8.7/17.1) Hz) and burst spike frequency (13.1 (2.3/23.9) Hz vs. 26.7 (18.0/35.5) Hz). There was no obvious effect of AP-18 on mechanotransduction.

Effect of Tranilast

Tranilast (blocker of TRPV2) was superfused in one cluster from one guinea pig. One neuron was activated by neurite stimulation before and after tranilast perfusion. The n number was too low to compare the spike frequency statistically. Nevertheless, the overall spike frequency (16.8 Hz vs. 15.5 Hz) and the burst spike frequency (17.6 Hz vs. 15.9 Hz) were similar.

Effect of cytochalasin D

Cytochalasin D (destabilizer of the cytoskeleton) incubation was tested in 16 clusters from one guinea pig. 3 different incubation times were tried in 3 different culture dishes: 28 h, 41 h and 45.5 h. All in all 31 spots on the neurites were mechanically stimulated. Stimulation of 17 spots (55%) induced in at least one neuron spike discharge. The percentage of mechanosensitive spots on the neurites in cytochalasin D was not significant different to the not treated myenteric neurons (45%). Nevertheless the response characteristics of cytochalasin D treated and not treated cultured myenteric neurons were statistically different (Figure 3.15). The overall spike frequency was significantly higher in cytochalasin D treated neurons (8.1 (4.3/12.6) Hz vs. 4.4 (2.2/9.8) Hz; $p=0.002$), as well as the burst spike frequency (17.1 (13.9/24.1) Hz vs. 13.4 (5.9/20.1) Hz; $p=0.001$). The spike frequency during dynamic phase was significantly higher after cytochalasin D incubation (28.1 (19.3/32.9) Hz vs. 9.4 (2.1/18.3) Hz; $p\leq 0.001$), but it was not during sustained phase (3.8 (2.1/7.8) Hz vs. 2.6 (0.7/8.1) Hz). Furthermore, the spike discharge started significantly earlier in cytochalasin D treated mechanosensitive neurons (8 (5/23) ms vs. 55 (13/153) ms; $p\leq 0.001$), but the burst duration was not different (781 (477/1,682) ms vs. 1,080 (418/1,576) ms).

3.5.5 Responses of multipolar neurons to multifocal mechanical stimulation

The ICA images clearly revealed that mechanosensitive myenteric neurons had several signal conducting neurites. To study if all neurites of an individual neuron are

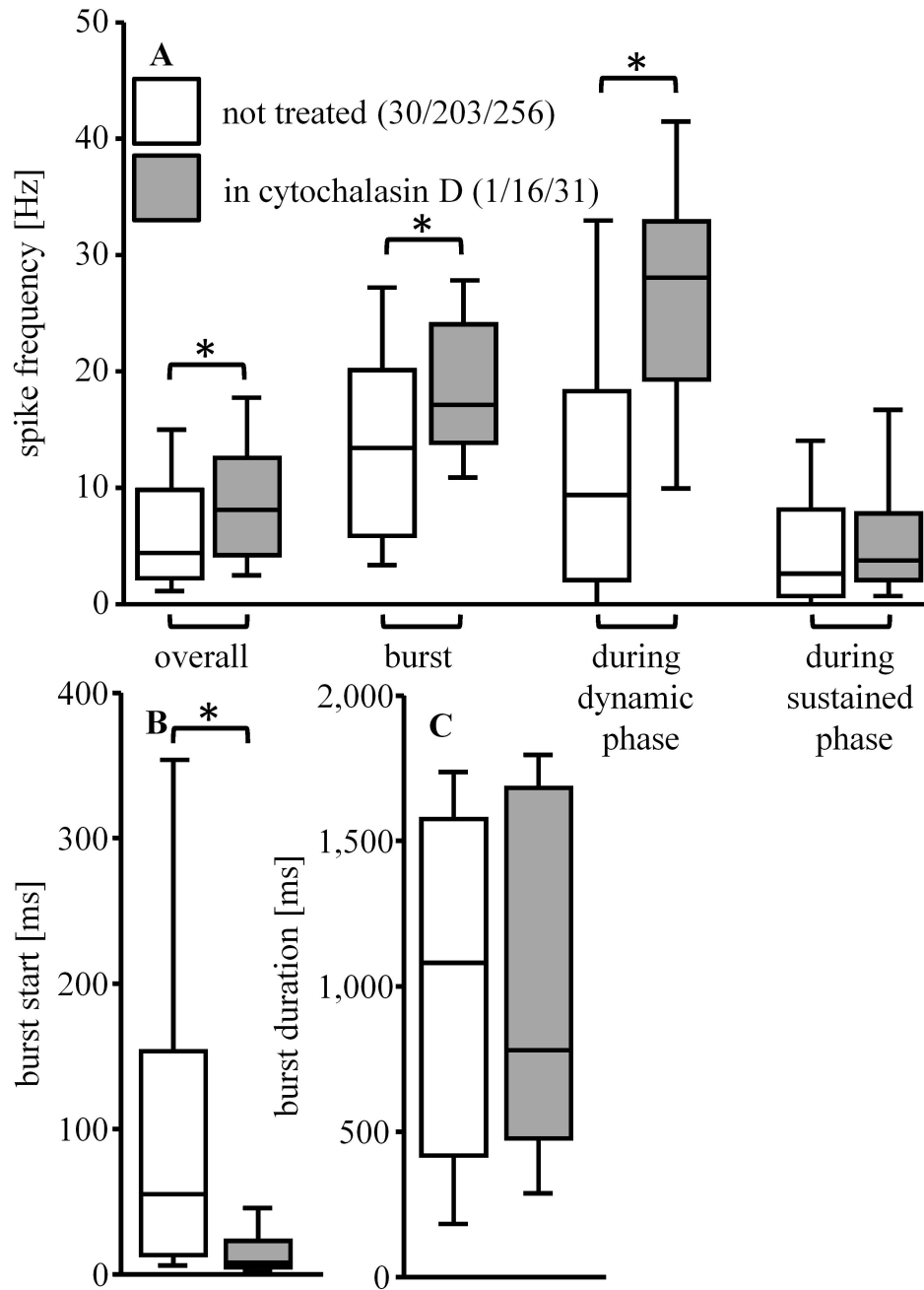


Figure 3.15: Comparison of the response characteristics of not treated and cytochalasin D treated mechanosensitive enteric neurons (Rank Sum test). (A) shows a significant higher overall and burst spike frequency as well as spike frequency during dynamic phase of cytochalasin D treated neurons. The action potential frequency during sustained phase is similar. The burst starts significantly earlier in cytochalasin D treated neurons (B). The burst duration is similar in not treated and cytochalasin D treated neurons (C). N numbers in parenthesis show the number of guinea pigs / clusters / neurons, respectively.

mechanosensitive; several neurites were probed of one particular neuron with the carbon fiber. Prior to probing neurites belonging to one neuron were identified with the ICA image generated by spike discharge in response to nicotine. All in all, the soma and neurites of 52 neurons in 15 clusters from 4 guinea pigs were identified. These neurons were classified by the percentage of mechanosensitive neurites. Of these neurons 8 were not mechanosensitive at all. In 21 neurons all probed neurites responded to carbon fiber stimulation. In 3 neurons 75% of the probed neurites were mechanosensitive, in 4 neurons 67%, in 8 neurons 50%, in 4 neurons 33%, in two neurons 25% and in two neurons 20% (Figure 3.16).

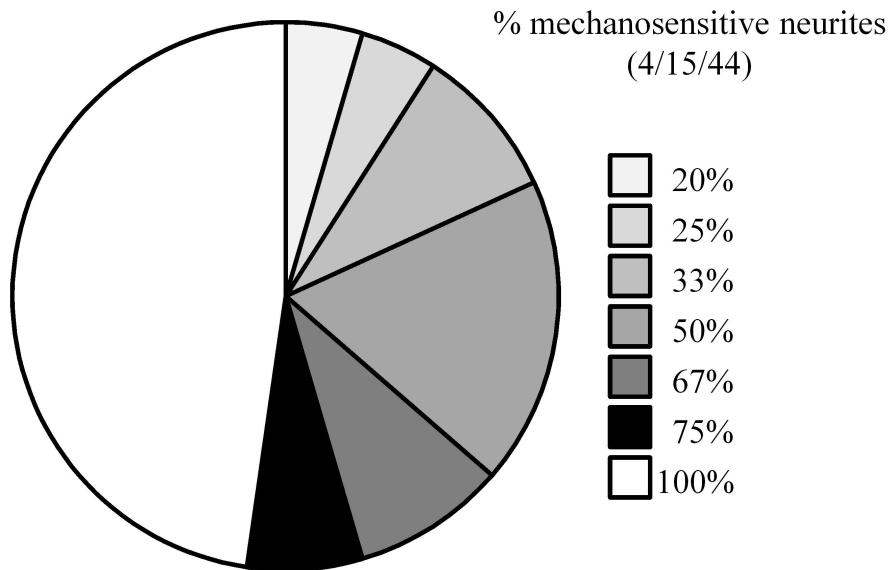


Figure 3.16: Mechanosensitive neurons possess multiple mechanosensitive neurites. Distribution of the percentages of mechanosensitive neurites per neuron is shown in a pie chart.

In those neurons that had at least 3 mechanosensitive neurites the responses were compared of each neurite stimulation. Probing different neurites from the same neuron evoked similar responses (Figure 3.17), the burst spike frequency (I: 14.5 (6.8/17.4) Hz vs. II: 15.3 (10.6/19.8) Hz vs. III: 15.8 (4.3/22.3) Hz) as well as the burst duration (I: 867 (398/1,258) ms vs. II: 551 (256/1,288) ms vs. III: 691 (172/1,481) ms) was comparable.

3.5.6 Mechanosensitivity is a property of entire neurites rather than hotspots

To clarify the question if mechanosensitive neurons have hotspots or their entire neurites are mechanosensitive stimulation was performed along one selected neurite. 13 mechanosensitive neurites were stimulated in 5 clusters from 4 guinea pigs 3 times along

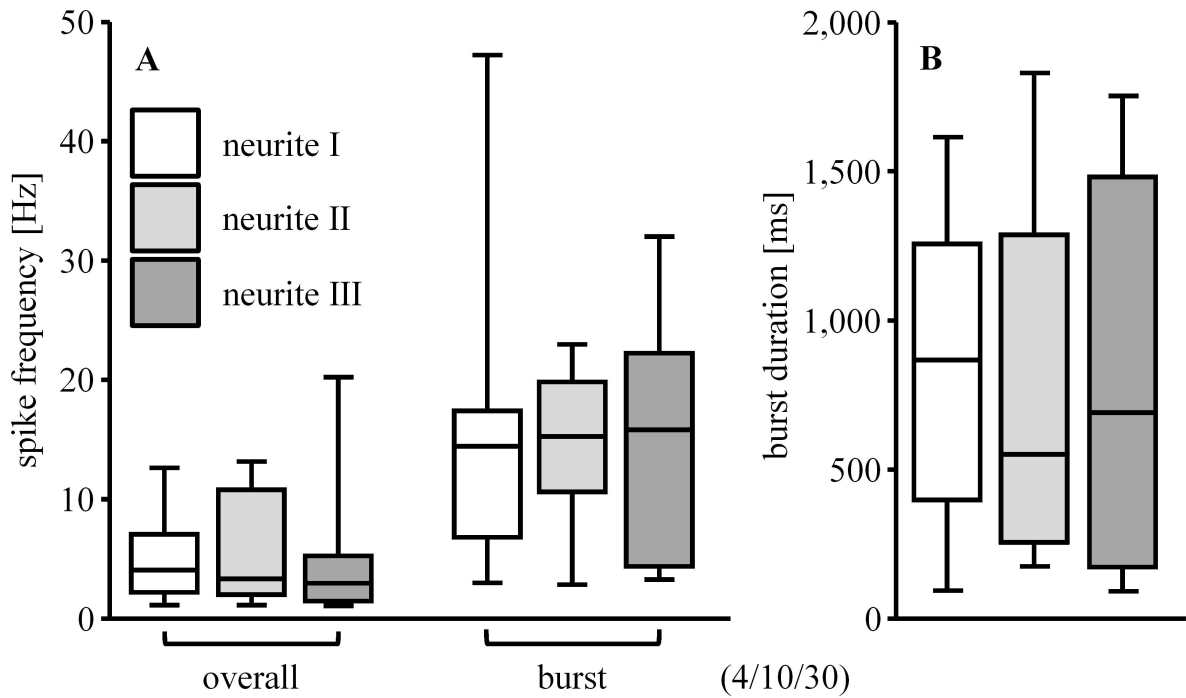


Figure 3.17: Comparison of the response to carbon fiber stimulation of 3 mechanosensitive neurites of the same neuron (Repeated Measurements ANOVA on Ranks test). (A) shows a similar overall and burst spike frequency for stimulation of 3 neurites of the same neuron. The duration of the spike burst is as well similar (B).

a fiber tract. The majority (77%) fired spikes in response to all 3 stimulations, whereas 3 neurons were only activated by two of them. This suggests that mechanosensitive neurons have mechanosensitive neurites rather than mechanosensitive hotspots on a neurite. Comparing the burst spike frequencies in a paired manner starting with the stimulation that was the most far away to the cluster to the one that was the closest to the cluster showed no significant difference (10.0 (3.4/21.3) Hz vs. 7.8 (3.2/15.4) Hz vs. 6.1 (4.8/11.8) Hz; Figure 3.18).

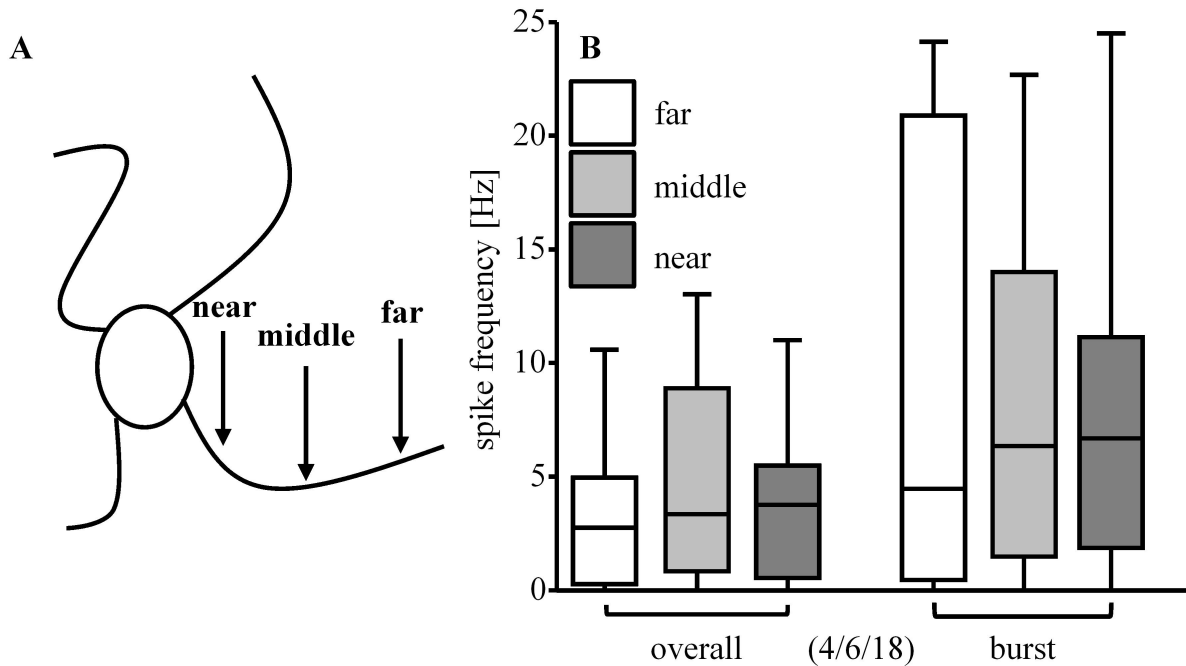


Figure 3.18: Comparison of the response to carbon fiber stimulation of 3 locations on one mechanosensitive neurite (Repeated Measurements ANOVA on Ranks test). The first location is far away from the neuronal cell body, the second location in a middle distance and the third location is the nearest to the cell body (A). There is neither a difference in the overall nor the burst spike frequency of the response to carbon fiber stimulation at the 3 different locations (B).

3.5.7 Reduced soma excitability affects spike invasion into neurites

Most of the mechanosensitive myenteric neurons were excited by stimulation of different neurites. This showed high excitability of the neurons at different sites. The gating concept was experimentally tested, which suggests that excitability of the soma controls spike invasion into neurites. Local application of adenosine (0.5 mM) was used to inhibit spike generation (Figure 3.19).

This phenomenon was shown in one cluster deriving from one guinea pig. Since neurites run together and many neurons can be activated by stimulation of one spot this was

3. RESULTS

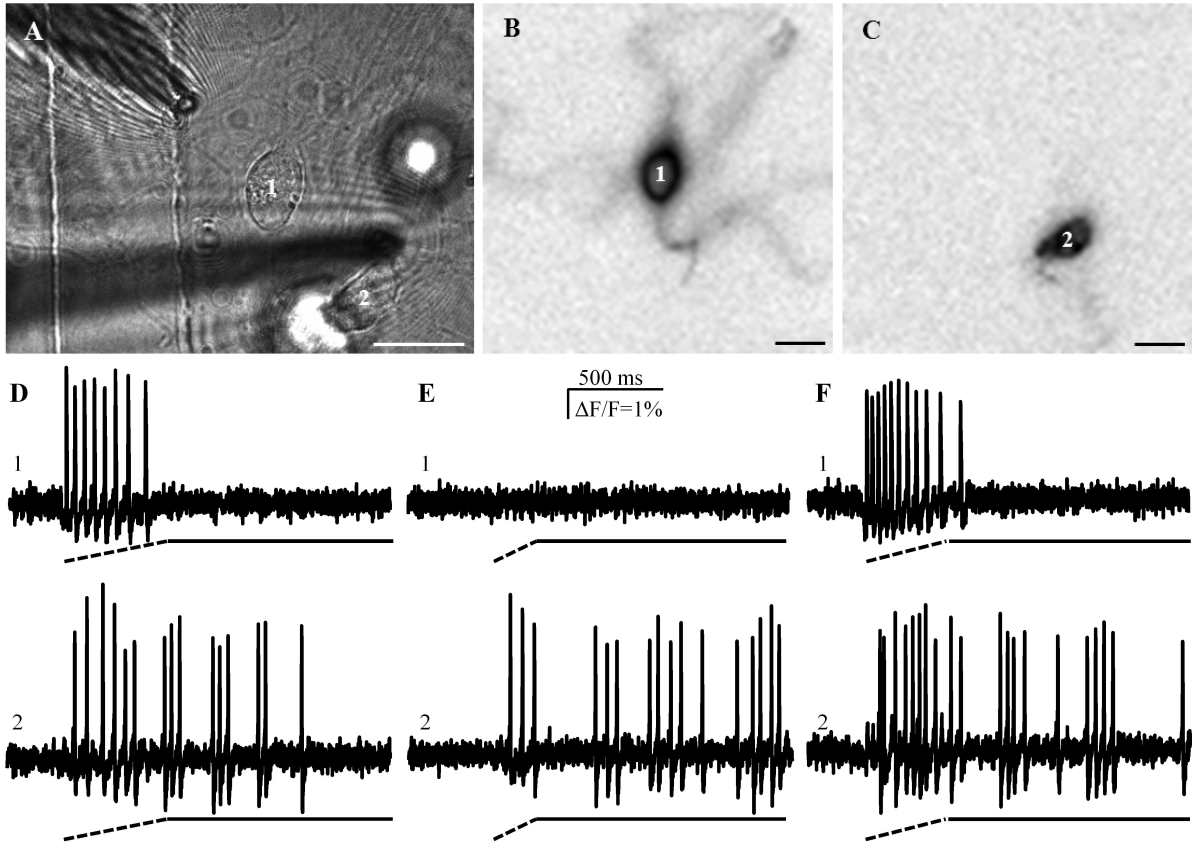


Figure 3.19: Modulation of mechanosensitive myenteric neurons by adenosine. (A) shows a bright field picture of two neurons. The carbon fiber is pressed on the neurite on the spot marked with the white arrow. Adenosine is applied with the micropipette marked with the black arrow. Neuron 1 (B) and neuron 2 (C) are mechanosensitive. The spike discharge is displayed in the traces, upper traces for neuron 1 and lower traces for neuron 2. (D) shows the response to carbon fiber stimulation. In (E) the traces of the mechanical response after local adenosine application on neuron 1 is shown. Spike discharge is blocked only in neuron 1, not in neuron 2. (F) shows the traces in response to carbon fiber stimulation after 10 min washout of adenosine. Both neurons fire spikes in response to the stimulation. Scale bar: 25 μm .

used and a cluster with two mechanosensitive neurons was stimulated (Figure 3.19 B-D). Adenosine was locally applied on only one of these somata. Adenosine totally blocked the spike discharge in this cell body and other neurites, whereas the other neuron still showed excitation by mechanical stimulation (Figure 3.19 E). After washout of adenosine both neurons responded to carbon fiber stimulation (Figure 3.19 F).

3.5.8 Mechanosensitive enteric neurons encode dynamic rather than sustained deformation

A noteworthy phenomenon could be observed when stimulating neurites. During advancement of the carbon fiber (dynamic phase) the neurons fired with a much higher spike frequency compared to the sustained phase of the deformation. It was investigated if the retraction of the carbon fiber as a dynamic change also excited myenteric neurons to support the hypothesis that myenteric neurons encode dynamic deformation. For these experiments the recording time was extended to 4-6 s. First the carbon fiber was pressed on a neurite and then retracted after 2-3 s. Experiments were performed in 30 neurons of 7 clusters from 3 guinea pigs. 63% (19 out of 30) of the neurons responded to both stimuli: application and release of the mechanical stress (Figure 3.20 A). 20% of the neurons (6 out of 30) responded when the carbon fiber was pressed down but not when it was retracted. 17% (5 out of 30 neurons) responded only when the carbon fiber was retracted (Figure 3.20 B).

The overall spike frequency (2.7 (1.2/5.0) Hz vs. 2.0 (1.0/6.7) Hz) as well as the burst spike frequency (6.4 (3.0/10.6) Hz vs. 4.6 (1.5/11.2) Hz) was not significantly different in neurons responding to both stimuli (Figure 3.20 C).

3.5.9 The site of mechanical stimulation is the site of origin of the electrical signal

With the 1 kHz sampling rate neurite deformation evoked spikes at the site of stimulation as well as the soma without measurable delay. In order to demonstrate that the spikes indeed originated in the neurite at the site of deformation TTX was locally applied via a small-tipped pipette proximal to the stimulus site. The local blockade was validated by showing that the local TTX application blocked invasion of spikes into the soma induced by electrical stimulation. In one cluster 3 neurons responded to neurite deformation with spike discharge in neurite and soma. Local TTX application prevented the spike invasion of the somata, which recovered after 10 min washout (Figure 3.21).

3.5.10 Conduction velocity

To calculate the conduction velocity in few experiments a 10 kHz sampling frequency was used, which however limited the field of view to 12 pixels x 80 pixels. With this technique spike propagation along neurites could be followed of 5 neurons. The conduction velocity was 0.19 ± 0.06 m/s (Figure 3.22).

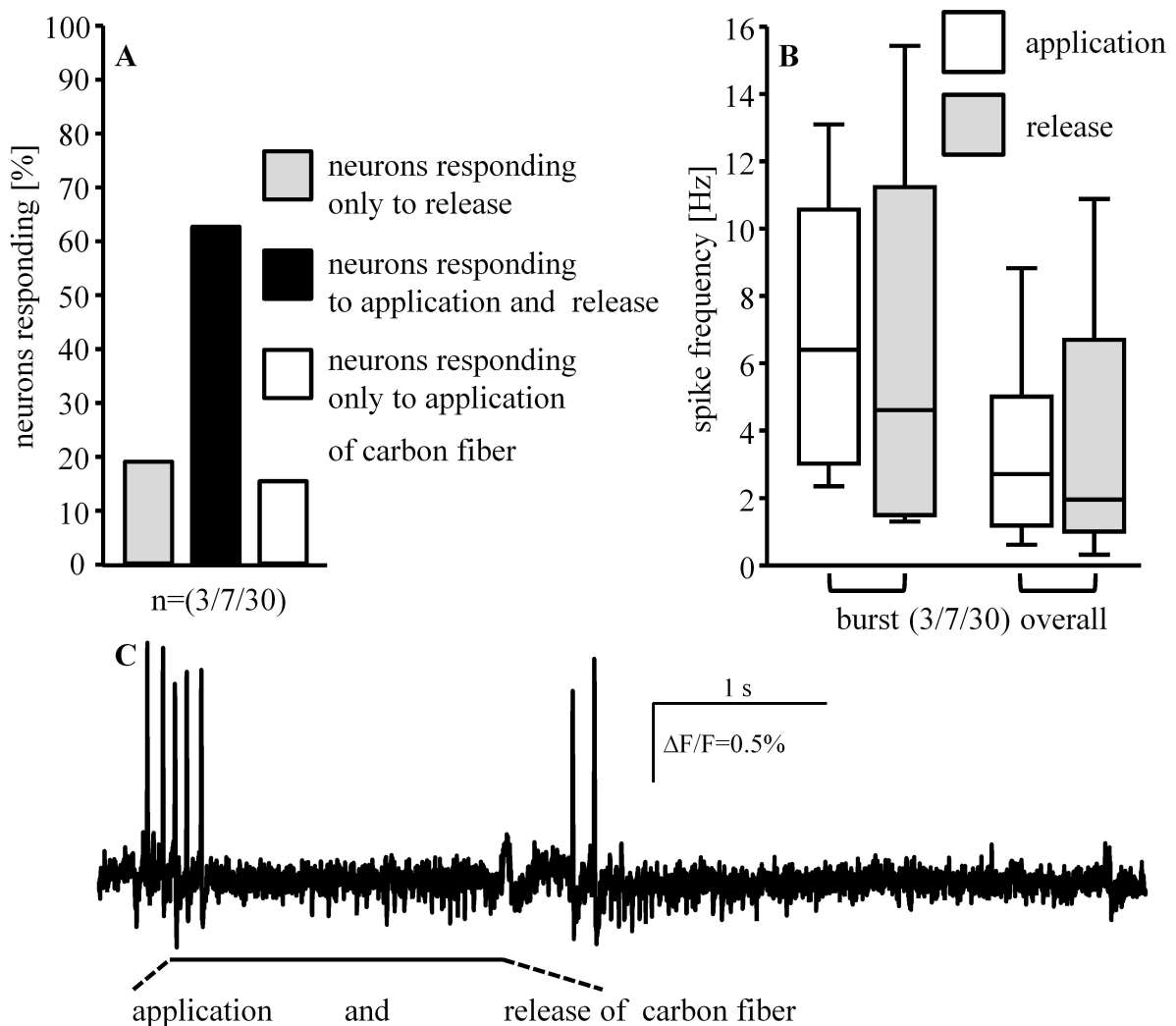


Figure 3.20: Application and release of the carbon fiber on a neurite leads to an excitatory response. In (A) are shown the percentages of the mechanosensitive populations that responded to both stimuli or one of the two stimuli. Comparison of the overall and burst spike frequencies of neurons responding to both stimuli shows no significant difference (B; Mann-Whitney Rank Sum test). (C) shows the response of a neuron excited by application as well as by release of the stimulus. The dashed lines correlate to each dynamic phase of the stimulation and the continuous line to the sustained phase.

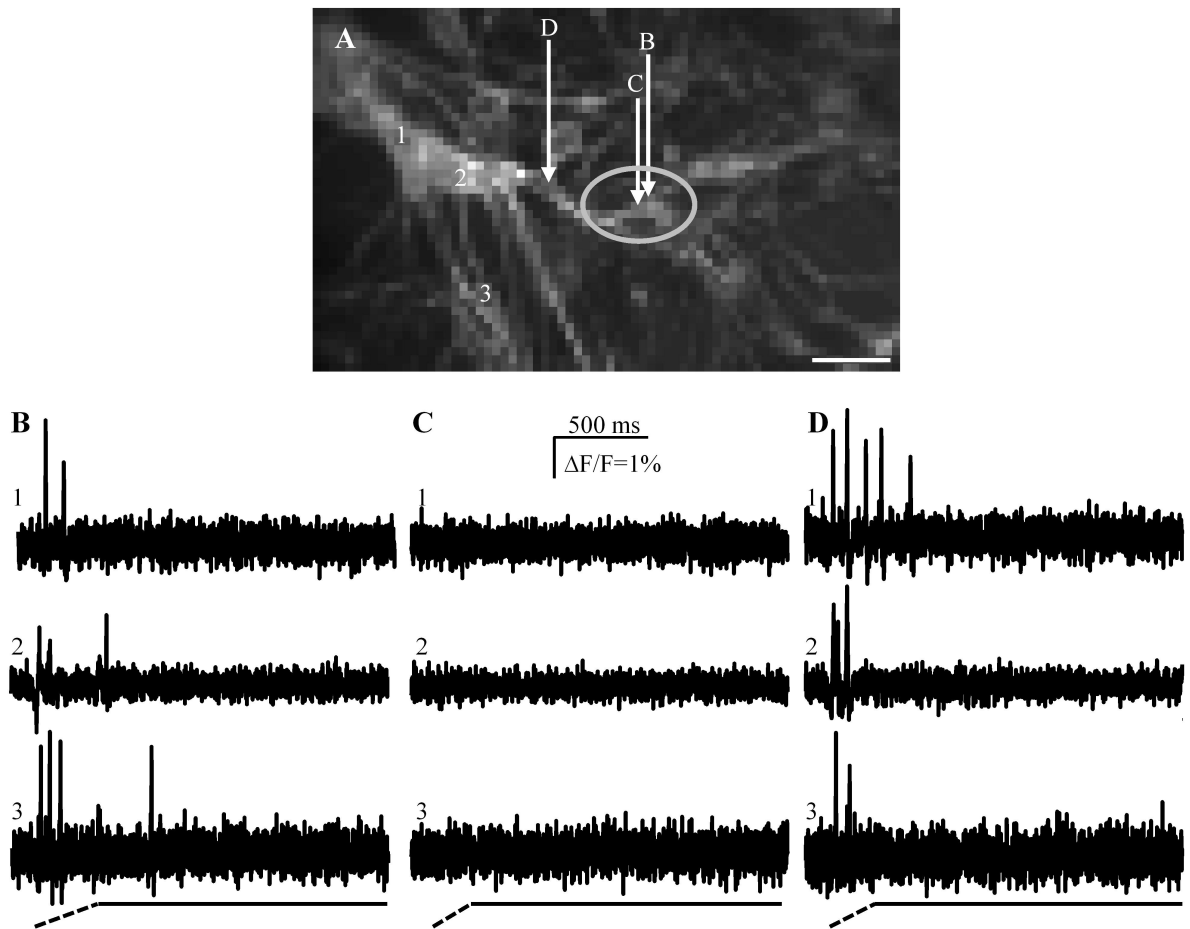


Figure 3.21: The site of mechanical stimulation is the site of the origin of the electrical signal. (A) shows a picture of the cluster. The carbon fiber stimulation is indicated by the white arrows at locations B, C and D. The traces of the three mechanosensitive neurons (1, 2 and 3) corresponding to the stimulation site B are shown in (B); the same is valid for (C) and (D). TTX is locally applied at the area encircled in grey to block neuronal activity. (B) shows spike discharge of all 3 neurons in response to carbon fiber stimulation B. In (C) all neurons are quiescent after local application of TTX and in (D) after 10 min washout of TTX all 3 neurons fire spikes in response to carbon fiber stimulation. Scale bar: 50 μm .

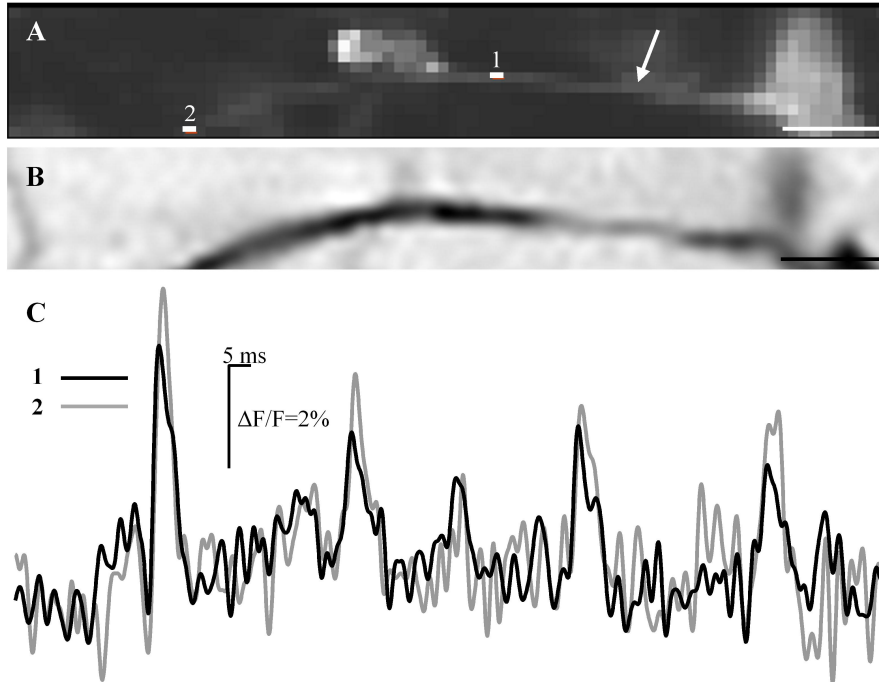


Figure 3.22: Method for the determination of the conduction velocity. (A) shows a picture of the field of view. The position of the carbon fiber stimulation is indicated with a white arrow. The positions marked with the white line and labelled with a number correspond to the positions of the site where the traces of (C) are derived. (B) shows the ICA image. Position 1 and 2 are on the same neurite. The traces of (C) are filtered with a Butterworth filter (402.4 low pass, 2.7 high pass) and a band-stop/pass-filter (9.9 right boundary) (timescale from 150 ms to 350 ms). Comparison of the two traces shows a slight time shift of every spike. Sale bar: 50 μm .

3.5.11 Timing of neuronal and non-neuronal responses

Non-neuronal responses were recorded with Ca^{2+} -sensitive dye. Thereby the relative timing of the different cell types was revealed. Experiments were performed in 23 clusters from 3 guinea pigs and were only used for descriptive purposes. The experiments showed that the increase of $[\text{Ca}^{2+}]_i$ in the neuron started exactly at the same time point in the spot on the neurite that is probed as well in the soma (Figure 3.23). On the other hand in other non-neuronal cells, in this case a fibroblast-like cell, the $[\text{Ca}^{2+}]_i$ increase started locally at the point, which was probed, and then from this point the signal was slowly (within seconds) transduced in the whole fibroblast (Figure 3.23).

3.5.12 Primary culture of human myenteric neurons show similar behaviour in response to mechanical stimulation

The translational aspects of the results were studied in primary culture of myenteric neurons from human tissue samples. Experiments were performed in 64 clusters from 19 human tissue samples. The ultra-fine carbon fiber was pressed on neurites, which led in 34% (86 from 251) of the neurons to spike discharge. The neurons activated by the mechanical stimulation fired with an overall spike frequency of 3.9 (2.2/6.8) Hz and a burst spike frequency of 6.0 (4.1/11.1) Hz. The duration of the dynamic phase of the stimulus was 320 (250/425) ms. The spike frequency of the dynamic phase was 7.0 (0.5/15.7) Hz. It was significantly higher than the spike frequency during sustained phase with 3.2 (1.5/5.7) Hz ($p \leq 0.001$). The first spike occurred 21 (10/216) ms after the advancement of the carbon fiber. The spike burst lasted 1,328 (1,071/1,607) ms.

Comparing the overall spike frequency of guinea pig and human in response to mechanical stimulation there was no significant difference (Figure 3.24 A). In contrast the burst spike frequency was significantly higher in guinea pig compared to human ($p \leq 0.001$; Figure 3.24 A). The spike frequency during dynamic phase and sustained phase was not significantly different between these two species (Figure 3.24 A). The start of the spike frequency was not different (Figure 3.24 B), whereas the burst time was significantly higher in human than in guinea pig ($p = 0.021$; Figure 3.24 C). The percentages of mechanosensitive neurites in guinea pig was significantly higher than in human ($p = 0.015$).

3. RESULTS

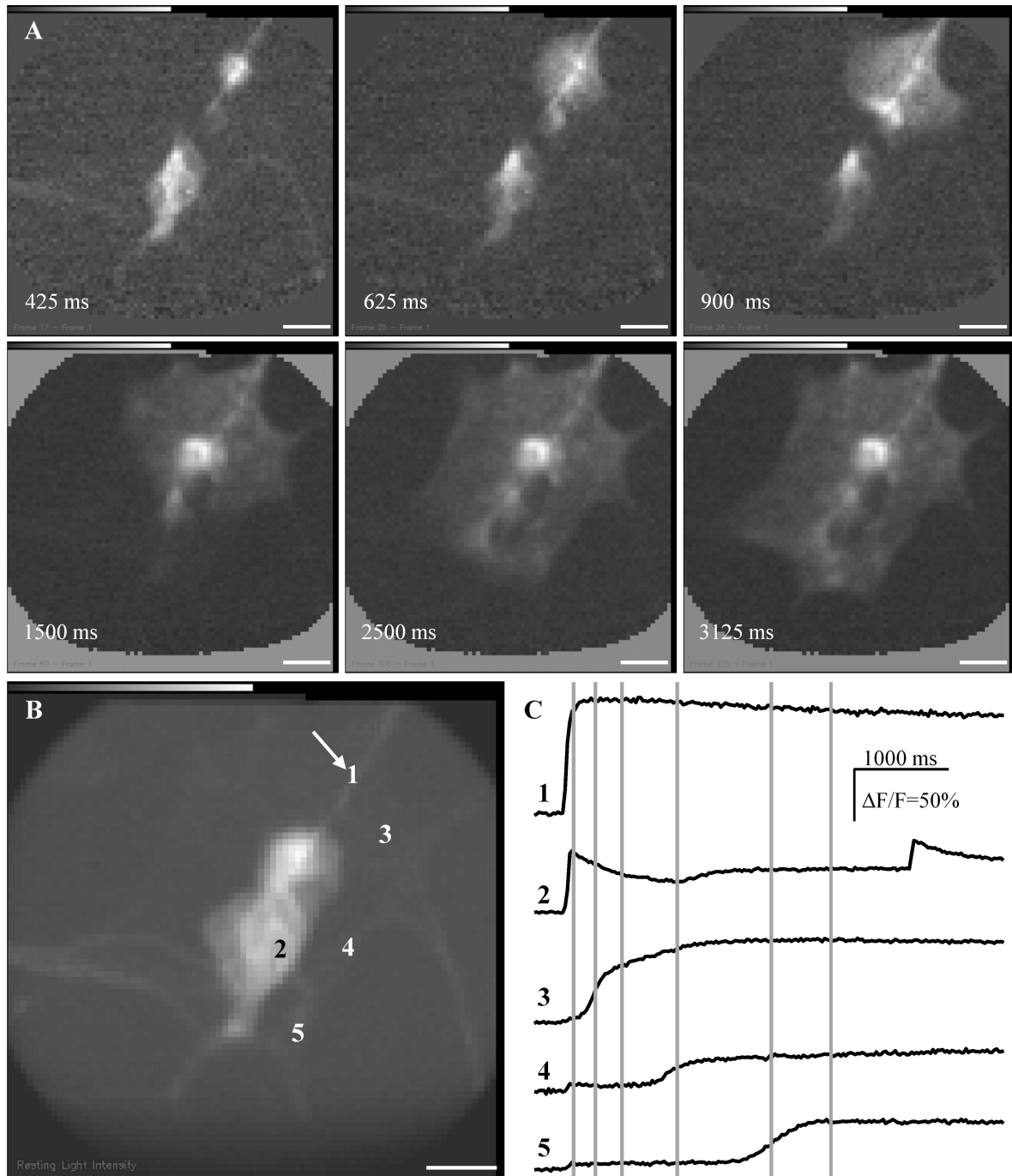


Figure 3.23: The timing of mechanosensitive responses in neuronal and non-neuronal cells is different. (A) shows frame subtraction images from the increase in intracellular calcium ($[Ca^{2+}]_i$) in the field of view at different time points as indicated in the picture. (B) shows the resting light intensity of the field of view. The place of mechanical stimulation is indicated with the white arrow. The area from which the traces in (C) are derived are numbered in (B). 1 is the stimulated neurite, 2 a soma, 3, 4 and 5 are different positions on a fibroblast. (C) shows the relative increase of $[Ca^{2+}]_i$ for the different positions. The gray lines indicate the different time points of (A). Scale bar: 25 μm .

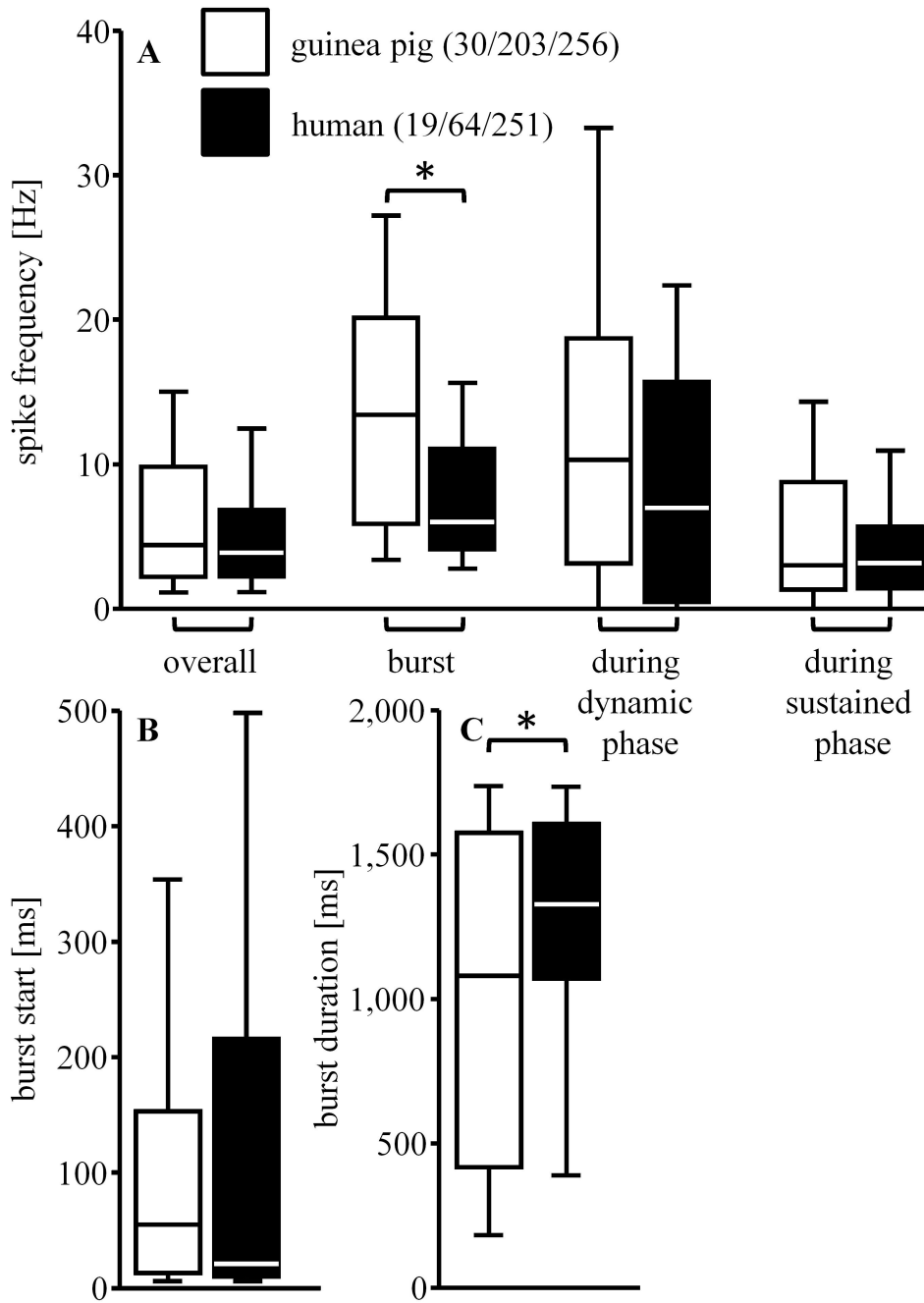


Figure 3.24: Comparison of the response characteristics of mechanosensitive myenteric neurons from guinea pig and human (Sum Rank test). (A) shows no significant difference of the overall spike frequency, but the burst spike frequency. The spike frequencies during dynamic and sustained phase are similar in both species. Comparison of the start of the spike burst (B) shows no significant difference. The burst duration (C) is significantly higher in human compared to guinea pig.

3.6 Identification of mechanical stimulus modalities exciting primary cultured myenteric neurons with non-contact methods

3.6.1 Normal stress

Hydrostatic pressure

With hydrostatic pressure mechanical stimulation occurring during phasic contraction was mimicked. Hydrostatic pressure was used to test the response to normal stress. First reproducibility of the stimulus was tested in 24 clusters with 206 neurons from 3 guinea pigs. Pulses with 1.0 bar were applied for 200 ms and recorded for 2 s. The percentage of responding neurons (80 (60/100) % vs. 75 (53/100) %) did not change. The overall spike frequency (1.6 (0.5/4.7) Hz vs. 2.1 (1.1/4.2) Hz) of the first and second application was not significant different.

For examination of the force strength dependency two different pressures were used. The microejection system was adjusted to 0.7 bar or 1.0 bar. The stimuli were applied in alternating order on 24 clusters with 330 neurons from 4 guinea pigs. To the higher stress a significantly higher percentage of neurons per cluster responded (17 (8/35) % vs. 35 (29/55) %; $p=0.005$; Figure 3.25 D). In addition, the overall spike frequency of all neurons responding at least once was significantly higher for the higher stress (5.3 (2.2/9.6) Hz vs. 1.1 (0.0/5.4) Hz; $p\leq 0.001$; Figure 3.25 E). Comparing the overall spike frequency of the responding neurons of each group showed the same (6.6 (3.9/10.6) Hz vs. 4.3 (2.1/11.1) Hz; $p=0.031$). The spike onset was significantly earlier for the higher stimulus (90 (48/141) ms vs. 132 (61/269) ms; $p=0.008$; Figure 3.25 F) and the spike discharge duration was longer (1,579 (730/1,818) ms vs. 1,429 (403/1,650) ms; $p\leq 0.001$; Figure 3.25 G).

Variation of the pulse duration was additionally tested. Pulses of 1 s and 2 s durations were tested with a recording time of 3 s. Experiments were performed in 39 clusters with 444 neurons from 4 guinea pigs. There was no difference in the percentage of neurons responding between the two pulse durations (1 s: 9 (0/20) % vs. 2 s: 7 (0/20) %; Figure 3.26 A). The overall spike frequency (1 s: 1.0 (0.0/2.8) Hz vs. 2 s: 0.3 (0.0/3.1) Hz; Figure 3.26 B) was similar. Furthermore the timing of the response was not different between the two stimulus durations. There was no difference in the onset of the spike discharge (1 s: 209 (45/643) ms vs. 2 s: 80 (44/358) ms; Figure 3.26 C) as well as in the burst duration (1 s: 523 (248/2,032) ms vs. 2 s: 1,270 (448/2,403) ms; Figure 3.26 D).

To test if the proportion of normal stress and shear stress plays a role in the mechanical response different angles of the application pipette to the dish surface (45 ° and 90 °) were tested on 26 clusters from 4 guinea pigs. Unfortunately the construction of the arch was not precise enough to adjust the pipette once and change only the angle,

3. RESULTS

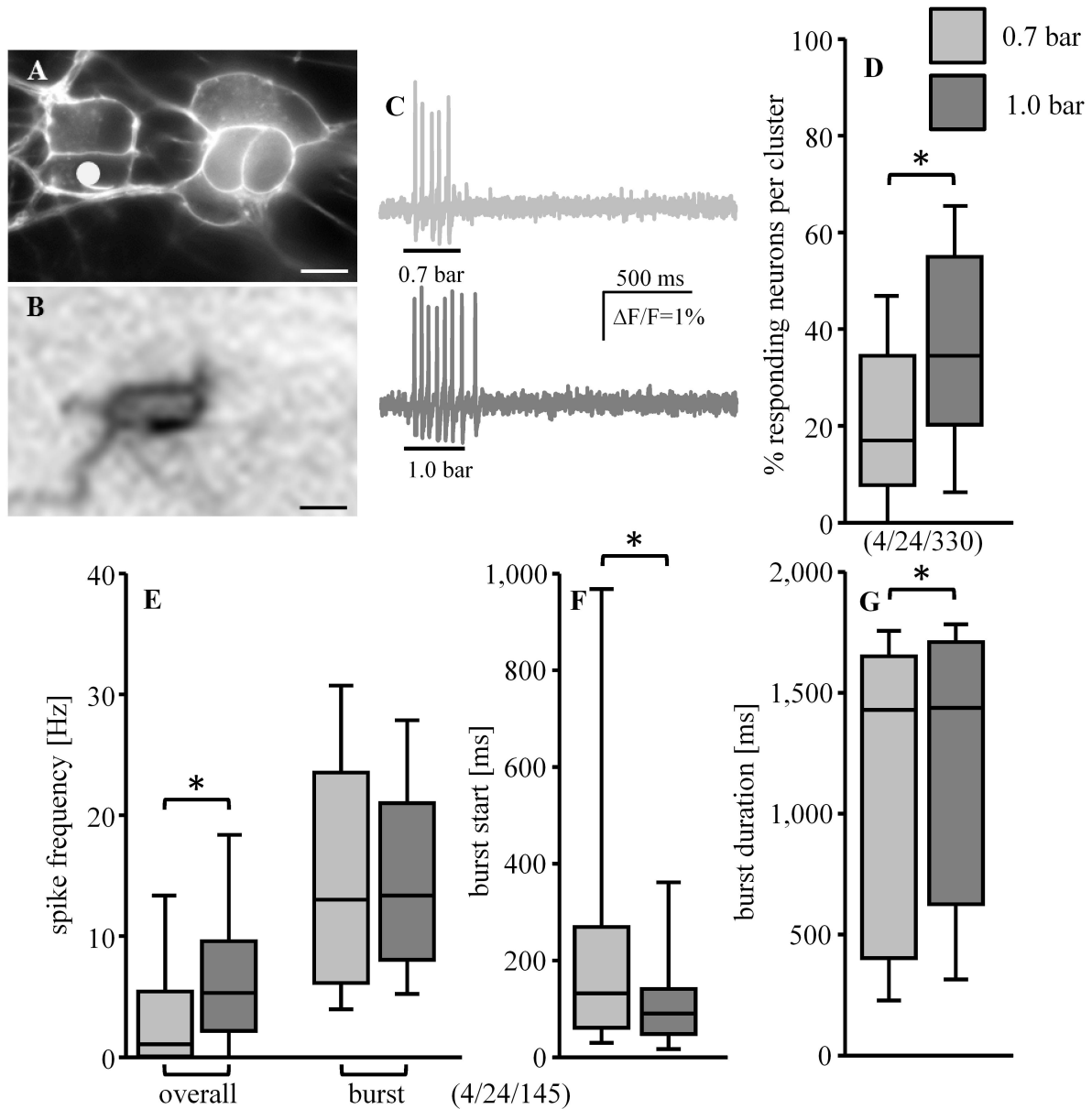


Figure 3.25: Comparison of the responses to different hydrostatic pressures (Sum Rank test). In (A) is a picture of the stimulated cluster. The neuron of interest is marked with the white dot, its ICA image is shown in (B). The response traces are shown in (C). The stimulation is indicated by the line below the trace with its corresponding pressure. The higher pressure induces a stronger spike discharge. The comparison of the percentage of neurons responding per cluster (D) shows that it is significantly higher for the higher hydrostatic pressure. The overall spike frequency (E) is significantly higher for the higher hydrostatic pressure, but not the burst spike frequency (E). The spike burst starts significantly earlier for the higher hydrostatic pressure (F). The spike burst duration (G) is significantly longer for the higher hydrostatic pressure. Scale bar: 10 μm .

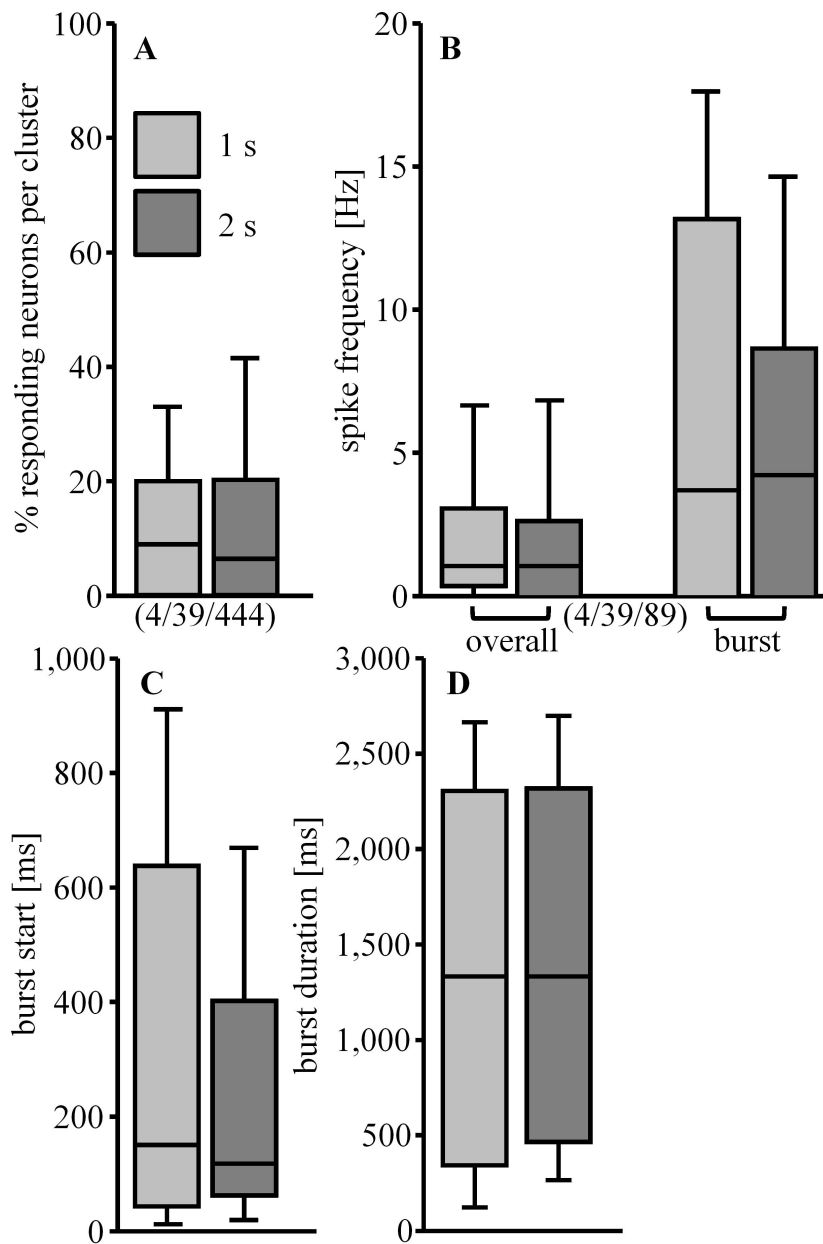


Figure 3.26: Comparison of the response characteristics for different pulse durations of hydrostatic pressure (Sum Rank test). The comparison of the percentage of neurons responding per cluster shows no significant difference (A). The overall and burst spike frequency is similar (B). The start of the spike burst (C) and the duration (D) is not significantly different between the two application times.

because then the distance varied enormously and this has also an effect on the applied force. Furthermore, with an angle of 90 ° it was not possible to visualize the pipette tip through the microscope, which is another disadvantage for the control of the distance. Therefore, experiments could not be performed paired and most pressure pulses did not activate the neurons. These experiments were not analyzed, because of these reasons.

Stretch

With stretch mechanical stimulation occurring during tonic contraction was mimicked. Stretch was also used to test the response to normal stress.

Validation of the coating procedures showed that only a combination of Poly-D-Lysine and human extracellular matrix can be used. On all other coatings the neurons did not attach or detached quickly.

In the first experiments it was tried to apply stretch with a glass pipette by indenting it 10 μm into the elastic bottom of the dish close to the cluster. This technique was used in 33 clusters from 9 guinea pigs. Indeed, spike discharge was induced with this technique (data not shown). Nevertheless, further analysis showed that with this technique it was not possible to really stretch neurons.

Therefore, a technique was used learned at the research center Jülich. Decaying deformation fields were induced by pulling an elastic surface with a gauge needle. With this method 93 clusters with 950 neurons from 15 guinea pigs were stretched. Of the stimulated neurons 13 (0/22) % per cluster responded to stretch with an overall spike frequency of 1.9 (0.7/3.2) Hz (Figure 3.27). The stimulation with the gauge needle resulted in a short dynamic phase lasting 425 (350/538) ms and a long sustained phase by not moving the gauge needle until the end of the recording time of 5 s. It was retracted after recording. Comparing the spike frequency during dynamic and sustained phase showed that it was significantly higher during sustained phase (0.0 (0.0/1.7) Hz vs. 1.9 (0.7/3.3) Hz; $p \leq 0.001$). The spike discharge started 532 (170/1,251) ms after the stimulation and lasted 4,040 (3,412/4,460) ms. In these experiments the analysis of the stretch in the plane parallel to the dish surface showed that in 91% of the activated neurons the \sum stretch of 2.9 (1.3/5.3) % was bigger than the \sum compression of 1.0 (0.5/1.7) % ($p \leq 0.001$; Figure 3.27 D). A range of \sum stretch of 0.1% - 30.4% was achieved. The maximal stretch in a neuron was 1.9 (0.8/3.7) % (range: 0.1 - 8.2%) in the line parallel to the deformation field. Correlation of the \sum stretch, \sum compression, maximal stretch and maximal compression for each neuron with the overall spike frequency and the burst spike frequency showed in none of the cases a correlation between the two values.

Furthermore, it was tried to induce the same deformation at the same cluster twice by pulling the gauge needle at the same position 10 min apart. Experiments were performed in 15 clusters with 166 neurons from 3 guinea pigs. Analysis of the \sum stretch of the responding neurons showed that it was not possible to induce exactly the same

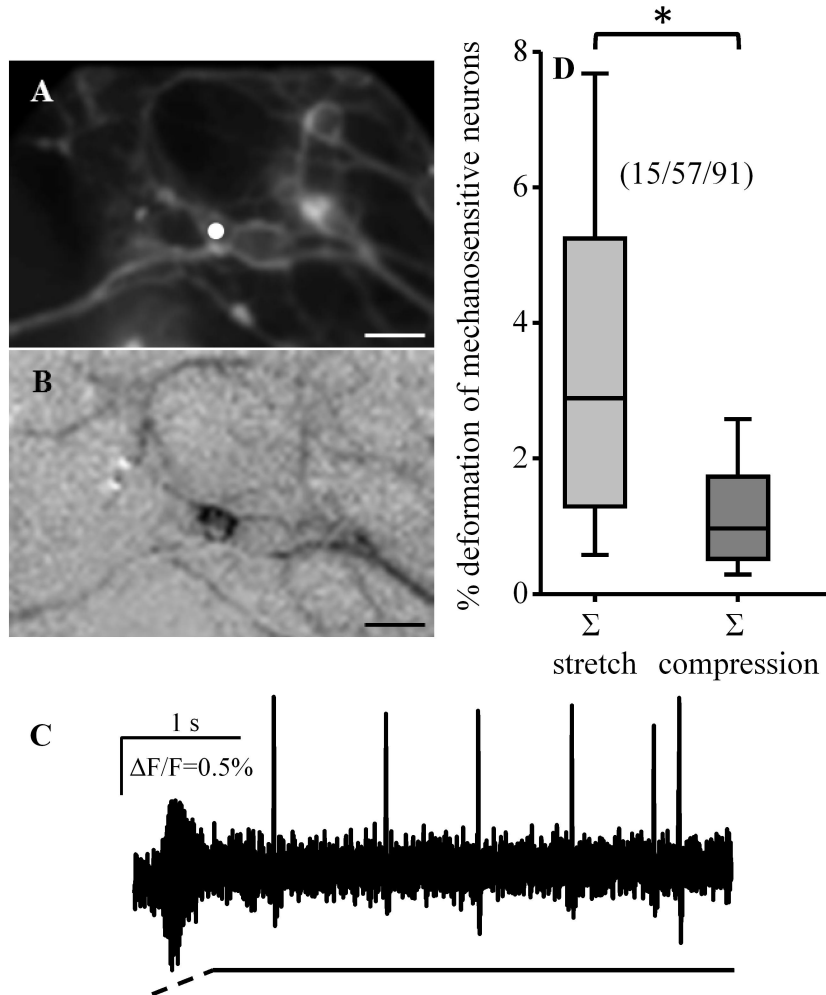


Figure 3.27: Stretching myenteric neurons induces spike discharge. (A) shows a picture of a cluster; a mechanosensitive neuron is marked with a white dot. The ICA image of this neuron is displayed in (B). The spike pattern in response to stretch is shown in (C). Comparison of the summed (Σ) stretch and the Σ compression (Sum Rank test) shows a significant higher Σ stretch (D). Scale bar: 25 μ m.

3. RESULTS

stretch and deformation field for each neuron twice. The \sum stretch between the first (2.7 (1.3/3.8) %) and the second (2.1 (1.1/3.5) %) application was significantly different ($p=0.012$). These experiments were used to test a force strength dependency of the neuronal response to stretch. The two stimulations were divided into two classes; the first one with lower maximal stretch and the second with higher maximal stretch (1.4 (0.7/1.9) % vs. 2.3 (1.3/3.9) %; $p\leq 0.001$; Figure 3.28 A). The overall spike frequency was in the second class as well significantly increased (0.0 (0.0/1.9) Hz vs. 1.9 (0.7/3.4) Hz; $p=0.01$; Figure 3.28 B). This demonstrated a force strength dependency in response to a stimulus mimicking tonic contractions.

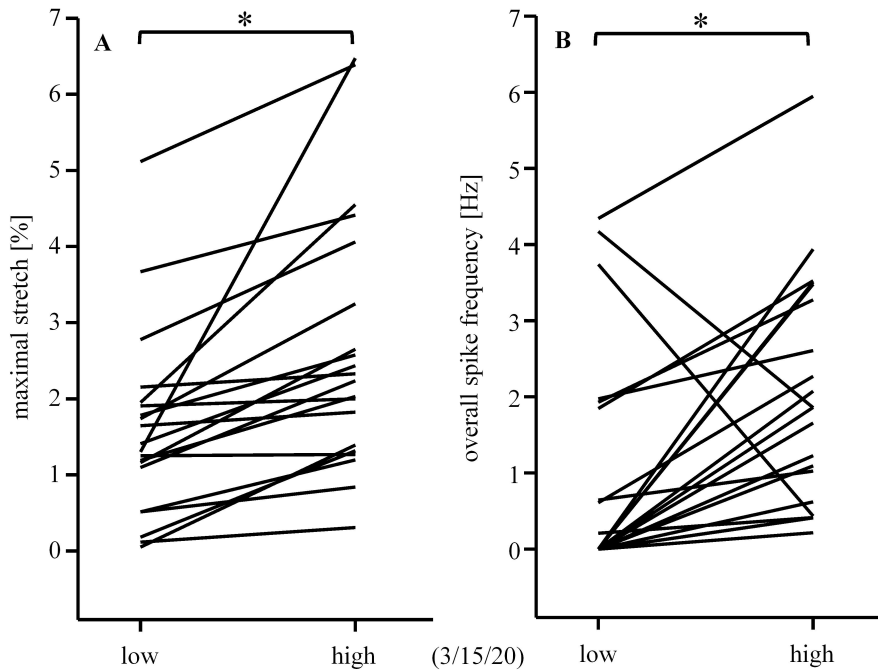


Figure 3.28: Two consecutive applications of stretch induce a different maximal stretch in the same neuron. Dividing the two stimulations in two classes in relation to their maximal stretch shows a significant difference (A). Comparing the overall spike frequency of the same two classes shows a significant increase for the high maximal stretch (B).

In 15 clusters from one guinea pig the gauge needle was additionally retracted during recording. In 4 clusters 7 neurons responded to retraction of the gauge needle. Comparing the micropatterned surface before stretching the neurons and after retracting the gauge needle, there was a shift of the beads in the surface. This means the initial state is not accomplished, the plasticity of the elastic surface did not allow this.

Hydrostatic pressure and stretch

In this set of experiments the two stimulation techniques applying normal stress were tested in a paired way. The myenteric neurons were grown on an elastic surface and then they were exposed to hydrostatic pressure via micropipette (1.0 bar) and stretch by pulling the elastic surface. Paired experiments were performed in 18 clusters with 122 neurons from 4 guinea pigs. 35 of 122 neurons (29%) were at least excited by one of the two stimuli. Of the mechanosensitive neuronal population 46% responded to both stimuli, 17% were only excited by hydrostatic pressure and 37% were only activated by stretch. Although the recording time of these two stimuli was different, we compared some response characteristics. The burst spike frequency to both stimuli was not significantly different (stretch: 2.0 (1.0/3.2) Hz vs. hydrostatic pressure: 2.6 (0.0/13.8) Hz; Figure 3.29 A). The timing of the responses to the two stimuli was different. The onset of the spike discharge was significantly later to stretch (711 (80/2,137) ms vs. 117 (76/392) ms; $p=0.019$; Figure 3.29 B) and the burst time was significantly longer in response to stretch (3,725 (2,566/4,579) ms vs. 652 (229/1,381) ms; $p\leq 0.001$; Figure 3.29 C).

3.6.2 Shear stress

To develop a technique for the application of shear stress first of all micro channels with different dimension were tested (micro channel 0.2: height: 200 μm , width: 5 mm; micro channel 0.4: height: 400 μm , width: 5 mm; micro channel 0.6: height: 600 μm , width: 5 mm; micro channel 0.8: height: 800 μm , width: 5 mm). 4 different channels were used and the shear stress range calculated that could be achieved with them (see Equation 2.4 and Table 3.3).

Further on the micro channel with the height of 400 μm was used because a shear stress range of 0.2 - 0.8 Pa could be achieved that is known to be physiological for endothelial cells (Fisher et al. 2001) and was already used for neurons (Kim et al. 2006).

First of all, as for the other stimuli reproducibility was tested of the stimulation technique using a shear stress of 0.2 - 0.8 Pa. Experiments were performed in 34 clusters with 734 neurons from 6 guinea pigs. Comparing the percentage of responding neurons per cluster a significant difference was found between the first and the second application (0 (0/5) % vs. 6 (0/13) %; $p=0.002$). All in all 64 neurons responded at least to one of the two stimulations but only 20% of them responded to both stimulations. Comparing the overall spike frequency in a paired manner of all neurons responding at least once a significant difference was found (0.0 (0.0/0.6) Hz vs. 0.4 (0.4/1.3) Hz; $p\leq 0.001$). Comparing only the neurons responding to both applications no difference was found (0.7 (0.4/1.7) Hz vs. 0.7 (0.4/1.4) Hz).

Although the response to this stimulus was not reproducible, a dose response relationship was tested. 0.2; 0.4; 0.6 and 0.8 Pa were applied in a random order on 34 clusters with

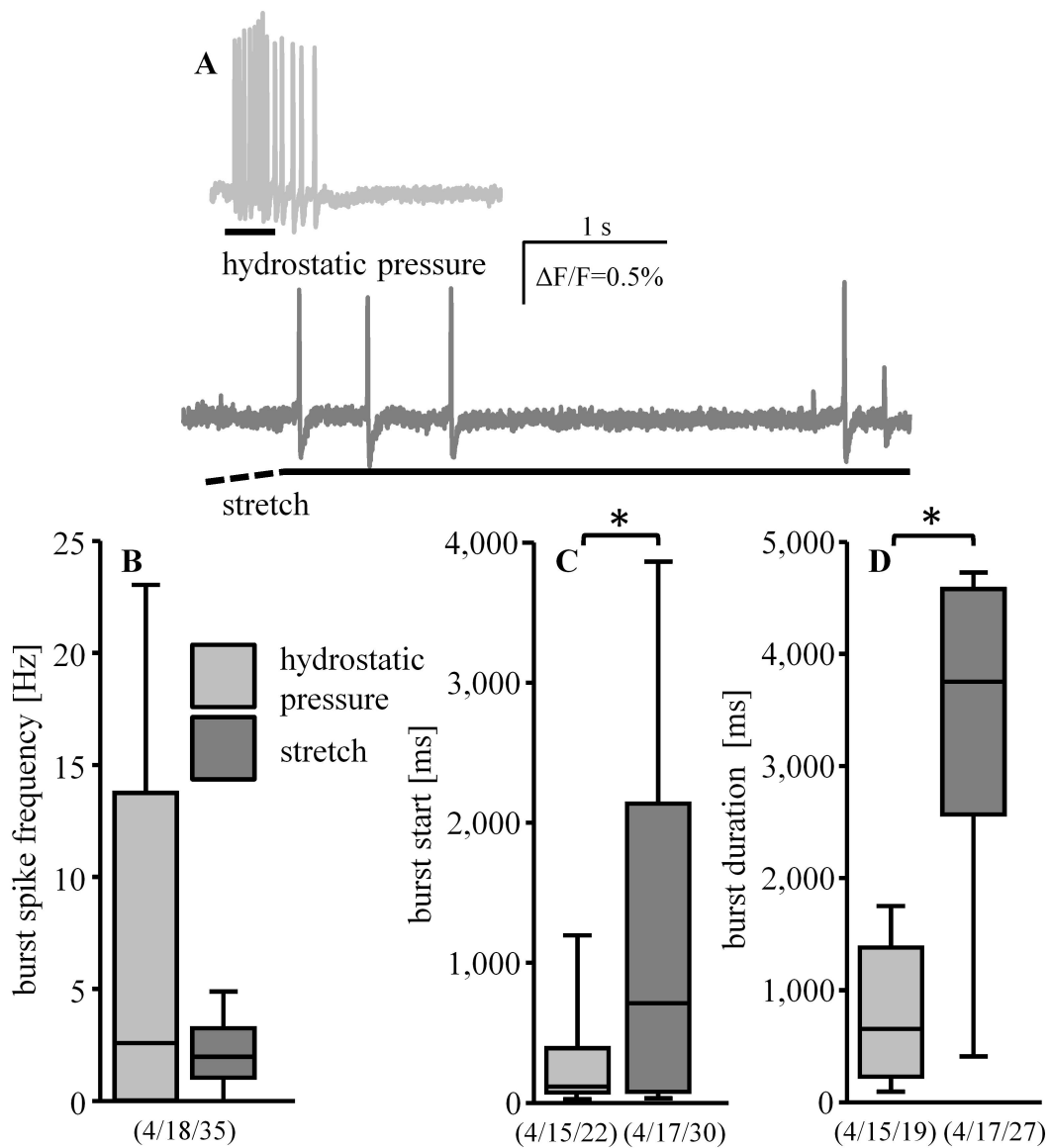


Figure 3.29: Comparison of the response characteristics of mechanosensitive neurons activated by hydrostatic pressure and stretch (Repeated Measurements ANOVA on Ranks test). In (A) are shown the traces of the same neuron responding to hydrostatic pressure and stretch. The burst spike frequency in response to the two stimuli is similar (B). The burst onset is significantly earlier to hydrostatic pressure compared to stretch (C) and the duration is significantly longer to stretch compared to hydrostatic pressure (D).

3. RESULTS

Table 3.3: Parameters for calculation of applied shear stress.

microslide	velocity $[\frac{ml}{min}]$	shear stress [Pa]
0.2	1	0.425
0.2	2	0.85
0.2	3	1.275
0.2	4	1.7
0.2	5	2.125
0.2	10	4.25
0.4	1	0.106
0.4	2	0.213
0.4	3	0.319
0.4	4	0.425
0.4	5	0.531
0.4	10	1.063
0.6	1	0.047
0.6	2	0.094
0.6	3	0.142
0.6	4	0.189
0.6	5	0.236
0.6	10	0.472
0.8	1	0.027
0.8	2	0.053
0.8	3	0.080
0.8	4	0.106
0.8	5	0.133
0.8	10	0.267

3. RESULTS

734 neurons from 6 guinea pigs. To different levels of stress different neurons responded. The percentage of neurons responding per cluster was not significantly different (0.2: 9 (5/19) %; 0.4: 6 (0/19) %; 0.6: 10 (0/19) %; 0.8: 8 (0/12) %; Figure 3.30 D). Neurons responding at least once were compared. Because not always the same neurons responded to all stress strengths the median was in all cases 0.0 Hz. The comparison showed that there was no significant difference in the overall spike frequency between the different stresses (0.2: 0.0 (0.0/0.8) Hz; 0.4: 0.0 (0.0/0.8) Hz; 0.6: 0.0 (0.0/1.1) Hz; 0.8: 0.0 (0.0/1.1) Hz; Figure 3.30 E).

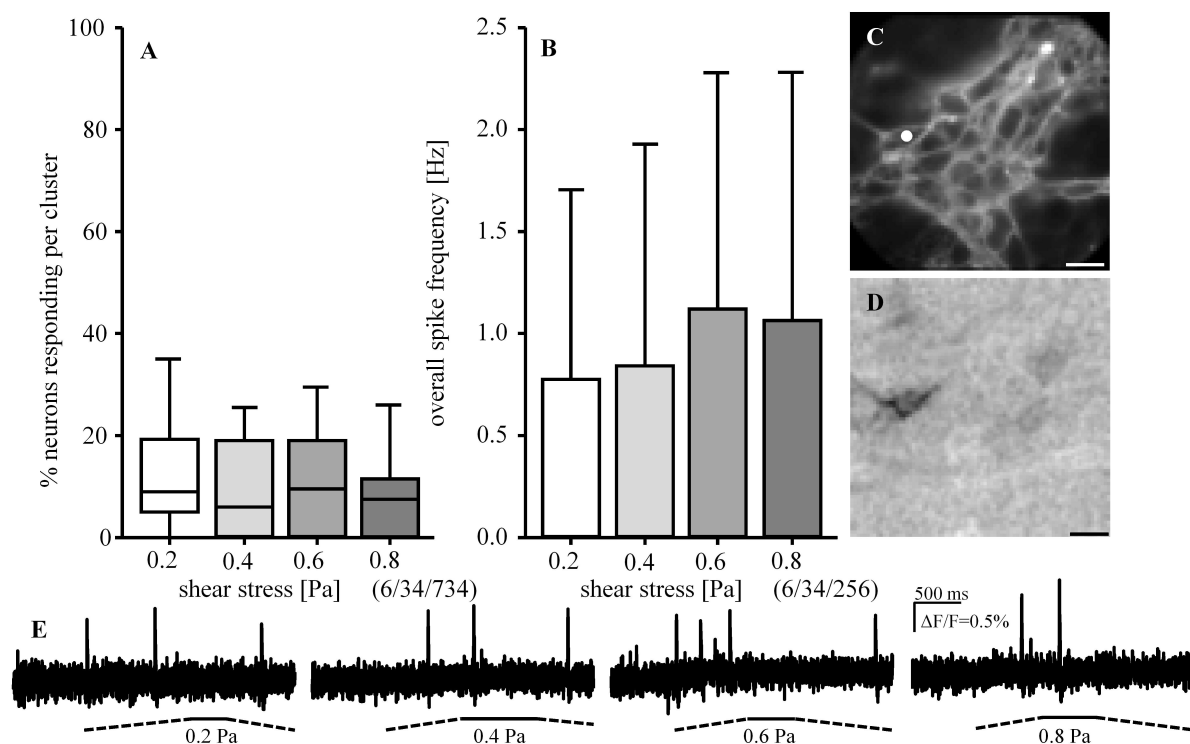


Figure 3.30: The response to shear stress is independent of the applied stress. Comparison of the response characteristics of mechanosensitive neurons activated by different shear stresses (Repeated Measurements ANOVA on Ranks test). Neither the percentage of neurons responding per cluster (A) nor the overall spike frequency (B) is significantly different between the different stresses. In (C) a picture of a stimulated cluster is shown. A mechanosensitive neuron is marked with a white dot. (D) displays its ICA image. The traces in response to different stresses of this neuron are shown in (E). The dashed lines under the traces indicate dynamic phases of the stimulation and the continuous lines the sustained phase. Scale bar: 25 μm .

3.6.3 Summary normal and shear stress

The responses to all 3 types of stimulation techniques showed different characteristics. This was likely to correlate to the fact that each stimulus used had a different strength. Therefore it was not possible to directly compare the response characteristics for all stimuli used. In the following table are the characteristics summarized for the pooled data of different stimulus strengths (Table 3.4).

Table 3.4: Summary of the response characteristics of the mechanical stimulus modalities.

	normal stress		shear stress
	hydrostatic pres- sure	stretch	
force [nN]	77 ± 52	< 50	1000 ± 516
stress duration [ms]	310 (260/370)	4,787 (4,762/4,812)	2,632 (2,467/2,760)
% responding	27 (12/45)	10 (0/27)	5 (0/13)
burst spike frequency [Hz]	13.0 (7.6/21.8)	2.6 (1.9/3.9)	3.0 (2.2/5.1)
reproducibility	yes	n. a.	no
strength dependency	yes	yes	no
burst start [ms]	100 (55/170)	345 (127/880)	660 (261/1,179)
burst duration [ms]	1,440 (579/1,694)	4,220 (3,593/4,464)	1,509 (871/2,012)
number of spikes	11 (6/20)	9 (5/17)	3 (2/5)
recording time [ms]	2,000	5,000	3,000

4 Discussion

This thesis presents several main findings on mechanosensitivity in the ENS.

Myenteric neurons have mechanosensitive neurites as well as somata. Mechanotransduction is not limited to specialized spots, but rather occurs along the entire neurite and soma. Characterization of the spike discharge pattern of mechanosensitive neurons in response to dynamic and sustained deformation, by compressing a small part of them, revealed that they primarily encode dynamic changes during deformation. The electrical signal induced by mechanical stimulation originated in the neurite and is then propagated towards the soma and invades other neurites. Mechanosensitive neurites not only transmit sensory information, but also function as motor neurites spreading the signal to other cells. Mechanosensitive neurons are capable of integrating and gating the stimuli they receive in order to provide an appropriate response. They share some properties with other sensory neurons, but also exhibit specific features very likely reflecting adaptation to their physiological function in the gut. Moreover, the study revealed that mechanosensitive properties are conserved across species as shown for guinea pig and human. Regarding mechanotransduction, normal stress plays a pronounced role in the activation of myenteric neurons, whereas shear stress shows only a marginal effect. Hydrostatic pressure, mimicking the deformation occurring during phasic contractions, and stretch, mimicking the deformation occurring during tonic contractions, both induce excitatory responses. Their different response patterns suggest that phasic contractions activate RAMEN, whereas tonic contractions activate SAMEN. Mechanosensitive neurons partly respond to both stimuli suggesting the presence of different mechanosensors on the same neuron.

4.1 Comparison primary cultured myenteric neurons of guinea pig and human

Culturing human myenteric neurons compared to guinea pig was challenging. In only half of the inoculated culture dishes were present neurons that responded to the viability test with nicotine and could be therefore used for experiments. One explanation might be the age of the patients (66 ± 13 years) that undergo surgery. Neuronal loss or degeneration during ageing have been widely reported and is associated with functional implications such as slowing of gastric emptying, decreased peristalsis and slowing of colonic transit (De Souza et al. 1993; Wade and Cowen 2004; Phillips and Powley 2007; Camilleri et al. 2008; Saffrey 2013; Mandić et al. 2013). It might be possible that the number of neurons in myenteric ganglia derived from adult human were already less

compared to the few weeks old guinea pigs. In addition the quantity of tissue used for the cultures was different, for guinea pig a 10-15 cm piece of the small intestine was used, in contrast the length from human tissue samples varied between 2 and 5 cm.

Indeed, immunohistochemical staining revealed that in human cultured myenteric clusters there were significantly less neurons compared to guinea pig.

In addition to the lower number of neurons per cluster the cellular composition of the cultured clusters was different. Immunohistochemical staining showed that in guinea pig clusters were present only neurons and glial cells. Other cell types such as fibroblast formed a separate layer all over the dish and also under the clusters but not within them. In human the clusters were formed by only a low number of neurons and a high number of glial cells and other cell types such as fibroblasts (see Figures 3.2 and 3.3).

Nevertheless, most response characteristics to carbon fiber stimulation of guinea pig and human were similar. Only the burst time was significantly higher in human and therefore also the burst spike frequency lower. Furthermore, the percentage of neurons responding was significantly lower in human. The lower percentage in human could be due to the composition of the cluster. As mentioned above there were only few neurons within a cluster, which were often located between other cell types such as glial cells and fibroblast-like cells. The carbon fiber pressed onto the cluster may first directly touch other cell types which lay above neurons. The stimulus strength reaching the neurons would be then attenuated. This strength difference can cause a lower percentage of mechanosensitive neurons identified in human compared to guinea pig. A force strength dependency of the neuronal response has been indeed shown for hydrostatic pressure and stretch.

With these results the translational aspect of this study was shown and with it the possible clinical relevance of the data. In addition, this reinforces the hypothesis that the concept of multifunctional enteric neurons, a concept recently proposed, is conserved across species (Mazzuoli and Schemann 2012).

4.2 Properties of mechanosensitive myenteric neurons identified with a contact method

The present study revealed that around half of the myenteric primary cultured neurons possess mechanosensitive properties. This proportion and their response pattern are comparable to the RAMEN identified in intact MP preparations (Mazzuoli and Schemann 2009). Mechanosensitive properties are not restricted to a single specialized region of the neuron; they are present in various spots located on the cell membrane of different neurites as well as of the soma. Indeed, it was shown with paired experiments that the response to neurite stimulation was comparable with the stimulation of the same neuron on the cell body. This finding contradicts the data of Kunze et al. that described a differential response of the two neuronal parts although as well in myenteric neurons,

but in a different experimental set. In this study in fact, while neurite stimulation excited the enteric neurons, the soma stimulation of IPANs failed to activate them and stimulation of spontaneously active IPANs on the soma reversibly inhibited their spike discharge (Kunze et al. 2000). It is possible that the data of these experiments have been biased by the patch clamp recording technique causing mechanical distortion by itself and therefore an alteration of the neuronal behaviour. This is even more likely for the soma stimulation, because the place where electrical signals are detected with an electrode and the place of the application of the mechanical stress is identical. This is especially true since the same pipette was used for patching and for stimulation. It was reported in the literature that patching cells can change their mechanical properties due to disruption of normal membrane structure and redistribution of ion channels at the site of the patch (Suchyna et al. 2009). In addition, because of technical problems a different step size for probing neurites and somata was used in this study (Kunze et al. 2000). With the “non-invasive” technique of recording in this study such problems are avoided. Only part of the mechanosensitive neurons identified in this study were multipolar, calbindin expressing and showing a Ca^{2+} hump on the falling phase of their spikes, which are characteristics of IPANs. Anyway these neurons showed also an excitatory response if stimulated on their somata.

Finally, it has been recently shown that during muscle contraction and relaxation neuronal cell bodies and neurites are distorted at the same time (Mazzuoli and Schemann 2009). A differential response of the two sites would cause a lower sensitivity of the neuronal network. A neuron would be activated by deformation of the neurite but at the same time inhibited by deformation of the soma, so the excitatory action would be always attenuated. This property would make no sense in gut physiology.

The hypothesis that gut regions which have to fulfill different functions require a different control on a neuronal basis was tested. Therefore we compared the response to mechanical stimulation of cultured myenteric neurons from small intestine and gastric corpus. A difference in the electrophysiological and synaptic behaviour of their neurons has been already shown (Wood 1987a; Wood 1987b; Wood 1989; Schemann and Wood 1989b; Schemann and Wood 1989a). In addition, AH-neurons are present only in guinea pig small intestine but not in the gastric corpus, whereas S-neurons are present in both regions (Hirst et al. 1974; Wood and Mayer 1978; Hodgkiss and Lees 1983; Schemann and Wood 1989b). Nevertheless, this study revealed similar response characteristics of myenteric neurons from small intestine and gastric corpus to mechanical stimulation. There was only a difference in the timing of the response: the burst duration was shorter in mechanosensitive myenteric neurons from gastric corpus. This results do not explain the different types of muscle activity in small intestine and gastric corpus. It is likely that under physiological conditions modulation of mechanosensitive neurons plays a pronounced role, especially since it is known that all myenteric neurons in the stomach and all mechanosensitive neurons from the small intestine receive fast synaptic input (Schemann and Wood 1989a; Mazzuoli and Schemann 2009). Indeed, this study showed that neuronal activity can be modulated by hyperpolarization of the soma. In addition different types of deformations as in phasic and tonic contractions caused different neu-

ronal responses.

As a proof of principle study the well-characterized mechanosensitive DRG neurons were used to validate the technique and to compare the results in the enteric neurons with other known sensory neurons (McCarter et al. 1999; Takahashi and Gotoh 2000; Gschossmann et al. 2000; Hao et al. 2013). In addition, neurons that have been previously known as non-mechanosensitive neurons, SCG neurons, were probed (McCarter et al. 1999). Using the same stimulus parameters as for the myenteric neurons activation of DRG neurons and surprisingly of SCG neurons was observed. The discharge pattern in response to neurite stimulation had similar characteristic to the one of the myenteric neurons. Noteworthy, the spike burst started significantly earlier in DRG neurons compared to both other types of neurons. DRG neurons transduce information from the periphery to the central nervous system. The fast response to mechanical stimuli in the periphery is crucial. Therefore, the requirements of mechanosensitive channels in DRG might be different compared to them in myenteric neurons where the sensory cells and the effector cells are close by. Noteworthy DRG neurons did not respond to mechanical stimulation with the carbon fiber on their somata. This might reflect the physiological situation, in which their cell bodies are *in vivo* protected by the backbone and are therefore not directly exposed to mechanical stress. Another study revealed that the stimulus strength activating DRG neurons is much higher for the soma compared to the neurite (Hu and Lewin 2006). This study unfortunately did not specify the stimulus strength, they quantified only the stimulation step, so there was not a force value to compare with. It might be possible that in the present study the threshold to excite the neurons by soma stimulation was not reached or that the stimulus used by the other study was an high threshold noxious stimuli. In addition, the culture age was different. In the mentioned study the time in culture was 16-48 h while the cultures of the present study were grown for at least 7 days before the experiments. A high plasticity in morphology and protein synthesis in adult DRG neurons *in vitro* and *in vivo* has been shown (Delree et al. 1993). DRG under *in vivo* conditions transform from bipolar to pseudounipolar, whereas in culture they show a wide variety of phenotypes (Delree et al. 1993). In the presence of fetal calf serum a high percentage of cultured DRG are multipolar (Delree et al. 1993). Furthermore neurites from 3 days old cultured DRG express markers for dendrites as well as axons but after 15 days only an axonal marker is expressed (Delree et al. 1993). It is possible that the first days of culture neuronal somata and neurites possess both mechanosensitive properties that are then lost for the soma after a certain time in culture. Experiments could not be performed directly after dissociation, because the neurons did not fully attach to the culture dish bottom during the first days and long neurites were required for stimulation.

Against the expectations SCG neurons responded as well to carbon fiber stimulation and their mechanosensitive properties were similar to the other sensory neurons. A physiological relevance of mechanosensitive function of SCG neurons is not known. They are supposed to be non-sensory neurons. It has been demonstrated that they do not show mechanically activated currents in response to lateral movement of a glass pipette towards the cell body as well as pressure application from a micro glass pipette (McCarter

et al. 1999). Nevertheless, neuroblastoma cells and SCG neurons have the same origin and show similar properties (Schubert et al. 1969; Hoehner et al. 1996; Wartiovaara et al. 2002). Mechanically activated currents in a neuroblastoma cell line has been previously reported (Coste et al. 2010). Piezo1 (previously known as FAM38A) has been identified in this neuroblastoma cell line and is the channel responsible for mechanically activated currents (Coste et al. 2010). Indeed, immunohistochemical staining revealed the presence of Piezo1 in neuronal cell bodies and neurites of SCG neurons (see Figure 3.14). The Piezo proteins have been recently identified as components of mechanically-activated cation channels (Coste et al. 2010; Coste et al. 2012).

In DRG Piezo2 (previously known as FAM38B) has been identified with a siRNA silencing technique to have a crucial role in mechanotransduction in a subset of DRG neurons (Coste et al. 2010). Immunohistochemical staining for Piezo1 and Piezo2 in DRG neurons in the present study were unfortunately unspecific (see Figure 3.13). In myenteric neurons the presence of Piezo1 and Piezo2 (see Figure 3.12) has been demonstrated in this thesis. Piezo1 was present in somata of myenteric cultured neurons, but only about half of the mechanosensitive neuronal population was Piezo1 positive. Piezo2 was mainly present in the neurites of the cultured neurons. Relation of the presence of Piezo2 to mechanosensitivity could have not been demonstrated because of difficulties to identify the exact spot of mechanical stimulation. Anyway, additional experiments are needed to test the involvement of Piezo1 or Piezo2 in mechanotransduction in myenteric neurons. One approach could be siRNA silencing of Piezo1 and Piezo2 if transfection of primary cultured myenteric neurons is reliable working. Another possibility could be the use of knock-out mice and experiments in intact tissue. Piezo1 might be a promising candidate as a mechanotransducing channel in a subset of mechanosensitive myenteric neurons.

As other candidates involvement of TRP channels was tested. The present study provided evidences that TRPA1 and TRPV2 channels are not involved in mechanotransduction in the ENS. However these results should be taken with care because the n-number was low and proper controls for the blockade are missing. More experiments are needed, especially since a functional role of TRPV2 in muscle relaxation and expression in inhibitory motor neurons and IPANs has been shown (Mihara et al. 2010).

An important role of the cytoskeleton in mechanotransduction has been in addition proposed for different mechanosensitive cell types (Hamill and Martinac 2001; Kraichely and Farrugia 2007; Chen 2008; Hoffman et al. 2011; Martinac 2014). The hypothesis was tested by destabilization of microtubules with a method that was already established in enteric neurons (Vanden Berghe et al. 2004). Treatment with cytochalasin D did not change the percent of mechanosensitive neurons. Based on these results, the microtubules cannot have a function as a tether to the mechanosensitive channel transferring the mechanical stimulus as suggested in the literature. Moreover, microtubule destabilization would reduce the mechanosensitive response, but the treated neurons showed a higher overall and burst spike frequency in respect to untreated neurons. This

could be explained by destabilization of the whole membrane and thereby increasing the open probability of mechanosensitive channels.

Local blockade of nerve activity by TTX at the site of mechanical stimulation revealed that this place is also the site of origin of the spike discharge. This was already proposed by another study, since spike discharge was observed although the site of mechanical stimulation was at great distance from the cell body and depolarization was not observed (Kunze et al. 2000). If the spike discharge would originate in the neuronal cell body triggered by a receptor potential from the location of the stimulation on the neurite; local TTX blockade on this site would not inhibit spike discharge in the neuronal cell body. In addition, these results give a further clue about the involved mechanosensitive channels that must be expressed on neurites as well as on cell bodies.

The most striking and at the same time puzzling finding was that neurites conduct spikes orthodromically and antidromically, suggesting that they have sensory as well as motor or integrative functions. In principle this conclusion agrees with previous findings that mechanosensitive myenteric neurons in intact tissue are multifunctional (Schemann and Mazzuoli 2010). This concept was based on the result that deformation of myenteric ganglia in the guinea pig ileum directly activated neurons generally considered as motor- or interneurons (Mazzuoli and Schemann 2009) and was further supported by the identification of sensory interneurons in the MP of the guinea pig colon (Smith et al. 2007). In the literature there are only two other examples of multifunctional neurites. The first one is the neuronal growth cones of peripheral neurons which play an important role as sensors, transducers and motor structures (Kater and Rehder 1995). The second one is the efferent function of axon collaterals from vagal sensory neurons (Wei et al. 1995). Recent studies suggest a shift in paradigm in that the strict classification of neurites by a sole function may be generally questioned. For example, it has been shown that axons can perform diverse functions, such as modulation of spike shape or integration of somatic spikes that extend beyond the prevailing model of axon physiology (Sasaki 2013).

The results clearly showed that mechanosensitive neurites not only generate spikes that propagate towards the soma but also conduct spikes generated in other neurites or in the soma. This is the plausible conclusion from the finding that neurite deformation caused invasion of spikes into other neurites, which also respond to deformation. Moreover, nicotine application caused spike discharge in the soma and along neurites, also those that responded to deformation. The ICA image of neurons responding to deformation and nicotine were identical. At this point, there is no conclusive explanation how myenteric neurons prevent collision of action potentials once several mechanosensitive neurites are activated. The results suggested that most, if not all, neurites of mechanosensitive myenteric neurons were activated by deformation and hence function as sensors. It cannot be excluded that this is a phenomenon of the culture, which resulted in excess expression of mechanosensitive channels, which is not reported in the literature. Altered expression of neurotransmitters in the *in vitro* vs. *in vivo* state has been shown in DRG neurons (Delree et al. 1993). In addition different morphology of DRG in culture and additional

expression of dendritic marker in cultures younger than 15 days was observed, which contradicts the *in vivo* state with pseudounipolar neurons with an axon only (Delree et al. 1993). In contrast it was shown that DRG *in vitro* express the same nociception properties as *in vivo* (Gold et al. 1996). These are evidences that cultured neurons can show partly different properties as the same neurons *in vivo* but not all their properties are changed. The physiological relevance of the results though is supported by the finding that stretch-activated channels such as TRAAK are highly expressed in the somata of virtually all kind of neurons (Maingret et al. 1999; Reyes et al. 1999). Nevertheless, mechanosensitivity of neuronal somata in intact tissue has been never shown, due to inaccessibility of the cell bodies. Although a particular spatial organization of these mechanosensitive neurites was not observed, there may be a preferred projection and a spatial preference of mechanosensitive neurites during neuronal development in the gut wall, which assures polarized activation of the soma from only one direction.

The ICA revealed the morphology of each mechanosensitive neuron based on independent spike discharge patterns. Whereas cultured DRG neurons are all well-characterized as pseudounipolar neurons (Dogiel 1908; Ranson 1912; Takahashi and Ninomiya 1987), myenteric neurons have different morphologies and are classified as Dogiel type I, Dogiel type II and Dogiel type III neurons (Dogiel 1895). In this study it was not possible to unequivocally classify each neuron according to the Dogiel categories. Most of them had multiple action potential conducting neurites, but differed in size. Multipolarity of neurons in culture has been also shown for DRG neurons (Delree et al. 1993).

A question that may come up from the data here proposed is if the neurites stimulated could be characterized as axons or as dendrites. Unfortunately there is no validated tool for the distinction of axons and dendrites in the ENS. In the central nervous system there are markers that could be used for this scope, but their validation in the ENS is until now not proven. Therefore, these markers were not tested in the present study. Just from the morphology it could not be concluded, which neurites are axons and which are dendrites, because they do not show a typical shape. Branching of short neurites could not be observed in the cultured neurons. It has been also shown that in short term culture neurites express dendritic and axonal markers at the same time (Delree et al. 1993).

To reveal the mechanism of mechanotransduction different approaches were followed. First of all it was tested if the response to mechanical stimulation is direct or synaptically driven. Synaptic blockade with ω -conotoxin GVIA significantly reduced the number of neurons responding to carbon fiber stimulation. This contradicts a previous study showing no change in the percent of neurons responding in ω -conotoxin GVIA or low Ca^{2+} /high Mg^{2+} conditions to intraganglionic volume injections (Mazzuoli and Schemann 2009; Mazzuoli and Schemann 2012). A possible reason could be a technical problem, due to the fact that the carbon fiber was not exactly placed on the same spot. This would change the exact stimulus strength in the stimulation after blocker perfusion. This also explains why the response to the second stimulation with the carbon fiber at the same spot was reduced. Thereby it might be that not all neurites running together

were stimulated or the threshold stimulus strength was not reached. This could not be controlled because ω -conotoxin GVIA is an irreversible blocker and a control stimulation after washout was not possible (Cruz and Olivera 1986). In addition, the reproducibility test, stimulating the same spot twice with the carbon fiber, revealed a similar effect. The response to the second stimulation was also here reduced. Therefore the validity of the finding is debatable.

Experiments with the Ca^{2+} -sensitive dye showed a simultaneous increase of $[\text{Ca}^{2+}]_i$ in the stimulated neurite and the corresponding neuronal cell body. The increase of $[\text{Ca}^{2+}]_i$ in other cell types, for example fibroblasts, started later than in the neurons (see Figure 3.23). The propagation of the signal within the fibroblast was quite slow; it took about 2.5 s until the whole fibroblast was reached by the Ca^{2+} -wave starting from the spot of mechanical stimulation. This is an evidence for a direct neuronal response. All neuronal mechanosensitive responses measured were much faster and it is unlikely that they were triggered by other cell types present in the culture.

The analysis with the ICA, made it possible to follow the electrical signal starting from the site of mechanical stimulation and reaching the soma or other neuronal branches, and to avoid the possible overlay of signals coming from other neurons. The experiments with multifocal stimulation revealed that the distance between the mechanical stimulation spot and the cell body does not play any role (see Figure 3.18). A similar finding was observed for DRG neurons (Usoskin et al. 2010). In addition, it indicated that there are no specialized mechanosensitive hotspots as reported for extrinsic afferent fibers innervating the gut (Zagorodnyuk and Brookes 2000; Lynn et al. 2003), but rather that the entire neurite possess mechanosensitive properties. This appears to be a useful property because the myenteric neurons can convert mechanical input at different sites. They seem to not have a specialized trigger zone, in which the receptor potential starts and is conducted to the cell body. If the amplitude of the receptor potential decreases over the distance, this would lead to a decrease of the spike frequency, but this was not the case in the present experiments with carbon fiber stimulations with different distances to the cell body. This means that the location where the receptor potential and the spike discharge starts must be close by. With the voltage-sensitive dye technique it was unfortunately not possible to resolve the receptor potential. This might be due to the restricted area where it appears and/or to the fact that mechanical stimulation causes artifacts at the site of stimulation by movement. Anyway, according to the literature, the amplitude of receptor potentials is < 1.5 mV (Gardner and Martin 2000), this cannot be resolved with the voltage-sensitive dye technique.

The uniform response of the mechanosensitive neuron to multifocal stimulation reflects the fact that the precise localization of the stimulus origin is in the gut not important unlike in the somatosensory system for visual or tactile stimuli.

In about half of the mechanosensitive neuron all probed neurites showed mechanosensitive function. This could lead to an “overdose” of stimuli crowding the neuronal cell body. The present study revealed that the enteric neurons have the capacity to modu-

late the input and therefore to adjust the output in a proper way. By local application of adenosine on single mechanosensitive somata it was shown that mechanosensitive responses are modulated by a gating mechanism. The concept of gating in enteric neurons was already proposed early on but not experimentally proven up to now (Wood and Mayer 1979). Also others shared the opinion that low stimulus fidelity is important to set the gain in a sensory network: differential responses to the same stimulus provide the basis for the sensory neurons to control the self-reinforcing network in a proper way that is dependent on the excitability level (Blackshaw et al. 2007; Mazzuoli and Schemann 2009). Neuronal as well as non-neuronal cells can exert modulatory action on the enteric network by secretion of neurotransmitters or other substances such as hormones.

Carbon fiber stimulation as a contact method resulted in a dynamic phase by placing the carbon fiber and a sustained phase by keeping the carbon fiber pressed onto the target. The spike discharge during dynamic phase was significantly higher compared to sustained phase. In the literature it is often discriminated between rapidly and slowly adapting mechanosensors (Delmas et al. 2011). Rapidly adapting mechanosensors encode the dynamic phase of a ramp and hold stimulus, whereas slowly adapting mechanosensors are activated throughout a sustained stimulus (Delmas et al. 2011). In this study it was tested if neurons could encode differently a dynamic and a sustained stimulus. It was tested if mechanosensitive myenteric neurons were also able to respond to release of mechanical stress as a further dynamic change. Indeed, more than half of the mechanosensitive neurons responded to both stimuli indicating that they encode a dynamic change. Similar findings were observed in mouse myenteric neurons in intact tissue preparations (Mazzuoli and Schemann 2012).

The forces that really act on the neurons during muscle contraction and relaxation have not been described until present. In this part of the present study a stimulation strength of 0.4 mN was used. One may argue that targeted mechanical stimulation never appears under physiological conditions. Nevertheless it was demonstrated that the response to carbon fiber stimulation is not an artifact. First, the response can be triggered more than one time, second the response can be modulated and third the conduction velocity (0.19 ± 0.06 m/s) was similar to what has been found in former studies in the ENS (Nishi and North 1973; Hendriks et al. 1990; Schemann et al. 2002). Furthermore, a former study showed that forces smaller than 1.0 mN failed to activate ileal myenteric neurons in intact tissue (Mazzuoli and Schemann 2009). Mechanoreceptors of rectal intraganglionic laminar endings (IGLEs) are activated by forces between 0.08 – 7 mN (Lynn et al. 2003) and IGLEs in the stomach responded to a von Frey hair with a force of 0.4 mN (Zagorodnyuk et al. 2001). Irreversible damage has been observed in rectal IGLEs for von Frey hairs with > 2 mN (Lynn et al. 2005). The stimulus strength in this study was well in the range what others used in the GI tract.

In addition, for the possible critic that the targeted stimulation is not happening under physiological conditions von Frey hair targeted stimulation in this study was used as a tool to reveal the properties of the different regions of mechanosensitive neurons.

4.3 Identification of the mechanical stimulus modalities exciting myenteric neurons

In the present study neurons were probed with normal and shear stress. Under physiological conditions during muscle activity myenteric ganglia are deformed (Gabella 1990; Mazzuoli and Schemann 2009). There is no study identifying the nature and strength of the stimulus that neurons undergo. Neuronal deformation is induced by muscle contraction and relaxation of the two muscle layers, in which the MP is sandwiched. It is most likely that neurons are compressed and stretched under these conditions. In addition shear stress is likely to affect them because of movement of the two muscle layers against each other. The appearance of compression and stretch in the GI tract have been also discussed elsewhere (Lynn et al. 2005). The present study demonstrated that myenteric neurons are mostly excited by normal stress and only marginal by shear stress. In addition two stimuli, one mimicking phasic and the other tonic contractions, activate in part the same neurons but exhibit different response patterns.

A marginal percentage of neurons (5%) responded to stimulation with shear stress, although the exerting force was rather high compared to the other stimuli. In addition, the neuronal response to shear stress was neither reproducible nor showing a stimulus strength dependency. A mechanosensor is generally able to respond to the same stimulus in the same way and its spike discharge normally encode the stimulus strength (Delmas et al. 2011). Both prerequisites were not fulfilled. It is possible that myenteric neurons do not react to this stimulus because shear stress does not provide important information for the gut to react to. It is likely that shear stress is only relevant for cell types that are surrounded by circulating liquid such as endothelial cells (Chen et al. 1999; Marchenko and Sage 2000; Meer et al. 2010; Park et al. 2011).

Normal stress is the prominent stimulus modalities in the GI tract and activates a high percentage of neurons. The activation of rectal mechanoreceptors to the same stimulus modality has been shown elsewhere (Lynn et al. 2005).

Both stimuli one mimicking phasic and the other tonic contractions were able to excite myenteric neurons.

Hydrostatic pressure with its short pulse duration mimicked phasic contractions. This stimulus resulted in a force of 77 ± 52 nN, which is much smaller as the force range that was exerted in the experiments with shear stress. Hydrostatic pressure induced reproducible responses indicating a physiological relevance. In addition, a force strength dependency of the response was demonstrated. Interestingly an increase of the stimulation time from 1 s to 2 s did not change the response characteristics. This phenomenon can be explained by adaptation of the mechanosensors activated by hydrostatic pressure. A similar effect has been observed in rectal IGLEs (Lynn et al. 2005).

The other stimulation technique used to simulate normal stress, stretch, mimicked tonic contractions. Stretch was a ramp and hold stimulus. The ramp phase of the stimulus lasted about 400 ms. At the end of the ramp the maximal exerting force was reached. This force was too small to detect it with the used methods. The cluster remained stretched until the end and no relaxation followed during the recording. For stretch reproducibility could not be tested, because pulling the elastic surface twice in the same way did not induce the same decaying deformation field. In addition, there was no correlation of the spike frequency with the maximal or with the \sum stretch. This can be due to the small range of different stresses (\sum stretch: 0.1% - 30.4%; maximal stretch: 0.1% - 8.2%) induced by this method and/or to the existence of different thresholds mechanosensitive neurons. Indeed, we could show that by grouping the two stimulations into two classes, an increase of the maximal stretch came along with an increase of the spike frequency indicating a force strength dependency. With light microscopy technique a quantitative study of the size variation of neurons and glial cells during muscle contraction and distension has been performed (Gabella and Trigg 1984). With this method a variation of the shape and size of myenteric ganglia was detected (Gabella and Trigg 1984). The guinea pig ileum can undergo profile area changes of ganglia from 200 μm^2 to 375 μm^2 , which corresponds to a change of 53% (Gabella and Trigg 1984). In a later study, on the basis of the study from Gabella and Trigg, a stretch of around 12.6% for single neurons was calculated (Gabella and Trigg 1984; Kunze et al. 2000). An increased membrane area of a single soma of 15% opened K^+ channels causing inhibition of the neuron (Kunze et al. 2000).

In the present study cell length changes of maximally of 0.1% - 8.2% in one direction were achieved, which is much smaller as reported under physiological conditions. Therefore it might be that only low-threshold mechanosensitive neurons are activated. Higher changes could not be achieved with the used technique.

Stretch induced by pulling of an elastic surface with a gauge needle resulted, as the carbon fiber stimulation, in a short dynamic phase and a longer sustained phase. Carbon fiber stimulation is a kind of compressive stress but just on a small membrane area ($\sim 50 \mu\text{m}^2$). The firing pattern was obviously different. To carbon fiber stimulation the induced spike discharge was significantly higher during dynamic compared to sustained phase, whereas for stretch it was the opposite. This suggests a faster adaptation to compressive stress than to stretch. In rectal IGLEs slow adaptation of low-threshold mechanoreceptors in response to maintained distension was shown (Lynn et al. 2003). This supports our results in guinea pig myenteric neurons in response to stretch.

Paired experiments with hydrostatic pressure and stretch revealed that the timing of the responses was different. The spike discharge in response to hydrostatic pressure started significantly earlier and lasted shorter than to stretch. This might be a hint that different mechanosensors, one coding dynamic changes and the other one encoding a sustained stimulus, are activated. In *in vivo* experiments the presence of two different types of mechanosensitive neurons (RAMEN and SAMEN) has been shown (Mazzuoli

and Schemann 2012). It is likely that phasic contractions activate RAMEN, whereas tonic contractions activate SAMEN.

Nevertheless, about half of the neuronal mechanosensitive population was able to respond to both stimulus modalities. That could mean that different mechanosensors are eventually expressed on the same cells. In the literature there are lots of data referring to possible multiple mechanisms of mechanotransduction. For instance blockade of mechanosensitive channels such as Piezo2 in DRG neurons only partially blocked the rapidly adapting mechanically-activated currents, which are only one group of mechanosensitive DRG neurons (Coste et al. 2010). Furthermore, deletion of TRPC3 and TRPC6 blocked only mechanically activated rapidly adapting currents in sensory neurons and cochlear hair cells (Quick et al. 2012).

Paired experiments were performed on elastic surface. This experimental setting reduced the percentage of neurons responding to 1.0 bar hydrostatic pressure (18% vs. 35%). 1.0 bar on the elastic surface activated about the same percentage as 0.7 bar on a normal surface (17%). This is due to the elastic properties of the PDMS surface. A stiff surface does not deform while applying a pressure pulse on it, whereas the elastic PDMS surface is deformed as well as the cells growing on it. This minimizes the force acting on the cells.

In this part of the study all forces inducing responses were in the nN range. Taking this in account, it is more likely that the neurons sense strain or deformation and not stress. Comparison of the modulus of elasticity, which is the ratio of stress to strain, of neurons and smooth muscle cells in the literature revealed an interesting feature. For neurons a modulus of elasticity mostly below 1 kPa is reported (Amin et al. 2012; Lu et al. 2006; Spedden et al. 2012). In contrast to this smooth muscle cells have a much higher stiffness, a modulus of elasticity between 3.5 – 22 kPa for vascular smooth muscle cells is reported (Hemmer et al. 2008; Zhu et al. 2012). This means much smaller stresses are needed to deform neurons, whereas for muscle cells higher stresses are needed. Under gut muscle movements stress is induced by the two muscle layers, in which the MP is sandwiched. This means that the deformation of the neurons is determined by the muscle layers. The stress acting on the neurons is only dependent of their mechanical properties. The neurons are very elastic therefore they just follow the muscle deformation without transmission of forces. This is a crucial clue to clarify the question if mechanoreceptors respond to stress or strain. This suggests that there is only marginal stress acting on the neurons therefore strain must be the critical factor.

The present study revealed that normal stress rather than shear stress activates myenteric neurons. Only normal stress causes deformation, whereas shear stress induces shape changes only. Different stimuli may activate different mechanosensors. This has to be taken in account for the future investigation of channels involved in mechanotransduction. It is furthermore most likely that mechanosensors primarily respond to strain rather than stress.

Future perspectives

The use of cultured neurons in combination with fast neuroimaging and ICA is a promising technique to reveal the whole mechanotransduction pathway. The present study elucidated new properties of enteric neurons that are partly distinctive for these sensory neurons and fulfil the requirements for their physiological functions. In addition, different stimuli may activate different pathways. It is only possible to speculate about the meaning of these data under *in vivo* conditions. The response of mechanosensitive neurons can be in fact, as was partially showed, modulated by a series of different factors (neuronal but also non-neuronal), that lead *in vivo* to an adequate response to the input of the microenvironment. It is still challenging to prove, which are the neurons initiating the peristaltic reflex. Mechanosensitive neurons can be the key but they can also only locally adjust the excitation of a particular neuronal network.

Bibliography

- Amin, L., E. Ercolini, R. Shahapure, E. Migliorini, and V. Torre (2012). “The role of membrane stiffness and actin turnover on the force exerted by DRG lamellipodia”. In: *Biophysical journal* 102.11, pp. 2451–2460 (cit. on p. 89).
- Anderson, C.R., J.B. Furness, H.L. Woodman, S.L. Edwards, P.J. Crack, and A.I. Smith (1995). “Characterisation of neurons with nitric oxide synthase immunoreactivity that project to prevertebral ganglia”. In: *Journal of the autonomic nervous system* 52.2, pp. 107–116 (cit. on p. 7).
- Auerbach, L. (1862). “Ueber einen Plexus myentericus, einen bisher unbekanntem ganglionnervösen Apparat im Darmkanal der Wirbeltiere”. In: *Verlag von E.Morgenstern, Breslau* (cit. on p. 5).
- Bae, C., F. Sachs, and P. A. Gottlieb (2011). “The mechanosensitive ion channel Piezo1 is inhibited by the peptide GsMTx4”. In: *Biochemistry*. 50.29, pp. 6295–6300 (cit. on p. 12).
- Barajas-Lopez, C., I. Berezin, E. E. Daniel, and J. D. Huizinga (1989). “Pacemaker activity recorded in interstitial cells of Cajal of the gastrointestinal tract”. In: *Am.J.Physiol.* 257, pp. C830–C835 (cit. on p. 8).
- Basbaum, A. I., D. M. Bautista, G. Scherrer, and D. Julius (2009). “Cellular and molecular mechanisms of pain”. In: *Cell*. 139, pp. 267–284 (cit. on p. 10).
- Bayliss, W. M. and E. H. Starling (1899). “The movements and innervation of the small intestine”. In: *J.Physiol.* 24.2, pp. 99–143 (cit. on p. 5).
- Belmonte, C. and F. Viana (2008). “Molecular and cellular limits to somatosensory specificity”. In: *Mol.Pain*. 4:14. doi: 10.1186;1744-8069-4-14. P. 14 (cit. on p. 10).
- Bertrand, P. P. and R. L. Bertrand (2010). “Serotonin release and uptake in the gastrointestinal tract”. In: *Auton.Neurosci.* 153.1-2, pp. 47–57 (cit. on p. 8).
- Bertrand, P. P. and E. A. Thomas (2004). “Multiple levels of sensory integration in the intrinsic sensory neurons of the enteric nervous system”. In: *Clin.Exp.Pharmacol.Physiol.* 31, pp. 745–755 (cit. on p. 8).
- Blackshaw, L. A., S. J. Brookes, D. Grundy, and M. Schemann (2007). “Sensory transmission in the gastrointestinal tract”. In: *Neurogastroenterol.Motil.* 19.1 Suppl, pp. 1–19 (cit. on p. 86).
- Bornstein, J. C. (1994). “Local neural control of intestinal motility: nerve circuits deduced for the guinea-pig small intestine”. In: *Clin.Exp.Pharmacol.Physiol.* 21, pp. 441–452 (cit. on pp. 7, 8).
- Bornstein, J.C., J.B. Furness, and M. Costa (1989). “An electrophysiological comparison of substance P-immunoreactive neurons with other neurons in the guinea-pig

- submucous plexus”. In: *Journal of the autonomic nervous system* 26.2, pp. 113–120 (cit. on p. 7).
- Brookes, S.J.H., A.C.B. Meedeniya, P. Jobling, and M Costa (1997). “Orally projecting interneurons in the guinea-pig small intestine”. In: *The Journal of physiology* 505.2, pp. 473–491 (cit. on p. 7).
- Brown, G. D., S. Yamada, and T. J. Sejnowski (2001). “Independent component analysis at the neural cocktail party”. In: *Trends Neurosci.* 24, pp. 54–63 (cit. on p. 33).
- Bulbring, E., R. C. Lin, and G. Schofield (1958). “An investigation of the peristaltic reflex in relation to anatomical observations”. In: *Q.J.Exp.Physiol Cogn Med.Sci.* 43.1, pp. 26–37 (cit. on p. 8).
- Camilleri, M., T. Cowen, and T.R. Koch (2008). “Enteric neurodegeneration in ageing”. In: *Neurogastroenterology & Motility* 20.3, pp. 185–196 (cit. on p. 78).
- Cesa, C. M., N. Kirchgessner, D. Mayer, U. S. Schwarz, B. Hoffmann, and R. Merkel (2007). “Micropatterned silicone elastomer substrates for high resolution analysis of cellular force patterns”. In: *Rev.Sci.Instrum.* 78, p. 034301 (cit. on p. 20).
- Chafik, D., D. Bear, P. Bui, A. Patel, N. F. Jones, B. T. Kim, C. T. Hung, and R. Gupta (2003). “Optimization of Schwann cell adhesion in response to shear stress in an in vitro model for peripheral nerve tissue engineering”. In: *Tissue Eng.* 9, pp. 233–241 (cit. on p. 11).
- Chen, C. S. (2008). “Mechanotransduction—a field pulling together?” In: *Journal of cell science* 121.20, pp. 3285–3292 (cit. on p. 82).
- Chen, K.D., Y.S. Li, M. Kim, S. Li, S. Yuan, S. Chien, and J.Y.J. Shyy (1999). “Mechanotransduction in response to shear stress roles of receptor tyrosine kinases, integrins, and Shc”. In: *Journal of Biological Chemistry* 274.26, pp. 18393–18400 (cit. on p. 87).
- Chen, M.X., S.A. Gorman, B. Benson, J.P. and Michel M.C. Singh K. and Hieble, S.N. Tate, and D.J. Trezise (2004). “Small and intermediate conductance Ca^{2+} -activated K^+ channels confer distinctive patterns of distribution in human tissues and differential cellular localisation in the colon and corpus cavernosum”. In: *Naunyn-Schmiedeberg’s archives of pharmacology* 369.6, pp. 602–615 (cit. on p. 39).
- Cheng, C. M., Y. W. Lin, R. M. Bellin, Jr. Steward R. L., Y. R. Cheng, P. R. LeDuc, and C. C. Chen (2010). “Probing localized neural mechanotransduction through surface-modified elastomeric matrices and electrophysiology”. In: *Nat.Protoc.* 5, pp. 714–724 (cit. on p. 11).
- Christensen, A. P. and D. P. Corey (2007). “TRP channels in mechanosensation: direct or indirect activation?” In: *Nat.Rev.Neurosci.* 8, pp. 510–521 (cit. on p. 12).
- Christensen, J. and G.A. Rick (1985). “Nerve cell density in submucous plexus throughout the gut of cat and opossum”. In: *Gastroenterology* 89, pp. 1064–1069 (cit. on p. 5).
- Colpaert, E. E., J.P. Timmermans, and R. A. Lefebvre (2002). “Immunohistochemical localization of the antioxidant enzymes biliverdin reductase and heme oxygenase-2 in human and pig gastric fundus”. In: *Free Radical Biology and Medicine* 32, pp. 630–637 (cit. on p. 5).

- Colquhoun, D. and J. M. Ritchie (1972). "The interaction at equilibrium between tetrodotoxin and mammalian non-myelinated nerve fibres". In: *J.Physiol.* 221, pp. 533–553 (cit. on p. 30).
- Costa, M., S.J.H. Brookes, P.A. Steele, I. Gibbins, E. Burcher, and C.J. Kandiah (1996). "Neurochemical classification of myenteric neurons in the guinea-pig ileum". In: *Neuroscience* 75, pp. 949–967 (cit. on pp. 6, 7).
- Coste, B., J. Mathur, M. Schmidt, T. J. Earley, S. Ranade, M. J. Petrus, A. E. Dubin, and A. Patapoutian (2010). "Piezo1 and Piezo2 are essential components of distinct mechanically activated cation channels". In: *Science* 330, pp. 55–60 (cit. on pp. 12, 49, 82, 89).
- Coste, B., B. Xiao, J. S. Santos, R. Syeda, J. Grandl, K. S. Spencer, S. E. Kim, M. Schmidt, J. Mathur, A. E. Dubin, M. Montal, and A. Patapoutian (2012). "Piezo proteins are pore-forming subunits of mechanically activated channels". In: *Nature* 483, pp. 176–181 (cit. on p. 12, 82).
- Couzon, C., A. Duperray, and C. Verdier (2009). "Critical stresses for cancer cell detachment in microchannels". In: *Eur.Biophys.J.* 38, pp. 1035–1047 (cit. on p. 11).
- Cruz, L. J. and B. M. Olivera (1986). "Calcium channel antagonists. Omega-conotoxin defines a new high affinity site". In: *J.Biol.Chem.* 261, pp. 6230–6233 (cit. on pp. 28, 85).
- Cunningham, S. M., S. Mihara, and H. Higashi (1998). "Presynaptic calcium channels mediating synaptic transmission in submucosal neurones of the guinea-pig caecum". In: *J.Physiol.* 509, pp. 425–435 (cit. on p. 28).
- Damann, N., T. Voets, and B. Nilius (2008). "TRPs in our senses". In: *Curr.Biol.* 18, R880–R889 (cit. on p. 12).
- De Souza, R.R., H.B. Moratelli, N. Borges, and E.A. Liberti (1993). "Age-induced nerve cell loss in the myenteric plexus of the small intestine in man". In: *Gerontology* 39.4, pp. 183–188 (cit. on p. 78).
- Delmas, P., J. Hao, and L. Rodat-Despoix (2011). "Molecular mechanisms of mechanotransduction in mammalian sensory neurons". In: *Nat.Rev.Neurosci.* 12, pp. 139–153 (cit. on pp. 12, 86, 87).
- Delree, P., Cl. Ribbens, D. Martin, B. Rogister, P.P. Lefebvre, J.M. Rigo, P. Leprince, J. Schoenen, and G. Moonen (1993). "Plasticity of developing and adult dorsal root ganglion neurons as revealed in vitro". In: *Brain research bulletin* 30.3, pp. 231–237 (cit. on pp. 81, 83, 84).
- Di Nardo, G., C. Blandizzi, U. Volta, R. Colucci, V. Stanghellini, G. Barbara, M. Del Tacca, M. Tonini, R. Corinaldesi, and R. De Giorgio (2008). "Review article: molecular, pathological and therapeutic features of human enteric neuropathies". In: *Aliment.Pharmacol.Ther.* 28, pp. 25–42 (cit. on p. 14).
- Diamant, M. L., H. W. Kosterlitz, and J. McKenzie (1961). "Role of the mucous membrane in the peristaltic reflex in the isolated ileum of the guinea pig". In: *Nature* 190:1205-6. Pp. 1205–1206 (cit. on p. 8).
- Dogiel, A.S. (1895). "Zur Frage ueber die Ganglien der Darmgeflechte bei den Saeugethieren". In: *Anat. Anz.* 10, pp. 517–528 (cit. on pp. 6, 84).

- Dogiel, A.S. (1899). "Ueber den Bau der Ganglien in den Geflechten des Darmes und der Gallenblase des Menschen und der Saeugethiere". In: *Arch. Anat. Physiol. Leipzig Anat. Abt. Jg*, pp. 130–158 (cit. on p. 6).
- (1908). "Der Bau der Spinalganglien des Menschen und der Saeugethiere". In: *Fischer*, pp. 1–151 (cit. on p. 84).
- Doran, J.F., P. Jackson, P.A.M. Kynoch, and R.J. Thompson (1983). "Isolation of PGP 9.5, a New Human Neurone-Specific Protein Detected by High-Resolution Two-Dimensional Electrophoresis". In: *Journal of neurochemistry* 40.6, pp. 1542–1547 (cit. on pp. 36, 49).
- Elson, E. L. (1988). "Cellular mechanics as an indicator of cytoskeletal structure and function". In: *Annu.Rev.Biophys.Biophys.Chem.* 17, pp. 397–430 (cit. on p. 11).
- Evans, D. H. and H. O. Schild (1953). "The reactions of plexus-free circular muscle of cat jejunum to drugs". In: *J.Physiol.* 119, pp. 376–399 (cit. on p. 8).
- Evans, R.J., M.M. Jiang, and A. Surprenant (1994). "Morphological properties and projections of electrophysiologically characterized neurons in the guinea-pig submucosal plexus". In: *Neuroscience* 59, pp. 1093–1110 (cit. on p. 7).
- Fisher, A. B., S. Chien, A. I. Barakat, and R. M. Nerem (2001). "Endothelial cellular response to altered shear stress". In: *Am.J.Physiol Lung Cell Mol.Physiol.* 281, pp. L529–L533 (cit. on p. 73).
- Franke, W.W., E. Schmid, M. Osborn, and K. Weber (1978). "Different intermediate-sized filaments distinguished by immunofluorescence microscopy". In: *Proceedings of the National Academy of Sciences* 75.10, pp. 5034–5038 (cit. on p. 39).
- Fromherz, P. and A. Lambacher (1991). "Spectra of voltage-sensitive fluorescence of styryl-dye in neuron membrane". In: *Biochim.Biophys.Acta.* 1068, pp. 149–156 (cit. on p. 21).
- Furness, J.B. (2006). *The enteric nervous system*. Blackwell Publishing Inc., 350 Main Street, Malden, Massachusetts, USA (cit. on pp. 5–7).
- Furness, J.B., M. Costa, and J.R. Keast (1984). "Choline acetyltransferase-and peptide immunoreactivity of submucous neurons in the small intestine of the guinea-pig". In: *Cell and tissue research* 237, pp. 329–336 (cit. on p. 7).
- Furness, J.B., J.R. Keast, S. Pompolo, J.C. Bornstein, M. Costa, P.C. Emson, and D.E.M. Lawson (1988). "Immunohistochemical evidence for the presence of calcium-binding proteins in enteric neurons". In: *Cell and tissue research* 252, pp. 79–87 (cit. on pp. 6, 9).
- Furness, J.B., K.C.K. Lloyd, C. Sternini, and J.H. Walsh (1991). "Evidence that myenteric neurons of the gastric corpus project to both the mucosa and the external muscle: myectomy operations on the canine stomach". In: *Cell and tissue research* 266.3, pp. 475–481 (cit. on p. 5).
- Furness, J.B., W.A. Kunze, P.P. Bertrand, N. Clerc, and J.C. Bornstein (1998). "Intrinsic primary afferent neurons of the intestine". In: *Prog.Neurobiol.* 54, pp. 1–18 (cit. on pp. 7, 8).

- Furness, J.B., C. Jones, K. Nurgali, and N. Clerc (2004). "Intrinsic primary afferent neurons and nerve circuits within the intestine". In: *Prog.Neurobiol.* 72, pp. 143–164 (cit. on p. 8).
- Gabella, G. (1990). "On the plasticity of form and structure of enteric ganglia". In: *Journal of the autonomic nervous system* 30, pp. 59–66 (cit. on p. 87).
- Gabella, G. and P. Trigg (1984). "Size of neurons and glial cells in the enteric ganglia of mice, guinea-pigs, rabbits and sheep". In: *Journal of neurocytology* 13, pp. 49–71 (cit. on p. 88).
- Gardner, E.P. and J.H. Martin (2000). *Coding of sensory information. In Principle of neural science.* Ed. by E.R. Kandel, J.H. Schwartz, and T.M. Jessel. Vol. 4th edn. Elsevier, pp. 411–428 (cit. on p. 85).
- Gayer, C.P. and M.D. Basson (2009). "The effects of mechanical forces on intestinal physiology and pathology". In: *Cellular signalling* 21.8, pp. 1237–1244 (cit. on pp. 11, 13).
- Geiger, B., K.T. Tokuyasu, A.H. Dutton, and S.J. Singer (1980). "Vinculin, an intracellular protein localized at specialized sites where microfilament bundles terminate at cell membranes". In: *Proceedings of the National Academy of Sciences* 77.7, pp. 4127–4131 (cit. on p. 36).
- Gershon, M.D. (1999). "The enteric nervous system: a second brain". In: *Hosp.Pract.* 34, pp. 31–8, 41 (cit. on p. 5).
- (2005). "Nerves, reflexes, and the enteric nervous system: pathogenesis of the irritable bowel syndrome". In: *J.Clin.Gastroenterol.* 39, pp. 184–193 (cit. on p. 8).
- Ginzl, K.H. (1959). "Are mucosal nerve fibres essential for the peristaltic reflex?" In: *Nature* 184, pp. 1235–1236 (cit. on p. 8).
- Gold, M.S., S. Dastmalchi, and J.D. Levine (1996). "Co-expression of nociceptor properties in dorsal root ganglion neurons from the adult rat *in vitro*". In: *Neuroscience* 71.1, pp. 265–275 (cit. on p. 84).
- Gschossmann, J.M., V.V. Chaban, J.A. McRoberts, H.E. Raybould, S.H. Young, H.S. Ennes, T. Lembo, and E.A. Mayer (2000). "Mechanical activation of dorsal root ganglion cells *in vitro*: comparison with capsaicin and modulation by kappa-opioids". In: *Brain Research* 856, pp. 101–110 (cit. on p. 81).
- Hamill, O. P. and B. Martinac (2001). "Molecular basis of mechanotransduction in living cells". In: *Physiol Rev.* 81, pp. 685–740 (cit. on pp. 11, 82).
- Hao, J., J. Ruel, B. Coste, Y. Roudaut, M. Crest, and P. Delmas (2013). "Piezoelectrically driven mechanical stimulation of sensory neurons". In: *Methods Mol.Biol.* Pp. 159–170 (cit. on p. 81).
- Hemmer, J.D., D. Dean, A. Vertegel, E. Langan, and M. LaBerge (2008). "Effects of serum deprivation on the mechanical properties of adherent vascular smooth muscle cells". In: *Proceedings of the Institution of Mechanical Engineers, Part H: Journal of Engineering in Medicine* 222.5, pp. 761–772 (cit. on p. 89).
- Hendriks, R., J.C. Bornstein, and J.B. Furness (1990). "An electrophysiological study of the projections of putative sensory neurons within the myenteric plexus of the guinea pig ileum". In: *Neurosci.Lett.* 110, pp. 286–290 (cit. on pp. 6, 9, 86).

- Hirst, G.D., S.M. Johnson, and D.F. Van Helden (1985a). "The calcium current in a myenteric neurone of the guinea-pig ileum." In: *The Journal of physiology* 361.1, pp. 297–314 (cit. on p. 6).
- (1985b). "The slow calcium-dependent potassium current in a myenteric neurone of the guinea-pig ileum." In: *The Journal of physiology* 361, pp. 315–337 (cit. on p. 6).
- Hirst, G.D.S., M.E. Holman, and I. Spence (1974). "Two types of neurones in the myenteric plexus of duodenum in the guinea-pig". In: *J.Physiol.* 236, pp. 303–326 (cit. on pp. 6, 9, 80).
- Hodgkiss, J.P. and G.M. Lees (1983). "Morphological studies of electrophysiologically-identified myenteric plexus neurons of the guinea-pig ileum". In: *Neuroscience* 8, pp. 593–608 (cit. on pp. 9, 80).
- (1986). "Transmission in enteric ganglia". In: *Autonomic and enteric ganglia*. Pp. 369–405 (cit. on p. 9).
- Hoefling, O. (1985). *Physik*. Ed. by O. Hoefling, B. Mirow, and G. Becker. Duemmler, pp. 267–274 (cit. on p. 10).
- Hoehner, J.C., C. Gestblom, F. Hedborg, and L. and Pålman S. Sandstedt B. and Olsen (1996). "A developmental model of neuroblastoma: differentiating stroma-poor tumors' progress along an extra-adrenal chromaffin lineage." In: *Laboratory investigation; a journal of technical methods and pathology* 75.5, pp. 659–675 (cit. on p. 82).
- Hoffman, B.D., C. Grashoff, and M.A. Schwartz (2011). "Dynamic molecular processes mediate cellular mechanotransduction". In: *Nature* 475.7356, pp. 316–323 (cit. on p. 82).
- Howe, J.F., J.D. Loeser, and W.H. Calvin (1977). "Mechanosensitivity of dorsal root ganglia and chronically injured axons: a physiological basis for the radicular pain of nerve root compression". In: *Pain* 3.1, pp. 25–41 (cit. on p. 45).
- Hu, J. and G.R. Lewin (2006). "Mechanosensitive currents in the neurites of cultured mouse sensory neurones". In: *J.Physiol.* 577, pp. 815–828 (cit. on pp. 45, 81).
- Hung, C.T., F.D. Allen, S.R. Pollack, E.T. Attia, J.A. Hannafin, and P.A. Torzilli (1997). "Intracellular calcium response of ACL and MCL ligament fibroblasts to fluid-induced shear stress". In: *Cell Signal.* 9, pp. 587–594 (cit. on p. 11).
- Inoue, R., Z. Jian, and Y. Kawarabayashi (2009). "Mechanosensitive TRP channels in cardiovascular pathophysiology". In: *Pharmacol. Ther.* 123, pp. 371–385 (cit. on p. 12).
- Iyer, V., J.C. Bornstein, M. Costa, J.B. Furness, Y. Takahashi, and T. Iwanaga (1988). "Electrophysiology of guinea-pig myenteric neurons correlated with immunoreactivity for calcium binding proteins". In: *J.Auton.Nerv.Syst.* 22, pp. 141–150 (cit. on pp. 6, 9).
- Izumi, N., H. Matsuyama, Y. Yamamoto, Y. Atoji, Y. Suzuki, T. Unno, and T. Takewaki (2002). "Morphological and morphometrical characteristics of the esophageal intrinsic nervous system in the golden hamster." In: *European journal of morphology* 40, pp. 137–144 (cit. on p. 5).
- Kamkin, A. and I. Kiseleva (2005). *Mechanosensitivity in Cells and Tissues*. Academia Publishing House Ltd. Moscow (cit. on p. 10).

- Kater, S.B. and V. Rehder (1995). “The sensory-motor role of growth cone filopodia”. In: *Current opinion in neurobiology* 5.1, pp. 68–74 (cit. on p. 83).
- Kim, I.A., S.A. Park, Y.J. Kim, S.H. Kim, H.J. Shin, Y.J. Lee, S.G. Kang, and J. W. Shin (2006). “Effects of mechanical stimuli and microfiber-based substrate on neurite outgrowth and guidance”. In: *J.Biosci.Bioeng.* 101, pp. 120–126 (cit. on p. 73).
- Kirchenbuchler, D., S. Born, N. Kirchgessner, S. Houben, B. Hoffmann, and R. Merkel (2010). “Substrate, focal adhesions, and actin filaments: a mechanical unit with a weak spot for mechanosensitive proteins”. In: *J.Phys.Condens.Matter.* 22, p. 194109 (cit. on pp. 11, 19).
- Kirchgessner, A.L., H. Tamir, and M.D. Gershon (1992). “Identification and stimulation by serotonin of intrinsic sensory neurons of the submucosal plexus of the guinea pig gut: activity-induced expression of Fos immunoreactivity”. In: *The Journal of neuroscience* 12, pp. 235–248 (cit. on p. 7).
- Komuro, T. and D.S. Zhou (1996). “Anti-c-ij i_{ij} kit_{ij}/i_{ij} protein immunoreactive cells corresponding to the interstitial cells of Cajal in the guinea-pig small intestine”. In: *Journal of the autonomic nervous system* 61.2, pp. 169–174 (cit. on pp. 39, 40).
- Kong, C.R., N. Bursac, and L. Tung (2005). “Mechanoelectrical excitation by fluid jets in monolayers of cultured cardiac myocytes”. In: *J.Appl.Physiol (1985.)*. 98, pp. 2328–2336 (cit. on p. 11).
- Kraichely, R.E. and G. Farrugia (2007). “Mechanosensitive ion channels in interstitial cells of Cajal and smooth muscle of the gastrointestinal tract”. In: *Neurogastroenterol.Motil.* 19, pp. 245–252 (cit. on pp. 8, 82).
- Kugler, E.M., G. Mazzuoli, I. E. Demir, G.O. Ceyhan, F. Zeller, and M. Schemann (2012). “Activity of protease-activated receptors in primary cultured human myenteric neurons”. In: *Frontiers in Neuroscience* 6 (cit. on p. 17).
- Kuhlbrodt, K., B. Herbarth, E. Sock, I. Hermans-Borgmeyer, and M. Wegner (1998). “Sox10, a novel transcriptional modulator in glial cells”. In: *The Journal of neuroscience* 18.1, pp. 237–250 (cit. on p. 36).
- Kuntz, A. (1938). “The structural organization of the celiac ganglia”. In: *Journal of comparative Neurology* 69, pp. 1–12 (cit. on p. 7).
- Kunze, W.A. and J.B. Furness (1999). “The enteric nervous system and regulation of intestinal motility”. In: *Annu.Rev.Physiol.* 61, pp. 117–142 (cit. on p. 9).
- Kunze, W.A., J.B. Furness, P.P. Bertrand, and J.C. Bornstein (1998). “Intracellular recording from myenteric neurons of the guinea-pig ileum that respond to stretch”. In: *J.Physiol.* 506, pp. 827–842 (cit. on pp. 9, 11).
- Kunze, W.A., N. Clerc, J.B. Furness, and M. Gola (2000). “The soma and neurites of primary afferent neurons in the guinea-pig intestine respond differentially to deformation”. In: *J.Physiol.* 526, pp. 375–385 (cit. on pp. 8–10, 13, 80, 83, 88).
- Kwak, B.R., P. Silacci, N. Stergiopoulos, D. Hayoz, and P. Meda (2005). “Shear stress and cyclic circumferential stretch, but not pressure, alter connexin43 expression in endothelial cells”. In: *Cell Commun.Adhes.* 12, pp. 261–270 (cit. on p. 11).

- Li, Z.S. and J.B. Furness (2000). "Inputs from intrinsic primary afferent neurons to nitric oxide synthase-immunoreactive neurons in the myenteric plexus of guinea pig ileum". In: *Cell Tissue Res.* 299, pp. 1–8 (cit. on p. 49).
- Lin, Y.W., C.M. Cheng, P.R. LeDuc, and C.C. Chen (2009). "Understanding sensory nerve mechanotransduction through localized elastomeric matrix control". In: *PLoS One* 4, e4293 (cit. on p. 11).
- Loop, F.T. van der, G. Schaart, E.D. Timmer, F.C. Ramaekers, and G.J. van Eys (1996). "Smoothelin, a novel cytoskeletal protein specific for smooth muscle cells." In: *The Journal of cell biology* 134.2, pp. 401–411 (cit. on p. 40).
- Lu, Y.B., K. Franze, G. Seifert, C. Steinhäuser, F. Kirchhoff, H. Wolburg, J. Guck, P. Janmey, E.Q. Wei, J. Käs, et al. (2006). "Viscoelastic properties of individual glial cells and neurons in the CNS". In: *Proceedings of the National Academy of Sciences* 103.47, pp. 17759–17764 (cit. on p. 89).
- Lumpkin, E.A. and M.J. Caterina (2007). "Mechanisms of sensory transduction in the skin". In: *Nature* 445, pp. 858–865 (cit. on p. 10).
- Lund, D.D., M.M. Knuepfer, M.J. Brody, R.K. Bhatnagar, P.G. Schmid, and R. Roskoski Jr (1978). "Comparison of tyrosine hydroxylase and choline acetyltransferase activity in response to sympathetic nervous system activation". In: *Brain research* 156.1, pp. 192–197 (cit. on p. 53).
- Lyford, G.L. and G. Farrugia (2003). "Ion channels in gastrointestinal smooth muscle and interstitial cells of Cajal". In: *Curr.Opin.Pharmacol.* 3, pp. 583–587 (cit. on p. 8).
- Lynn, P., V. Zagorodnyuk, M. Hennig G.and Costa, and S. Brookes (2005). "Mechanical activation of rectal intraganglionic laminar endings in the guinea pig distal gut". In: *The Journal of physiology* 564.2, pp. 589–601 (cit. on pp. 86, 87).
- Lynn, P.A., C. Olsson, V. Zagorodnyuk, M. Costa, and S.J. Brookes (2003). "Rectal intraganglionic laminar endings are transduction sites of extrinsic mechanoreceptors in the guinea pig rectum". In: *Gastroenterology* 125, pp. 786–794 (cit. on pp. 85, 86, 88).
- Maingret, F., M. Fosset, F. Lesage, M. Lazdunski, and E. Honoré (1999). "TRAAK is a mammalian neuronal mechano-gated K⁺ channel". In: *Journal of Biological Chemistry* 274.3, pp. 1381–1387 (cit. on p. 84).
- Mandić, P., S. Leštarević, T. Filipović, N. Đukić, and M. Šaranović (2013). "Age-related structural changes in the myenteric nervous plexus ganglion along the anterior wall of the proximal human duodenum: A morphometric analysis". In: *Vojnosanitetski pregled* 70.2, pp. 177–181 (cit. on p. 78).
- Mann, P.T., J. B. Furness, S. Pompolo, and M. Mader (1995). "Chemical coding of neurons that project from different regions of intestine to the coeliac ganglion of the guinea pig". In: *Journal of the autonomic nervous system* 56, pp. 15–25 (cit. on p. 7).
- Mao, Y., B. Wang, and W. Kunze (2006). "Characterization of myenteric sensory neurons in the mouse small intestine". In: *J.Neurophysiol.* 96, pp. 998–1010 (cit. on p. 8).

- Marchenko, S.M and S.O. Sage (2000). “Effects of shear stress on $[Ca^{2+}]_i$ and membrane potential of vascular endothelium of intact rat blood vessels”. In: *Experimental physiology* 85.1, pp. 43–48 (cit. on p. 87).
- Martinac, B. (2014). “The ion channels to cytoskeleton connection as potential mechanism of mechanosensitivity”. In: *Biochimica et Biophysica Acta (BBA)-Biomembranes* 1838.2, pp. 682–691 (cit. on p. 82).
- Mayer, C.J. and J.D. Wood (1975). “Properties of mechanosensitive neurons within Auerbach’s plexus of the small intestine of the cat”. In: *Pfluegers Arch.* 357, pp. 35–49 (cit. on pp. 8, 10).
- Mazzuoli, G. and M. Schemann (2009). “Multifunctional rapidly adapting mechanosensitive enteric neurons (RAMEN) in the myenteric plexus of the guinea pig ileum”. In: *J.Physiol.* 587, pp. 4681–4694 (cit. on pp. 8–10, 44, 79, 80, 83, 84, 86, 87).
- (2012). “Mechanosensitive enteric neurons in the myenteric plexus of the mouse intestine”. In: *PLoS One* 7, e39887 (cit. on pp. 8, 9, 79, 84, 86, 88).
- McCarter, G.C., D.B. Reichling, and J.D. Levine (1999). “Mechanical transduction by rat dorsal root ganglion neurons in vitro”. In: *Neurosci.Lett.* 273, pp. 179–182 (cit. on pp. 13, 45, 81).
- Meer, A.D. van der, Feijen J. Poot A.A., and I. Vermes (2010). “Analyzing shear stress-induced alignment of actin filaments in endothelial cells with a microfluidic assay”. In: *Biomicrofluidics* 4, p. 11103 (cit. on pp. 11, 87).
- Meissner, G. (1857). “Ueber die Nerven der Darmwand”. In: *Z.Ration.Med.N.F.* 8, pp. 364–366 (cit. on p. 5).
- Merkel, R., N. Kirchgessner, C.M. Cesa, and B. Hoffmann (2007). “Cell force microscopy on elastic layers of finite thickness”. In: *Biophys.J.* 93, pp. 3314–3323 (cit. on p. 19).
- Michel, K., R. Zeller F.and Langer, H. Nekarda, D. Kruger, T.J. Dover, C.A. Brady, N.M. Barnes, and M. Schemann (2005). “Serotonin excites neurons in the human submucous plexus via 5-HT₃ receptors”. In: *Gastroenterology* 128, pp. 1317–1326 (cit. on p. 22).
- Michel, K., M. Michaelis, G. Mazzuoli, K. Mueller, P. Vanden Berghe, and M. Schemann (2011). “Fast Calcium and voltage sensitive dye imaging in enteric neurons reveal calcium peaks associated with single action potential discharge”. In: *J.Physiol.* 589, pp. 5941–5947 (cit. on p. 21).
- Mihara, H., A. Boudaka, K. Shibasaki, A. Yamanaka, T. Sugiyama, and M. Tominaga (2010). “Involvement of TRPV2 activation in intestinal movement through nitric oxide production in mice”. In: *The Journal of Neuroscience* 30.49, pp. 16536–16544 (cit. on pp. 30, 82).
- Milkiewicz, M., J.L. Doyle, T. Fudalewski, E. Ispanovic, M. Aghasi, and T.L. Haas (2007). “HIF-1alpha and HIF-2alpha play a central role in stretch-induced but not shear-stress-induced angiogenesis in rat skeletal muscle”. In: *J.Physiol.* 583, pp. 753–766 (cit. on p. 11).
- Minke, B. and B. Cook (2002). “TRP channel proteins and signal transduction”. In: *Physiol Rev.* 82, pp. 429–472 (cit. on p. 12).

- Narahashi, T., J.W. Moore, and W.R. Scott (1964). "Tetradotoxin blockage of sodium conductance increase in lobster giant axons". In: *J.Gen.Physiol* 47, pp. 965–974 (cit. on p. 30).
- Neunlist, M., S. Peters, and M. Schemann (1999). "Multisite optical recording of excitability in the enteric nervous system". In: *Neurogastroenterol.Motil.* 11, pp. 393–402 (cit. on pp. 21, 22).
- Nishi, S. and R.A. North (1973). "Intracellular recording from the myenteric plexus of the guinea-pig ileum". In: *J.Physiol.* 231, pp. 471–491 (cit. on p. 86).
- Nocka, K., S. Majumder, P. Chabot B.and Ray, M. Cervone, A. Bernstein, and P. Besmer (1989). "Expression of c-kit gene products in known cellular targets of W mutations in normal and W mutant mice—evidence for an impaired c-kit kinase in mutant mice." In: *Genes & development* 3.6, pp. 816–826 (cit. on p. 40).
- North, R.A. (1973). "The calcium-dependent slow after-hyperpolarization in myenteric plexus neurones with tetrodotoxin-resistant action potentials". In: *British journal of pharmacology* 49, pp. 709–711 (cit. on p. 6).
- (1986). "Mechanisms of autonomic integration". In: *Comprehensive Physiology*, pp. 115–153 (cit. on p. 9).
- O’Neil, R.G. and S. Heller (2005). "The mechanosensitive nature of TRPV channels". In: *Pfluegers Archiv* 451.1, pp. 193–203 (cit. on p. 12).
- Park, J., Z. Fan, and C.X. Deng (2011). "Effects of shear stress cultivation on cell membrane disruption and intracellular calcium concentration in sonoporation of endothelial cells". In: *Journal of biomechanics* 44.1, pp. 164–169 (cit. on p. 87).
- Petrus, M., A. M. Peier, M. Bandell, S. W. Hwang, T. Huynh, N. Olney, T. Jegla, and A. Patapoutian (2007). "A role of TRPA1 in mechanical hyperalgesia is revealed by pharmacological inhibition". In: *Mol Pain* 3.40, pp. 1–8 (cit. on p. 30).
- Phillips, R.J. and T.L. Powley (2007). "Innervation of the gastrointestinal tract: patterns of aging". In: *Autonomic Neuroscience* 136.1, pp. 1–19 (cit. on p. 78).
- Quick, K., J. Zhao, N. Eijkelkamp, J.E. Linley, F. Rugiero, J.J. Cox, R. Raouf, M. Gringhuis, J.E. Sexton, J. Abramowitz, R. Taylor, A. Forge, J. Ashmore, N. Kirkwood, C.J. Kros, G.P. Richardson, M. Freichel, V. Flockerzi, L. Birnbaumer, and J.N. Wood (2012). "TRPC3 and TRPC6 are essential for normal mechanotransduction in subsets of sensory neurons and cochlear hair cells". In: *Open biology* 2.5, p. 120068 (cit. on p. 89).
- Quinson, N., H. Robbins, M. Clark, and J. Furness (2001). "Calbindin immunoreactivity of enteric neurons in the guinea-pig ileum". In: *Cell and Tissue Research* 305, pp. 3–9 (cit. on pp. 9, 49).
- Ranson, S.W. (1912). "Degeneration and regeneration of nerve fibers." In: *J.comp.Neurol.* 22, pp. 487–537 (cit. on p. 84).
- Reyes, R., I. Lauritzen, F. Lesage, M. Ettaiche, M. Fosset, and M. Lazdunski (1999). "Immunolocalization of the arachidonic acid and mechanosensitive baseline traak potassium channel in the nervous system". In: *Neuroscience* 95.3, pp. 893–901 (cit. on p. 84).

- Rugiero, F., M. Mistry, D. Sage, J. A. Black, S. G. Waxman, M. Crest, N. Clerc, P. Delmas, and M. Gola (2003). “Selective expression of a persistent tetrodotoxin-resistant Na⁺ current and NaV1.9 subunit in myenteric sensory neurons”. In: *The Journal of neuroscience* 23, pp. 2715–2725 (cit. on p. 6).
- Saffrey, J.M. (2013). “Cellular changes in the enteric nervous system during ageing”. In: *Developmental biology* (cit. on p. 78).
- Sanchez, D., N. Johnson, C. Li, P. Novak, J. Rheinlaender, Y. Zhang, U. Anand, P. Anand, J. Gorelik, G.I. Frolenkov, C. Benham, M. Lab, V.P. Ostanin, T.E. Schaffer, D. Klenerman, and Y.E. Korchev (2008). “Noncontact measurement of the local mechanical properties of living cells using pressure applied via a pipette”. In: *Biophys.J.* 95, pp. 3017–3027 (cit. on p. 11).
- Sasaki, T. (2013). “The axon as a unique computational unit in neurons”. In: *Neuroscience research* 75.2, pp. 83–88 (cit. on p. 83).
- Schabadasch, A. (1930). “Die Nerven des Magens der Katze”. In: *Zeitschrift fuer Zellforschung und Mikroskopische Anatomie* 10, pp. 254–319 (cit. on p. 5).
- Schemann, M. and G. Mazzuoli (2010). “Multifunctional mechanosensitive neurons in the enteric nervous system”. In: *Auton.Neurosci.* 153, pp. 21–25 (cit. on pp. 9, 83).
- Schemann, M. and J.D. Wood (1989a). “Electrical behaviour of myenteric neurones in the gastric corpus of the guinea-pig.” In: *The Journal of physiology* 417.1, pp. 501–518 (cit. on pp. 9, 80).
- (1989b). “Synaptic behaviour of myenteric neurones in the gastric corpus of the guinea-pig.” In: *The Journal of physiology* 417.1, pp. 519–535 (cit. on pp. 9, 80).
- Schemann, M., D. Reiche, and K. Michel (2001). “Enteric pathways in the stomach”. In: *The Anatomical Record* 262, pp. 47–57 (cit. on p. 5).
- Schemann, M., K. Michel, S. Peters, S.C. Bischoff, and M. Neunlist (2002). “Cutting-edge technology. III. Imaging and the gastrointestinal tract: mapping the human enteric nervous system”. In: *Am.J.Physiol Gastrointest.Liver Physiol.* 282, G919–G925 (cit. on pp. 21, 86).
- Schmid, E., S. Tapscott, G.S. Bennett, J. Croop, S.A. Fellin, H. Holtzer, and W.W. Franke (1979). “Differential location of different types of intermediate-sized filaments in various tissues of the chicken embryo”. In: *Differentiation* 15.1, pp. 27–40 (cit. on p. 39).
- Schofield, G.C. (1960). “Experimental studies on the innervation of the mucous membrane of the gut”. In: *Brain* 83.3, pp. 490–514 (cit. on p. 5).
- Schubert, D., S. Humphreys, C. Baroni, and M. Cohn (1969). “In vitro differentiation of a mouse neuroblastoma”. In: *Proceedings of the National Academy of Sciences* 64.1, pp. 316–23 (cit. on p. 82).
- Sharif-Naeini, R., A. Dedman, J.H. Folgering, F. Duprat, A. Patel, B. Nilius, and E. Honore (2008). “TRP channels and mechanosensory transduction: insights into the arterial myogenic response”. In: *Pfluegers Arch.* 456, pp. 529–540 (cit. on p. 12).
- Smith, T.K., N.J. Spencer, G.W. Hennig, and E.J. Dickson (2007). “Recent advances in enteric neurobiology: mechanosensitive interneurons”. In: *Neurogastroenterol.Motil.* 19, pp. 869–878 (cit. on pp. 8, 9, 83).

- Sommer, E.W., J. Kazimierzczak, and B. Droz (1985). "Neuronal subpopulations in the dorsal root ganglion of the mouse as characterized by combination of ultrastructural and cytochemical features". In: *Brain Res.* 346, pp. 310–326 (cit. on p. 45).
- Song, Z.M., S.J.H. Brookes, and M. Costa (1991). "Identification of myenteric neurons which project to the mucosa of the guinea-pig small intestine". In: *Neuroscience letters* 129, pp. 294–298 (cit. on p. 6).
- Song, Z.M., S.J.H. Brookes, P.A. Steele, and M. Costa (1992). "Projections and pathways of submucous neurons to the mucosa of the guinea-pig small intestine". In: *Cell and tissue research* 269, pp. 87–98 (cit. on p. 7).
- Spedden, E., J.D. White, E.N. Naumova, and C. Kaplan D.L. and Staii (2012). "Elasticity maps of living neurons measured by combined fluorescence and atomic force microscopy". In: *Biophysical journal* 103.5, pp. 868–877 (cit. on p. 89).
- Spencer, N.J. and T.K. Smith (2004). "Mechanosensory S-neurons rather than AH-neurons appear to generate a rhythmic motor pattern in guinea-pig distal colon". In: *The Journal of physiology* 558.2, pp. 577–596 (cit. on p. 9).
- Spencer N.J., Nicholas S.J. Robinson L. Kyloh M. Flack N. Brookes S.J. Zagorodnyuk V.P. and D.J. Keating (2011). "Mechanisms underlying distension-evoked peristalsis in guinea pig distal colon: is there a role for enterochromaffin cells?" In: *Am.J.Physiol Gastrointest.Liver Physiol.* 301, G519–G527 (cit. on p. 8).
- Stach, W. (1981). "Zur neuronalen Organisation des Plexus myentericus (Auerbach) im Schweinedunndarm II. Typ II-Neurone". In: *Z mikrosk-anat Forsch* 95, pp. 161–182 (cit. on p. 6).
- Stach, W., R. Weiss, and R. Radke (1975). "Licht-und elektronenmikroskopische Untersuchungen ueber die Nervengeflechte der Magenschleimhaut und deren Beziehungen zu Beleg-und Mastzellen". In: *Dtsch Z Verdauungs-Stoffwechselkr* 35, pp. 205–218 (cit. on p. 5).
- Steele, P.A., S.J.H. Brookes, and M. Costa (1991). "Immunohistochemical identification of cholinergic neurons in the myenteric plexus of guinea-pig small intestine". In: *Neuroscience* 45, pp. 227–239 (cit. on p. 6).
- Suchyna, T.M., V.S. Markin, and F. Sachs (2009). "Biophysics and structure of the patch and the gigaseal". In: *Biophys.J.* 97, pp. 738–747 (cit. on p. 80).
- Szurszewski, J.H. and S.M. Miller (1994). "Physiology of prevertebral ganglia". In: *Physiology of the gastrointestinal tract*, pp. 795–877 (cit. on p. 7).
- Takahashi, A. and H. Gotoh (2000). "Mechanosensitive whole-cell currents in cultured rat somatosensory neurons". In: *Brain Res.* 869, pp. 225–230 (cit. on p. 81).
- Takahashi, K. and T. Ninomiya (1987). "Morphological changes of dorsal root ganglion cells in the process-forming period". In: *Prog.Neurobiol.* 29, pp. 393–410 (cit. on p. 84).
- Tassicker, B.C., G.W. Hennig, M. Costa, and Brookes S.J. (1999). "Rapid anterograde and retrograde tracing from mesenteric nerve trunks to the guinea-pig small intestine in vitro." In: *Cell Tissue Res.* 295(3), pp. 437–452 (cit. on p. 7).

- Thevenaz, P., U.E. Ruttimann, and M. Unser (1998). “A pyramid approach to subpixel registration based on intensity”. In: *Image Processing, IEEE Transactions on* 7.1, pp. 27–41 (cit. on p. 24).
- Trendelenburg, P. (1917). “Physiologische und pharmakologische Versuche ueber die Duenn darmperistaltik”. In: *Archiv fuer experimentelle Pathologie und Pharmakologie* 81, pp. 55–129 (cit. on p. 5).
- Tsuji, S., P. Anglade, T. Ozaki, T. Sazi, and S. Yokoyama (1992). “Peristaltic movement evoked in intestinal tube devoid of mucosa and submucosa”. In: *Jpn.J.Physiol.* 42, pp. 363–375 (cit. on p. 8).
- Usoskin, D., M. Zilberter, S. Linnarsson, J. Hjerling-Leffler, P. Uhlen, T. Harkany, and P. Ernfors (2010). “En masse in vitro functional profiling of the axonal mechanosensitivity of sensory neurons”. In: *Proc.Natl.Acad.Sci.U.S.A.* 107, pp. 16336–16341 (cit. on p. 85).
- Vanden Berghe, P., S. Molhoek, L. Missiaen, J. Tack, and J. Janssens (2000). “Differential Ca(2+) signaling characteristics of inhibitory and excitatory myenteric motor neurons in culture”. In: *Am.J.Physiol Gastrointest.Liver Physiol.* 279, G1121–G1127 (cit. on p. 15).
- Vanden Berghe, P., G.W. Hennig, and T.K. Smith (2004). “Characteristics of intermittent mitochondrial transport in guinea pig enteric nerve fibers”. In: *American Journal of Physiology-Gastrointestinal and Liver Physiology* 286, G671–G682 (cit. on pp. 30, 82).
- Vilceanu, D. and C. L. Stucky (2010). “TRPA1 mediates mechanical currents in the plasma membrane of mouse sensory neurons”. In: *PLoS One* 5, e12177 (cit. on p. 12).
- Wade, P.R. and T. Cowen (2004). “Neurodegeneration: a key factor in the ageing gut”. In: *Neurogastroenterology & Motility* 16.s1, pp. 19–23 (cit. on p. 78).
- Ward, S.M., E.A.H. Beckett, X.Y. Wang, F. Baker, M. Khoyi, and K.M. Sanders (2000). “Interstitial cells of Cajal mediate cholinergic neurotransmission from enteric motor neurons”. In: *The Journal of Neuroscience* 20, pp. 1393–1403 (cit. on p. 8).
- Wartiovaara, K., F. Barnabae-Heider, F. D. Miller, and D. R. Kaplan (2002). “N-myc promotes survival and induces S-phase entry of postmitotic sympathetic neurons”. In: *The Journal of neuroscience* 22.3, pp. 815–824 (cit. on p. 82).
- Wei, J.Y., D.W. Adelson, Y. Taché, and V.L.W. Go (1995). “Centrifugal gastric vagal afferent unit activities: another source of gastric efferent control”. In: *Journal of the autonomic nervous system* 52.2, pp. 83–97 (cit. on p. 83).
- Wood, J.D. (1987a). “Neurophysiological theory of intestinal motility”. In: *Jpn J Smooth Muscle Res* 23, pp. 143–186 (cit. on pp. 9, 80).
- (1987b). “Signal transduction in intestinal neurons”. In: *Cellular Physiology and Clinical*, pp. 55–69 (cit. on pp. 9, 80).
- (1989). “Electrical and synaptic behavior of enteric neurons”. In: *Comprehensive Physiology*, pp. 465–517 (cit. on pp. 9, 80).

- Wood, J.D. and C.J. Mayer (1978). “Intracellular study of electrical activity of auerbach’s plexus in guinea-pig small intestine”. In: *Pfluegers Archiv European Journal of Physiology* 374, pp. 265–275 (cit. on pp. 9, 80).
- (1979). “Intracellular study of tonic-type enteric neurons in guinea pig small intestine”. In: *J.Neurophysiol.* 42, pp. 569–581 (cit. on pp. 9, 86).
- Zafirov, D.H., J.M. Palmer, P.R. Nemeth, and J.D. Wood (1985). “Cyclic 3’, 5’-adenosine monophosphate mimics slow synaptic excitation in myenteric plexus neurons”. In: *Brain research* 347.2, pp. 368–371 (cit. on p. 31).
- Zagorodnyuk, V.P. and S.J. Brookes (2000). “Transduction sites of vagal mechanoreceptors in the guinea pig esophagus”. In: *J.Neurosci.* 20, pp. 6249–6255 (cit. on p. 85).
- Zagorodnyuk, V.P. and N.J. Spencer (2011). “Localization of the sensory neurons and mechanoreceptors required for stretch-evoked colonic migrating motor complexes in mouse colon”. In: *Frontiers in physiology* 2, p. 98 (cit. on p. 11).
- Zagorodnyuk, V.P., B.N. Chen, and S.J.H Brookes (2001). “Intraganglionic laminar endings are mechano-transduction sites of vagal tension receptors in the guinea-pig stomach”. In: *The Journal of physiology* 534.1, pp. 255–268 (cit. on p. 86).
- Zhu, Y., H. Qiu, J.P. Trzeciakowski, Z. Sun, Z. Li, Z. Hong, M.A. Hill, W.C. Hunter, D.E. Vatner, S.F. Vatner, et al. (2012). “Temporal analysis of vascular smooth muscle cell elasticity and adhesion reveals oscillation waveforms that differ with aging”. In: *Aging cell* 11.5, pp. 741–750 (cit. on p. 89).

List of Tables

2.1	List of antibodies used for staining primary cultured neurons.	32
3.1	Comparison of the response characteristics of paired neurite and soma stimulations as well as soma stimulation with and without prior neurite stimulation.	44
3.2	Comparison of percentages of mechanosensitive neurites and somata of MP, DRG and SCG neurons.	47
3.3	Parameters for calculation of applied shear stress.	75
3.4	Summary of the response characteristics of the mechanical stimulus modalities.	77

List of Figures

2.1	Cell suspension during the procedure of fishing myenteric ganglia.	17
2.2	Schematic illustration of the components used for the production of the self-made elastic surface culture dishes.	19
2.3	Schematic illustration of the neuroimaging set-up.	20
2.4	Schematic drawing of a stimulation of a neuronal cluster with a von Frey hair made of carbon fiber.	23
2.5	Schematic drawing of a stimulation of a neuronal cluster with hydrostatic pressure via micropipette.	24
2.6	Illustration of the resulting force by its decomposition in normal and shear force.	25
2.7	Custom-made arch for application of hydrostatic pressure with different angles used on the experimental set-up.	26
2.8	Schematic drawing of the application of stretch on cultured neurons adherent to a micropatterned elastic surface by side movement of a gauge needle dipped into the elastic surface.	26
2.9	Schematic drawing of the stimulation of cultured neurons with shear stress by fluid flow through a micro channel.	27
2.10	Measurements of cell length changes induced by stretch.	29
2.11	Picture of the experimental set for the local blockade of neuronal activity with tetrodotoxin (TTX).	30
2.12	Advantages of the signal detection of single neurons with the independent component analysis (ICA).	34
3.1	Cell growth during day 0 - 9 of the culture of guinea pig myenteric neurons.	37
3.2	Overlay of protein gene product 9.5 (PGP 9.5) positive and SOX positive cells.	38
3.3	Overlay of PGP 9.5 positive and Vinculin positive cells.	39
3.4	Overlay of PGP 9.5 positive and vimentin positive cells.	40
3.5	Myenteric neurons are activated by carbon fiber stimulation on their neurites.	42
3.6	Myenteric neurons are excited by carbon fiber stimulation on their soma.	43
3.7	Carbon fiber stimulation on the neurites of cultured dorsal root ganglia (DRG) neurons is excitatory.	46
3.8	Cultured sympathetic chain ganglia (SCG) neurons are excited by carbon fiber stimulation on their neurites.	47

LIST OF FIGURES

3.9	Comparison of the response characteristics of mechanosensitive myenteric plexus (MP), DRG and SCG neurons.	48
3.10	Overlap of the ICA images of a neuron in response to nicotine and carbon fiber stimulation.	49
3.11	The mechanosensitive neuronal population is partly showing characteristics of intrinsic primary afferent neurons (IPANs).	50
3.12	Piezo1 and Piezo2 are present in myenteric neurons.	51
3.13	Piezo1 and Piezo2 stainings are not specific in DRG neurons.	52
3.14	Piezo1 and Piezo2 is present in SCG neurons.	53
3.15	Comparison of the response characteristics of not treated and cytochalasin D treated mechanosensitive enteric neurons.	55
3.16	Mechanosensitive neurons possess multiple mechanosensitive neurites. . .	56
3.17	Comparison of the response to carbon fiber stimulation of 3 mechanosensitive neurites of the same neuron.	57
3.18	Comparison of the response to carbon fiber stimulation of 3 locations on one mechanosensitive neurite.	58
3.19	Modulation of mechanosensitive myenteric neurons by adenosine.	59
3.20	Application and release of the carbon fiber on a neurite leads to an excitatory response.	61
3.21	The site of mechanical stimulation is the site of the origin of the electrical signal.	62
3.22	Method for the determination of the conduction velocity.	63
3.23	The timing of mechanosensitive responses in neuronal and non-neuronal cells is different.	65
3.24	Comparison of the response characteristics of mechanosensitive myenteric neurons from guinea pig and human.	66
3.25	Comparison of the responses to different hydrostatic pressures.	68
3.26	Comparison of the response characteristics for different pulse durations of hydrostatic pressure.	69
3.27	Stretching myenteric neurons induces spike discharge.	71
3.28	Two consecutive applications of stretch induce a different maximal stretch in the same neuron.	72
3.29	Comparison of the response characteristics of mechanosensitive neurons activated by hydrostatic pressure and stretch.	74
3.30	The response to shear stress is independent of the applied stress.	76

Abbreviations

[Ca ²⁺] _i	Intracellular Calcium concentration
5-HT	5-Hydroxytryptamine
AFM	Atomic force microscopy
AH	After-hyperpolarizing
CCD	Cooled coupled device
ChAT	Choline acetyltransferase
DRG	Dorsal root ganglia
EPSP	Excitatory postsynaptic potential
FST	Fine Science Tools
GI	Gastrointestinal
HEPES	2-(4-(2-Hydroxyethyl)- 1-piperazinyl)-ethansulfonsäure
ICA	Independent component analysis
ICC	Interstitial cells of Cajal
IPAN	Intrinsic primary afferent neuron
LMMP	Longitudinal muscle – myenteric plexus
MP	Myenteric plexus
PBS	Phosphate Buffered Saline
PDMS	Polydimethylsiloxane
PGP	Proteine gene product
RAMEN	Rapidly adapting mechanosensitive enteric neurons
RT	Room temperature
S	Synaptic
SAMEN	Slowly adapting mechanosensitive enteric neurons
SCG	Sympathetic chain ganglia
SK3	Small conductance Ca ²⁺ - activated potassium channel type 3 protein
SMP	Submucous plexus
TH	Tyrosine hydroxylase
TRP	Transient receptor potential
TRPA	Transient receptor potential ankyrin
TRPC	Transient receptor potential canonical
TRPM	Transient receptor potential melastin
TRPML	Transient receptor potential mucolipin
TRPP	Transient receptor potential polycystin
TRPV	Transient receptor potential vanilloid
TTX	Tetradotoxin
VIP	Vasoactive intestinal peptide
Vs.	Versus

Acknowledgements

Ich möchte Herrn Prof. Dr. Michael Schemann dafür danken, dass ich meine Doktorarbeit in seinem Labor anfertigen durfte und hervorragend betreut wurde. Er hat mir dabei geholfen über mich hinaus zu wachsen und mir immer die nötigen Denkanstöße gegeben. Ich möchte mich auch dafür bedanken, dass ich die Möglichkeit hatte an einer Vielzahl von nationalen und internationalen Kongressen teilzunehmen.

Dr. Gemma Mazzuoli-Weber danke ich, dass sie mir so unverhofft diese Stelle angeboten hat. Ohne sie hätte ich wahrscheinlich nie eine Doktorarbeit geschrieben. Ich danke ihr für die Möglichkeit an ihrem Projekt mitzuarbeiten. Sie war eine sehr aufmerksame und herzliche Betreuerin. Der intellektuelle Austausch mit ihr hat mir sehr weitergeholfen. Liebe Gemma du bist mir sehr ans Herz gewachsen nicht nur als Betreuerin, sondern auch als Freundin. Vielen Dank, dass du dir trotz Elternzeit so viel Zeit für mich genommen hast. Ich wünsche dir und deiner kleinen Familie alles Gute für die Zukunft!

Ganz besonders möchte ich mich auch bei Dr. Klaus Michel bedanken. Ohne seine aufopfernde Hilfe bei Computerproblemen sowie bei Schwierigkeiten am Set-up wäre ich wohl nicht weit gekommen. Das Programmieren der ICA in Igor hat mir sehr bei meiner Auswertung geholfen.

Unseren TA's Birgit Kuch und Marlene Redl möchte ich danken, dass sie mir immer mit Rat und Tat zur Seite standen.

Mein herzlicher Dank gilt auch allen anderen Kollgen des Lehrstuhls für Humanbiologie, die mich stets bei meiner Arbeit unterstützt haben. Ganz besonders möchte ich meinen Bürokollegen im International Office danken, ohne sie wäre die Zeit nur halb so schön gewesen. Aber nicht nur die kleinen Pausen wurden durch meine Kollegen versüßt, auch der intellektuelle Austausch und die Diskussion meiner Daten haben mir sehr geholfen. Das nette Arbeitsklima in der Humanbiologie wird mir sehr fehlen.

Ich möchte mich auch bei meinen Kooperationspartnern in Jülich bedanken. Sie haben mir die Möglichkeit gegeben eine Technik zum Stretchen der Nervenzellen zu erlernen und haben mich stets mit Rat und passender Software für die Auswertung unterstützt.

Zuletzt danke ich meiner Familie für die Unterstützung. Ganz besonders möchte ich auch meinem Freund Riccardo danken, der mich stets beim Üben meiner Vorträge unterstützt hat, obwohl er nicht viel vom Vortrag selbst verstanden hat.

Curriculum Vitae

Persönliche Daten

Name: Eva Maria Kugler

Geburtsdatum: 07.04.1985

Ausbildung

seit 05.2010 Doktorarbeit, Lehrstuhl für Humanbiologie, Technische Universität München; Thema: Mechanosensitivität in isolierten myenterischen neuronalen Netzwerken

10.2004–09.2009 Dipl.Biologie, Technische Universität München, Abschlussnote: 1,0; Diplomarbeit: Prosekretorische Wirkung von Allylthiocyanat und Cinnamaldehyd auf das Meerschweinchenkolon und den Humandarm

09.1995–05.2004 Allgemeine Hochschulreife, Gymnasium Wolnzach, Abschlussnote: 1,9

Praktika

04.2007–07.2007 Helmholtz Zentrum München, Abteilung Genvektoren; Etablierung eines konditionalen Expressionssystem für das LMP1 Onkogen des Epstein-Bar-Viruses

11.2006–02.2007 Technische Universität München, Lehrstuhl für Genetik; Keimblattentwicklung bei Arabidopsis

Nebentätigkeiten

01.2006–07.2006 Studentische Hilfskraft, Technische Universität München, Lehrstuhl für Genetik

Preise und Auszeichnungen

07.2013 Reisestipendium für die Teilnahme am Kongress der „International Society of Autonomic Neuroscience“

09.2012 Reisestipendium für die Teilnahme am „International Neurogastroenterology and Motility Meeting“

09.2012 Abstract Auszeichnung: Abstract unter den Besten 5% aller eingereichten Abstracts